Tumor Immunogenicity Unlocked: Multi-omics Models Predict Immunotherapy Response and Survival

Dissertation
der Mathematisch-Naturwissenschaftlichen Fakultät
der Eberhard Karls Universität Tübingen
zur Erlangung des Grades eines
Doktors der Naturwissenschaften
(Dr. rer. nat.)

vorgelegt von
Axel Gschwind
aus Crailsheim

Tübingen
2026

Gedruckt mit Genehmigung der Mathematisch-Naturwissenschaftlichen Fakultät der Eberhard Karls Universität Tübingen.

Tag der mündlichen Qualifikation:	24.06.2026
Dekan:	Prof. Dr. Thilo Stehle
1. Berichterstatter:	Prof. Dr. Stephan Ossowski
2. Berichterstatter:	Prof. Dr. Sven Nahnsen

License

WIDMUNG

Gewidmet allen durch das Gesetz über befristete Arbeitsverträge in der Wissenschaft (WissZeitVG) Geschädigten.

This work is dedicated to all scientists who were aggrieved by the Gesetz über befristete Arbeitsverträge in der Wissenschaft (WissZeitVG).

Abstract

Background: Immune Checkpoint Inhibitor (ICI) outcomes are highly heterogeneous among cancer patients. Some individuals experience remarkable treatment success and durable responses, whereas others do not show any benefit from ICI therapy. Concurrently, patients may experience severe or even potentially life-threatening adverse effects. Although currently available individual biomarkers, such as the gold-standards tumor mutation burden (TMB) or *PDL1* expression, correlate with ICI outcomes, their predictive accuracy remains limited. More reliable models that predict ICI treatment outcomes with higher accuracy are urgently needed to identify patients who are likely to benefit from ICI therapy. Integrating distinct biomarkers from multiple omics layers into predictive models is a promising strategy for improving ICI outcome predictions.

Methods: Various genomic and transcriptomic biomarkers that are predictive of ICI outcomes and that describe different aspects of tumor biology were derived from next-generation sequencing (NGS) data. These included tumor-intrinsic properties, such as TMB, *PDL1* expression, immune cell infiltration, and known mechanisms of ICI response, as well as host factors such as HLA-related metrics. Subsequently, the biomarkers were combined into multi-omics models using machine learning (ML) approaches and interpretable scoring methods to predict ICI outcomes with higher accuracy than individual biomarkers. The models were trained on cohorts of melanoma patients with annotated clinical ICI outcomes. Subsequent analyses were performed using additional datasets of various cancer types.

Results: This cumulative dissertation resulted in two scientific, peer-reviewed publications. In the first study, we developed Least Absolute Shrinkage and Selection Operator (LASSO) models that integrate biomarkers derived form bulk RNA sequencing (RNA-seq) and whole exome sequencing (WES) to predict ICI outcomes. The predictions of these multi-omic models outperformed those of the gold-standard ICI biomarker TMB. SHapley Additive exPlanations (SHAP) values were applied to provide explanations of the predictions. The second study focused on an interpretable multi-omics model, the Multi-Omics Tumor Immunogenicity score (MOTIscore), which extended the outcome prediction to survival analyses and investigated underlying molecular mechanics of the tumors. This MOTIscore accurately predicted ICI outcomes, and discriminated patient groups with survival benefits following ICI treatment. The MOTIscore revealed the predictive role of genes that are part of the C-X-C motif ligand pathway, which plays an important role in immune cell activation.

Conclusion: This cumulative work demonstrated that integrating multi-omics data substantially improved the prediction of ICI outcomes compared to individual biomarkers. The multi-omics models developed in this study offer a promising tool for the selection of patients for treatment with ICIs. Using SHAP-based explanations and the interpretable MOTIscore model, we provided explanations for the predictions, which is a crucial prerequisite for a clinical decision-making tool. However, prospective studies are necessary to validate all the findings of our study for potential clinical applications, preferably with a larger patient cohort for which sequencing is performed.

Zusammenfassung

Hintergrund: Krebsbehandlungen mit Immuncheckpointinhibitoren (ICIs) zeigen sehr unterschiedliche Behandlungsergebnisse. Bei manche Patienten führt die Behandlung zu bemerkenswerten Ergebnissen mit dauerhaftem Behandlungserfolg, während andere Patienten kaum oder überhaupt nicht auf die Behandlung mit ICIs ansprechen. Gleichzeitig können starke Nebenwirkungen auftreten, die bis hin zum Tod führen können. Obwohl einzelne derzeit verfügbare Biomarker, wie z.B. die beiden Goldstandards Tumormutationslast (TMB) oder *PDL1*-Expression, mit den Ergebnissen einer ICIs-Behandlung korrelieren, bleibt ihre Vorhersage-Genauigkeit begrenzt. Zuverlässigere Modelle mit genauerer Vorhersage des ICIs-Behandlungserfolgs werden dringend benötigt. Dadurch können Patienten, die von einer Immuntherapie profitieren könnten, aber bisher noch nicht für diese Behandlung ausgewählt werden, treffsicherer identifiziert werden. Ein vielversprechender Ansatz hierfür ist es, verschiedene Biomarker aus mehreren Omics-Schichten in prädiktiven Modellen zu integrieren.

Methoden: Mehrere genomische und transkriptomische Biomarker wurden aus Next-Generation-Sequencing-Daten abgeleitet. Diese beschrieben verschiedene Aspekte der Tumorbiologie, beispielsweise tumor-intrinsische Eigenschaften wie TMB, *PDL1*-Expression, Immunzellinfiltration und bekannte ICI-Resistenzmechanismen. Außerdem berücksichtigten wir Host-Faktoren wie beispielsweise Biomarker, die das HLA-System charakterisieren. Diese Biomarker wurden in Multi-Omics Modelle integriert, die mittels Machine Learning-Ansätzen und interpretierbaren Scoring-Modellen ICI-Ergebnisse genauer vorhersagen sollen als bisher etablierte einzelne Biomarker. Die Modelle wurden mit einer Kohorte von Melanompatienten trainiert, die mit klinischen ICI-Ergebnissen annotiert waren. Anschließende Analysen wurden mit zusätzlichen Datensätzen verschiedener Krebstypen durchgeführt.

Ergebnisse: Die vorliegende kumulative Dissertation besteht aus zwei wissenschaftlichen Publikationen, die beide ein Peer Review durchlaufen haben. In der ersten Studie haben wir Least Absolute Shrinkage and Selection Operator (LASSO)-Modelle zur Vorhersage des ICI-Therapieansprechens entwickelt. Diese LASSO-Modelle integrieren Biomarker, die aus RNA-Bulksequenzierungen (RNA-seq) und Gesamtexomsequenzierungen (WES) abgeleitet wurden. Die Vorhersagen dieser Multi-Omics-Modelle übertrafen diejenigen des Goldstandards TMB. Wir benutzten SHapley Additive exPlanations (SHAP) Werte, um Erklärungen für die Modellvorhersagen zu liefern. In der zweiten Studie konzentrierten wir uns auf ein interpretierbares Multi-Omics-Modell, dem Multi-Omics Tumor Immunogenicity score (MOTIscore). Diese Studie erweiterte die reine Outcome-Analyse um Überlebensanalysen und Analysen zugrundeliegender molekularer Mechanismen der Tumore. Der MOTIscore sagte die ICI-Ergebnisse präzise voraus und erwies sich als geeigneter Prädiktor für Überlebensvorteile in der Patientengruppe mit hohem MOTIscore nach ICI-Behandlung. Die Analysen zeigten darüber hinaus die prädiktive Rolle von Genen, die Teil des C-X-C motif ligand Signalwegs sind, der eine wichtige Rolle bei der Aktivierung von Immunzellen spielt.

Fazit: In dieser kumulativen Arbeit konnten wir zeigen, dass die Integration von Multi-Omics Daten die Vorhersage von ICI-Ergebnissen im Vergleich zu einzelnen Biomarkern sub-

stantiell verbessern kann. Die Multi-Omics-Modelle dieser Dissertation stellen ein vielversprechendes Werkzeug dar, um die Auswahl von Patienten für eine Behandlung mit ICIs zu verbessern. Unser Ansatz benutzt SHAP-Werte und das interpretierbare MOTIscore-Modell, um Erklärungen für die Vorhersagen bereitzustellen, einer wichtigen Voraussetzung für eine klinische Entscheidungshilfe. Dennoch müssen prospektive Studien durchgeführt werden, um alle Befunde dieser Dissertation zu bestätigen, insbesondere im Hinblick auf potentielle klinische Anwendungen. Dabei sollte eine große klinische Krebspatientenkohorte zusammengestellt werden, für die eine umfassende Sequenzierung durchgeführt wird.

Acknowledgments

First, I would like to thank my first supervisor, Prof. Dr. Stephan Ossowski, for the great opportunity to do my dissertation in his computational genomics group. I also thank him for his excellent supervision and guidance over the last few years. Moreover, I would also like to thank Prof. Dr. Sven Nahnsen for accepting my offer to be the second supervisor of this dissertation. Many thanks to Prof. Dr. Manfred Claassen for being part of the thesis advisory committee (TAC), which he formed together with Prof. Dr. Ossowski and Prof. Dr. Nahnsen. I valued every piece of scientific advice given by the TAC.

Additionally, I would like to thank the director of the Institute for Medical Genetics and Applied Genomics, Prof. Dr. Olaf Rieß, for enabling the great working framework and contract under which I have worked on this dissertation. He enabled me to attend several computational biology conferences in Europe. This is something that should not be taken for granted, as PhD candidates from other institutions were not allowed to attend a single conference. Most importantly, without the sheer amount of free coffee, I would never ever have finished this thesis so quickly. I would also like to thank Prof. Dr. Rieß and Prof. Dr. Ossowski for taking care of the full-time funding of this PhD project and the corresponding salaries.

I would also like to express my gratitude to our collaborators of the molecular tumor board (MTB) at the University Hospital Tübingen. To emphasize a few names, Calogero Maurici and Öznür Öner helped me to obtain the metadata of MTB cancer patients and Prof. Dr. Andrea Forschner and Dr. Markus Reitmajer gave scientific advice and analyzed additional metadata of melanoma patients. Many thank to Prof. Dr. Sorin Armeanu-Ebinger for volunteering as the last author of the second integral scientific publication forming this cumulative dissertation.

Special thanks to Dr. Stefan Rein, who helped negotiate the legal details of the labor contract used for this doctoral thesis.

Last but not least, my deepest gratitude goes to my colleagues and intriguing people who have contributed to this work outside the strict scientific framework. Particularly, I mention German, Dominic, Länie and Ali. Without your daily support, the work on this thesis would have been extremely boring.

Contents

List of Abbreviations

AI artificial intelligence

AUC area under the curve

BAM Binary Alignment Map

COSMIC Catalogue of Somatic Mutations in Cancer

CR complete response

CNV copy number variant

dbGaP database of Genotypes and Phenotypes

DEG differentially expressed gene

ECCB European Conference on Computational Biology

ECOG Eastern Cooperative Oncology Group

FOG Festival of Genomics & Biodata

GSEA gene set enrichment analysis

HR hazard ratio

ICI Immune Checkpoint Inhibitor

inDel insertion and Deletion

ISMB Intelligent Systems For Molecular Biology

LASSO Least Absolute Shrinkage and Selection Operator

LIME Local Interpretable Model-agnostic Explanations

MELD Model for End-stage Liver Disease

MHC major histocompatibility complex

ML machine learning

MOTIscore Multi-Omics Tumor Immunogenicity score

MTB molecular tumor board

NGS next-generation sequencing

NSCLC non-small cell lung cancer

ORR objective response rate

OS overall survival

PFS progression-free survival

PD progressive disease

PR partial response

RECIST Response Evaluation Criteria in Solid Tumors

ROC receiver operating characteristic

RNA-seq bulk RNA sequencing

SD stable disease

SNV single nucleotide variant

SRA Sequence Read Archive

SHAP SHapley Additive exPlanations

TAC thesis advisory committee

TCR T-cell receptor

TMB tumor mutation burden

TME tumor microenvironment

TüBMI Tübingen Bioinformatics and Medical Informatics Day

VEP Variant Effect Predictor

WES whole exome sequencing

Chapter 1

Introduction

Immune Checkpoint Inhibitors (ICIs) have revolutionized the treatment of many solid tumors. Unlike classical cytotoxic anti-cancer drugs, which directly target rapidly dividing tumor cells, ICIs enhance anti-tumor immunity[1]. Durable therapy responses and long-term survival have been observed in a subset of cancer patients who otherwise have a poor prognosis using conventional treatment strategies. However, only a minority of patients benefit from ICI treatment, whereas the majority suffer from potential side effects but do not show any benefit from the therapy[2]. Predicting ICI outcomes in patients with advanced disease with higher accuracy is an urgent need, and several approaches are conceivable.

1.1 Carcinogenesis and Tumor Evolution

To understand why only a minority of patients benefit from ICI treatment, it is necessary to comprehend the biological mechanisms underlying tumor evolution and related immune interactions. Cancer evolves through the gradual accumulation of genomic alterations in somatic cells over time[3]. Such mutations can occur randomly during cell division and are triggered by various mutational processes that can alter or modify the human DNA. Widely known examples include tobacco smoke, ultraviolet radiation, exposure to radioactive materials, and, most importantly, aging. Cancer is initiated when a mutation causes a selective growth advantage in a somatic cell, typically by altering important cellular control mechanisms[4]. The affected cells divide slightly faster than their neighboring cells and quickly accumulate more mutations. Over time, this slight increase in cell division can result in a large tumor containing billions of cells[5]. Most cancer cells acquire additional mutations during cell division, resulting in different genomic traits within the tumor mass. Some of these alterations provide further growth advantages, whereas others remain neutral. As a consequence, most tumors are composed of heterogeneous subclones with different genomic profiles. Of note, most anti-cancer drugs further shape this intratumoral heterogeneity, because potentially drug-resistant cells outgrow subclones that respond to the treatment[6]. However, early clonal mutations are shared among all subclones in most cases. Alterations that cause selective growth advantages are called driver mutations, whereas neutral mutations

are called passenger mutations.

Both types of genomic alterations can also influence the immunogenicity of the tumor[7]. Many mutations lead to altered protein peptide sequences, a subset of which are presented by major histocompatibility complex (MHC) molecules on the surface of cancer cells. Mutant peptides, known as neoantigens, are expressed only in tumor tissue and not in healthy cells. Therefore, neoantigens can be recognized as non-self by the T-cell receptor (TCR) of antigen-specific T-cells (Figure 1.1). However, only a small subset of somatic mutations

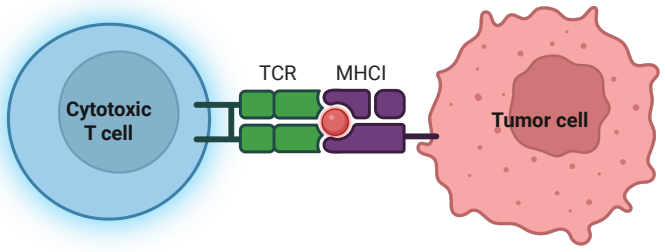

Figure 1.1: Recognition of neoantigens by the immune system. The antigen-specific TCR of a cytotoxic T cell binds to an MHC–neopeptide complex on the surface of a tumor cell, thereby recognizing the neoantigen as non-self. This figure was created using Biorender.

become immunogenic neoantigens that are successfully recognized by the immune system[8]. Importantly, the mutated peptides must bind to the patient-specific MHC molecules, a prerequisite that is often not met. Consequently, tumor immunogenicity is determined not only by the total number of mutations but also by the quality of the resulting neoantigens. Subclonal neoantigens result in suboptimal T-cell activation because they are only presented in a subset of cancer cells[9]. In contrast, clonal neoantigens are expressed in every tumor cell, potentially leading to better immune cell activation.

Cancer normally develops under the constant selective pressure of the immune system. As tumor cells accumulate mutations and neoantigens, the immune system gains the ability to recognize cancer cells and interacts closely with the tumor. Hence, the molecular properties of malignant cells are shaped by an evolutionary process known as immunoediting[10]. This process is typically described as a three-phase model: elimination, equilibrium, and escape. During the elimination phase, the immune system may recognize and eliminate highly immunogenic subclones, whereas subclones with lesser immunogenicity survive. As a result, the overall immunogenicity of the tumor decreases, leading to the following equilibrium phase. During the equilibrium phase, the pressure of the immune system still moderates tumor growth, but only subclones with low immunogenicity persist. Over time, tumor cells acquire mutations that allow them to evade the immune response, culminating in the escape phase of immunoediting. In this phase, malignant cells have gained the ability to escape the immune system, and the tumor microenvironment (TME) becomes increasingly immunosuppressive[11].

The TME not only consists of malignant tumor cells, but also includes a mixture of healthy cells, such as tumor-infiltrating immune cells, stromal cells, and extracellular matrix components[12]. Tumors with a high percentage of infiltrating lymphocytes are often described as inflamed or “hot” tumors and generally show good responses to ICI treatment. In

contrast, "cold" tumors are characterized by very few or absent infiltrating lymphocytes and are frequently resistant to ICIs[13]. However, the molecular changes during immunoediting can limit tumor immunogenicity, even if the tumor is characterized as "hot." Importantly, the presence of highly immunogenic antigens and corresponding tumor-infiltrating T-cells alone is not sufficient to induce an effective immune response. Infiltrating T-cells may exhibit functional exhaustion, or immune cell activity may be suppressed by regulatory T-cells[14], [15]. Another example of factors limiting tumor immunogenicity is resistance mutations as a result of immunoediting, such as loss of antigen presentation due to defects in the MHC or the up-regulation of inhibitory immune checkpoints, such as *PDL1*[10]. Notably, the spatial organization and anatomical location of the tumor can also affect the TME if the tumor location prevents immune cells from infiltrating the tumor tissue. For instance, tumors located in the brain develop an immune-specialized environment in which the blood–brain barrier and other local immunoregulatory factors limit lymphocyte infiltration[16]. Similarly, a dense stromal architecture can prevent immune cells from entering a tumor or parts of the tumor, as in urothelial cancer[17].

Thus, the molecular changes of the tumor cells and the surrounding TME during immunoediting not only promote tumor progression, but also limit the effectiveness of the natural immune response. As a consequence, restoring or enhancing the pre-existing tumor immunogenicity to trigger an immune response is a promising target for modern anti-cancer drugs, such as ICIs.

1.2 Immune Checkpoint Inhibitors

ICIs are a relatively new class of anti-cancer drugs that have transformed the treatment landscape for many cancer patients in the past decade[18]. Unlike classical cytotoxic therapies, ICIs do not directly attack tumor cells but instead improve the anti-tumor activity of the immune system. ICIs block the inhibitory signals of T-cell activation, thereby improving anti-tumor immunity. Figure 1.2 shows a schematic of the biological mechanisms underlying anti-PD1 cancer treatment. T-cells recognize neoantigens if their TCR binds to a specific peptide–MHC molecule presented on the surface of somatic or tumor cells. The interaction between the TCR and the MHC leads to the activation of neoantigen-specific T-cells, triggering an immune response[19]. However, T-cells typically express inhibitory signals, such as PD1 or CTLA4, on their cell surface. These receptors are known as immune checkpoints. If they bind to their counterparts on the membrane of a tumor cell or an antigen-presenting cell, T-cell activity is downregulated. For example, PD1 binds to the membrane protein ligand PDL1. As a result of immune evasion, *PDL1* is over-expressed in many cancer cells[20].

ICIs are monoclonal antibodies that block the interactions between these immune checkpoints, leading to increased immune cell activity (Figure 1.2). Commonly used ICIs include the anti-PD1 antibodies pembrolizumab and nivolumab, both of which directly target PD1 proteins. The efficacy of both drugs has been demonstrated in many solid cancer types, including metastatic melanoma and non-small cell lung cancer (NSCLC)[21][22]. However, only

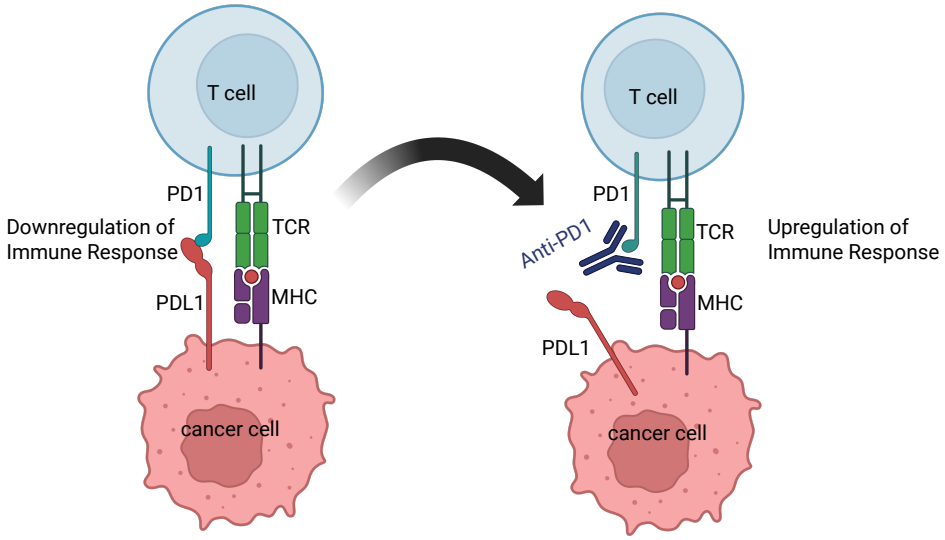

Figure 1.2: General molecular mechanisms of cancer treatment using ICIs. **Left:** A T-cell recognizes a neoantigen presented on the cancer cell surface using its TCR. However, the concurrent interaction between the immune checkpoints PD1 and PDL1 downregulates the immune response. **Right:** An Anti-PD1 antibody is blocking the immune checkpoint, thereby leading to an increased immune response. This figure was created using Biorender.

a minority of patients with metastatic cancer respond to ICI, although patients are selected for ICI treatment based on those molecular properties of the tumor that are predictive of ICI outcomes. This highlights the need to identify novel biomarkers and models that can predict ICI outcomes with higher accuracy than the currently established metrics.

1.3 Sequencing and ICI Biomarker Extraction

Several such biomarkers have been approved for the selection of ICIs in personalized treatment strategies, but their accuracy in predicting ICI outcomes is limited. For instance, *PDL1* expression is an FDA-approved biomarker for selecting patients with advanced NSCLC for ICI treatment, but typical objective response rates (ORRs) to pembrolizumab are modest, with only approximately 25 % in *PDL1*-positive versus 14 % in *PDL1*-negative patients[23]. In melanoma, tumor mutation burden (TMB) is an FDA-approved biomarker for the selection of ICIs in patients with metastatic disease. However, ORRs to pembrolizumab of only 29 % were observed in patients with high TMB versus 6 % in patients with low TMB in a recent study[24]. These findings underscore the urgent need to identify more robust biomarkers that can predict ICI outcomes with higher accuracy.

The advent of next-generation sequencing (NGS) in the early 2000s has facilitated the extraction of both DNA and RNA biomarkers for routine clinical diagnostics. In contrast to earlier technologies, such as Sanger sequencing, NGS is characterized by a very high throughput, enabling the low-cost sequencing of an entire human genome at a time[25]. In current clinical settings, Illumina provides the leading platform for high-throughput sequencing. It leverages the massively parallel sequencing of short DNA fragments on a flow cell, with characteristic short read lengths of 75 up to 300 base pairs. A typical laboratory protocol for the Illumina sequencing-by-synthesis approach includes DNA extraction, shearing of DNA,

adapter ligation, target enrichment, library amplification, and sequencing[26]. In the case of RNA sequencing, the RNA molecules are first reverse-transcribed into complementary DNA before the fragmentation step is performed. The final sequencing-by-synthesis step is usually performed using Illumina sequencers, such as NovaSeq or HiSeq. In the target enrichment step, certain parts of the genome are selected for sequencing. This is typically achieved using sequence-specific oligonucleotide probes, also known as "baits," which selectively hybridize with the genomic regions of interest. Target enrichment normally selects a specific set of genes, known as a gene panel, or targets all protein-coding regions of the human genome, that is, it selects all exons of known genes. Targeted sequencing of all known exonic regions is called whole exome sequencing (WES)[27]. In contrast, the sequencing of all transcribed RNA molecules, known as bulk RNA sequencing (RNA-seq), does not require target enrichment[28].

Genomic biomarkers can be easily extracted using WES, whereas RNA-seq can be employed to extract transcriptomic biomarkers. Data generated by both sequencing technologies are becoming increasingly available as part of standard cancer diagnostics, enabling personalized treatment strategies[29]. However, several steps are necessary *in silico* to extract and analyze biomarkers from the raw sequencing data obtained from the sequencers. The basic steps of a typical clinical bioinformatics data analysis pipeline are outlined in Figure 1.3. The

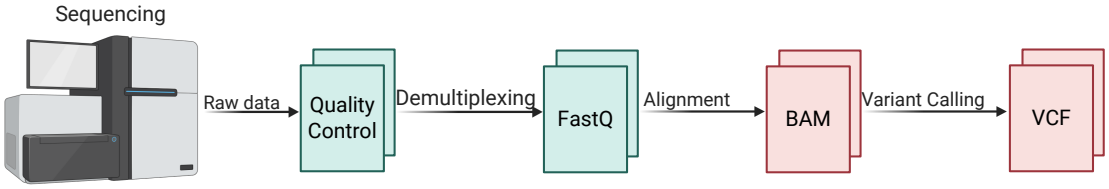

Figure 1.3: Basic steps of a typical bioinformatics sequence analysis pipeline used for the analysis of clinical DNA samples. The most important steps are quality control, demultiplexing, read alignment, and variant calling. The downstream extraction of more complex biomarkers is normally based on the outputs of these steps. This figure was created using Biorender.

first step after sequencing involves quality control, which includes the inspection of base quality scores at the read level as well as the inspection of the GC content. Corrupted sequencing runs can heavily damage later biomarker extraction, making quality control crucial before proceeding with the next steps[30]. For Illumina platforms, this preliminary quality control step can be performed using the Illumina Sequence Analysis Viewer. If the quality of the run was good, the raw base calls will be demultiplexed using, for example, *bcl2fastq*. That is, the sequencing data of the pooled samples will be separated and converted into FASTQ files. Subsequently, the sequencing reads stored in the FASTQ files are aligned against a reference genome, such as GRCh37 or GRCh38. Various algorithms and tools can be used for read alignment, such as *bwa mem* for DNA or *STAR* for RNA short reads[31], [32]. Notably, the alignment step of many bioinformatics pipelines often includes additional post-alignment steps, such as insertion and Deletion (inDel) realignment, sorting, and indexing. Variant calling can be performed once the aligned reads are stored in Binary Alignment Map (BAM) or compressed reference-specific CRAM files. Widely used variant callers are *freebayes* and *strelka2*, both of which have been used in this dissertation[33], [34]. In germline DNA samples,

freebayes detects deviations from the reference genome, so-called single nucleotide and inDel polymorphisms. In tumor DNA samples, strelka2 detects deviations from the corresponding normal sample, that is, mutations in the form of single nucleotide variants (SNVs) and small inDels. The analysis of RNA-seq samples normally does not include variant calling. Instead, the last basic analysis step in RNA-seq is usually the normalization and quantification of transcripts, giving rough estimates of gene expression[35].

These basic bioinformatics steps convert raw sequencing signals into structured genomic and transcriptomic outputs that can subsequently be used to extract higher-level biomarkers. The detected somatic variants in WES are annotated with data from various sources providing meaningful genomic information. For instance, the impact of a mutation on proteins is annotated using the Ensembl Variant Effect Predictor (VEP), whereas the oncogenic relevance of an SNV can be estimated from the Catalogue of Somatic Mutations in Cancer (COSMIC) database[36], [37]. Higher-level ICI biomarkers can be derived from these annotated variants. Examples include TMB, mutations in immune-related pathways, mutational signatures or predicted neoantigens. Other relevant ICI biomarkers, such as HLA genotypes, can be derived from aligned DNA sequences in the BAM file. Of note, copy number variants (CNVs) are estimated based on coverage data, which are typically derived from the BAM file. CNV calls are another source of higher-level biomarkers, for example, loss-of-heterozygosity events or deletions of tumor suppressor genes[38]. In contrast, the basic output of an RNA-seq analysis pipeline is gene expression, quantified as transcript counts normalized by sequencing depth and gene length. While the expression of certain genes, such as *PDL1*, is a predictive ICI biomarker, RNA-seq can also be used to derive higher-level biomarkers. For instance, the cell composition in tumors can be quantified using gene expression values, serving as a proxy for immune cell infiltration in the tumor sample[39]. Using RNA-seq data, TCR clones present in the tumor samples can be reconstructed using tools such as TRUST4[40]. These TCR clone counts can be used to calculate the TCR diversity in terms of Shannon entropy. Importantly, gene fusions are biomarkers in many cancer types, such as *ALK* fusions in NSCLC, and can be detected using RNA-seq data and various fusion callers such as Arriba[41], [42].

The biomarkers derived from WES and RNA-seq provide complementary data[43]. For example, WES can be used to obtain biomarkers describing mutational processes of the tumor, such as TMB or mutations in known pathways of ICI resistance or response. Conversely, RNA-seq biomarkers capture transcriptomic data, such as gene expression profiles or immune cell infiltration. Thus, biomarkers from different omic layers describe distinct aspects of the anti-tumor immune response. WES is typically performed using paired tumor- and blood samples, extending the spectrum of available genomic information to germline biomarkers[44]. Manyfold metrics have been described as predictors of ICI outcomes.

To better conceptualize this diversity, biomarkers are often grouped into three categories: host-related (germline), tumor-intrinsic (somatic), and TME-related[45]. This classification and typical examples are shown in Figure 1.4. Somatic biomarkers reflect the properties of cancer cells, with TMB being a prominent example. In contrast, germline biomarkers

describe the properties of the host, such as HLA genotypes. TME-related metrics cover aspects of dynamic tumor-host interactions, such as immune cells that infiltrate the tumor tissue. Biomarkers from each category cover various aspects of tumor biology, and these

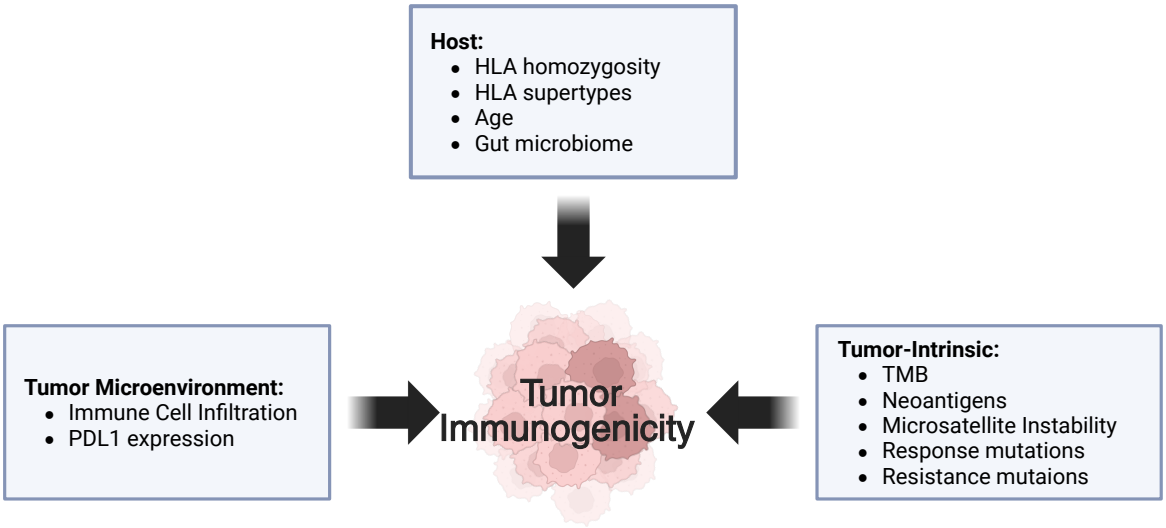

Figure 1.4: ICI biomarkers can be grouped into three broad categories covering different aspects of tumor biology; host, tumor-intrinsic, and TME-related. The superset of all biomarkers describes a model of tumor immunogenicity, that is, its ability to evoke an immune response. This figure was created using Biorender.

metrics are typically extracted using the different sequencing technologies introduced above. For instance, most TME-related metrics require RNA-seq, whereas tumor-intrinsic and host-related biomarkers are derived from WES. Of note, not all potentially relevant biomarkers can be extracted from NGS data, such as age or smoking status.

Although most single-omics biomarkers from these categories have been shown to correlate with ICI outcomes, their predictive accuracy remains limited. Therefore, a more accurate prediction of ICI outcomes is an urgent need[46].

1.4 Multi-Omics Biomarker Integration

The integration of several predictive biomarkers from both WES and RNA-seq into a comprehensive multi-omics model could improve the prediction of ICI outcomes, suggesting a potential avenue of escape. Several methods can be used to combine biomarkers from different sources into one model for the prediction of ICI outcomes, including artificial intelligence (AI) and machine learning (ML) models. Such algorithms have become very popular tools in many branches of science, and state-of-the-art AI models have already been applied in biomedical cancer research[47]. In particular, AI methods have been used to explore ICI treatment. For example, several recent studies have applied ML models to predict ICI outcomes using multiple biomarkers. Despite their complexity, most existing studies have used only a single molecular layer, that is, either clinical variables or single-omics.

For instance, some of these studies have combined simple non-NGS clinical features, such as age, serum albumin, or sex, to predict ICI outcomes [48], [49], [50]. The models showed

good predictive performance, but a major limitation is that their predictions may just reflect the general health status of the patients and the overall stage of their disease. For example, Yoo et al.[48] used serum albumin and Eastern Cooperative Oncology Group (ECOG) status as features in their ML model to predict ICI outcomes. Low serum albumin levels were associated with poor ICI outcomes, whereas a high ECOG status was associated with good ICI outcomes, as they showed in a feature importance analysis. However, both serum albumin and ECOG performance status are well-established prognostic factors that reflect the general well-being of the patient and disease stage[51], [52]. Therefore, both biomarkers may just be prognostic factors and correlate with survival independently of the actual ICI efficacy. The same limitation may apply to Benzekry et al.[49]. They found ECOG performance status and hemoglobin levels to be the most important features in their multivariate models. As a result of these limitations, the models solely based on blood values may identify patients with limited life expectancy rather than those whose tumors are biologically unlikely to benefit from ICI treatment.

Hence, the integration of a more comprehensive set of biomarkers is desirable. Several other studies have developed ML models predictive of ICI outcomes using either genomic or transcriptomic NGS-derived biomarkers but did not combine both single-omics layers into a multi-omics model[53], [54]. For instance, Bigelow et al. developed a random forest classifier predictive of anti-PD1 ICI outcomes, leveraging an initial set of 92 WES-derived biomarkers[53]. Their feature selection reduced the feature count to approximately a dozen genomic biomarkers. However, the random forest model of Bigelow et al. showed only a moderate increase in predictive performance compared to TMB alone. The training cohort comprised only 104 patients, which is relatively small for complex ML models. Furthermore, the pan-cancer setting of their cohorts may limit the inferences from this model. In contrast, Schina et al. developed various ML models predictive of ICI outcomes based only on transcriptomics biomarkers derived from RNA-seq[54]. The features of these models focused on biomarkers that describe the properties of the TME, such as the TCR repertoire or *PDL1* expression. Similar to the model presented by Bigelow et al., the ML models presented by Schina et al. only moderately outperformed univariable predictors across several cancer types. However, neither Bigelow et al. nor Schina et al. developed models that integrated both genomic and transcriptomic biomarkers.

As of 2026, we found only one study that combined WES and RNA-seq data into a multi-omics ML model. Litchfield et al. developed an XGBoost model that predicts ICI outcomes by integrating a total of 11 multi-omics biomarkers[55]. Similar to the aforementioned studies, their model led to an improved predictive performance compared to TMB alone, which was, however, only moderate. Another limitation may be that this model was trained using sequencing data from different cancer types (in a pan-cancer setting). On the other hand, Litchfield et al. reached a comparatively large size of more than 1000 ICI samples for the training cohort.

The classification ML algorithms used in the preliminary studies varied widely. Typical ML models used for ICI outcome prediction included logistic regression[56], random

forests[57], support vector machines[58], and gradient boosting algorithms[59]. Importantly, some ML algorithms require an appropriate feature selection before model training. Of note, the automatic selection an optimal ML algorithm out of several alternatives is possible if the selection process is performed on the training cohort, as demonstrated by Schina et al.[54]. The existing ML models were usually trained using a binary ICI outcome classification derived from radiological imaging technologies; ICI-responders and ICI-nonresponders.

In addition to ML-based models, straightforward scoring approaches, such as weighted sum or product scores, are conceivable for the integration of NGS-based biomarkers. Prominent examples include polygenic risk scores, which are calculated as the weighted sum of risk alleles in a (poly)genic disease[60]. Another example, the Model for End-stage Liver Disease (MELD) score, is defined as the weighted sum of laboratory variables for estimating the severity of liver failure[61]. For such scores, it is necessary to normalize the constituting biomarkers, for example, using z-standardization. Unlike ML models, such scores do not require large training datasets and are typically easy to compute and interpret by humans.

1.5 Multi-Omics Model Challenges

While integrating multi-omics biomarkers into models for improved ICI outcome prediction is a promising approach, their application is accompanied by several challenges. Multi-omic datasets are normally high-dimensional, that is, there are several features but only a limited number of available training samples. This imbalance between model biomarker count and sample count increases the risk of model overfitting[62]. An independent validation cohort is necessary o show that a model did not overfit and generalizes well to other datasets. However, this further reduces the effective size of the training cohort, because the cohort is usually randomly split into training and test datasets[63].

Selecting an appropriate ML model for biological questions is not straightforward. In addition to the high dimensional features in multi-omics datasets, many biological features are not independent of each other. As a result of highly interconnected biological processes, NGS-derived biomarkers are often highly correlated[64]. For example, *PDL1* expression and immune cell infiltration may reflect overlapping biological mechanisms. This multicollinearity in the feature space can affect the performance and stability of the ML model. This problem must be addressed by proper feature selection and an appropriate choice of the ML algorithm[65]. For instance, regularized linear models explicitly address multicollinearity and may be an appropriate choice for ML models. By shrinking the coefficient sizes of correlated features to zero, such models improve the stability and performance of the model[66].

Another important challenge is the heterogeneity of multi-omics datasets[67]. Biomarkers derived from different NGS technologies have different measurement scales and can be diversely represented as categorical, rank-based, or continuous metrics. For example, alterations in ICI resistance pathway genes may be represented on a binary categorical scale; altered pathway versus non-altered pathway, whereas gene expression of the same pathway may be represented as a continuous metric. Therefore, integrating biomarkers defined using

diverse scales requires a careful normalization of these metrics[68]. Without normalization, features that were originally defined on a large numerical scale may dominate the model, regardless of their true biological relevance, thus leading to poor predictions. Furthermore, ML models trained on a specific cancer type may not generalize well to other cohorts, particularly those representing other cancer types.

A major challenge in multi-omics modeling is the limited number of patients for whom both WES and RNA-seq data are available, along with annotated clinical ICI outcomes[69]. Although tumor sequencing is nowadays often performed as part of standard care, systematic clinical outcome annotation is often unavailable. Additionally, consent restrictions and privacy regulations further reduce the number of samples available for research purposes. Hence, sequencing data from different cancer centers and studies are often combined to increase the effective cohort sizes. This can potentially introduce batch effects that arise, for example, from differences in sample processing and laboratory protocols[70]. Batch effects are particularly challenging in RNA-seq expression data and require batch correction to eliminate biases in downstream analyses. Furthermore, WES enrichment kits used at different sequencing centers do not fully overlap in their target regions[71]. Therefore, an overlapping target region must be constructed to avoid batch effects, reducing the effective target size.

Another common problem with ML and AI models is their limited explainability and interpretability. It is often difficult or impossible to understand how a complex ML model reaches its conclusions. Although these terms are closely interconnected, there is no broadly accepted definition for either. In general, explainability can be defined as algorithms that "explicitly consider human comprehensibility of their decisions as a criteria in their computations." This encompasses post-hoc methods and tools to explain the algorithmic predictions made by black-box AI[72]. In contrast, interpretability normally refers to intrinsic model properties that can be directly recognized and understood by humans[73]. Clear explainability and interpretability of the predictions are crucial prerequisites for the clinical application of a model in precision oncology[74]. For example, a model that is interpretable-by-design could apply the weighted sum scoring schemes or product scores mentioned above to integrate several biomarkers into a single metric. Such a scoring model keeps the predictions of the model interpretable and explainable according to the aforementioned definitions.

1.6 Thesis Objectives and Results

The overall objective of this thesis is to improve ICI outcome predictions by integrating genomic and transcriptomic biomarkers into multi-omic models. Thereby, we acquired sequencing data from several public ICI cohorts and derived biomarkers from RNA-seq and WES data. An additional cohort of sequencing data was provided by the local molecular tumor board (MTB), which comprised several cancer types[75]. Using these datasets, we investigated ML and scoring models in melanoma and other cancers to enhance ICI outcome predictions. The candidate's work resulted in two peer-reviewed publications, which constitute this cumulative thesis.

First, we developed Least Absolute Shrinkage and Selection Operator (LASSO) regression models integrating genomic and transcriptomic biomarkers in melanoma[76]. We carefully examined and compared three distinct model outcomes: genomic, transcriptomic, and multi-omic models. As part of the research, we addressed several of the aforementioned problems and challenges. For instance, we selected the LASSO algorithm because it is a regularized linear regression model that effectively handles multicollinearities in the input feature space and that selects the most important biomarkers. Furthermore, our study carefully examined methodologies to explain the ML predictions. We used techniques like permutation feature importance for the selection of biomarkers and to estimate biomarker contributions on a cohort-wide scale. Similarly, we applied SHapley Additive exPlanations (SHAP) values for explanations on a post-hoc per-sample base[77], [78].

Second, we developed the Multi-Omics Tumor Immunogenicity score (MOTIscore) model in a subsequent study. This model leveraged a weighted sum scoring scheme to integrate biomarkers derived from WES and RNA-seq[79]. Using this method, we kept the model transparent and interpretable by its design. The weights were determined using statistical significance testing in a melanoma cohort. This study not only investigated ICI outcomes in terms of binary Response Evaluation Criteria in Solid Tumors (RECIST) outcomes, but also using Kaplan Meier curves of progression-free survival (PFS) and overall survival (OS) across several cancer types[80]. The corresponding Cox model revealed significant differences for the MOTIscore as a predictor of survival. The MOTIscore was also tested for its generalizability to different cancer types. Using MOTIscore for analysis of differentially expressed genes (DEGs), we gained insights into general tumor immune biology across cancers[81].

Besides these two core papers, the candidate contributed as a co-author to more than ten publications that were relevant to the field of oncogenetics.

1.7 Thesis Structure and Scope

The remainder of this cumulative thesis is organized as follows. We explicitly define the main research goals of this dissertation in Chapter 2. In the following Chapter 3, we list all scientific works of the candidate, including co-authored publications, talks, teaching, peer reviewing, and conference contributions. All the scientific findings which were obtained in the two core publications of this thesis are summarized in Chapter 4. Thereby, we present each research result with respect to the goals defined earlier in Chapter 2. The overall discussion can be found in Chapter 5. Full copies of both core papers constituting this thesis are provided in Appendix A and Appendix B, respectively. Finally, copies of certificates of courses and scientific activities which the candidate obtained during his dissertation are provided in Appendix C.

Chapter 2

Research Objectives

The overall goal of this cumulative thesis is to develop and evaluate models that integrate several NGS-derived biomarkers to predict ICI outcomes with higher accuracy than that of currently established individual biomarkers. In particular, we use multi-omics biomarkers extracted from WES and RNA-seq data and apply ML and statistical scoring models for biomarker integration. In the following subsections of this chapter, we briefly define and describe the research objectives of this cumulative thesis as they were addressed in the two main publications. The results will be summarized with respect to these research goals in Chapter 4.

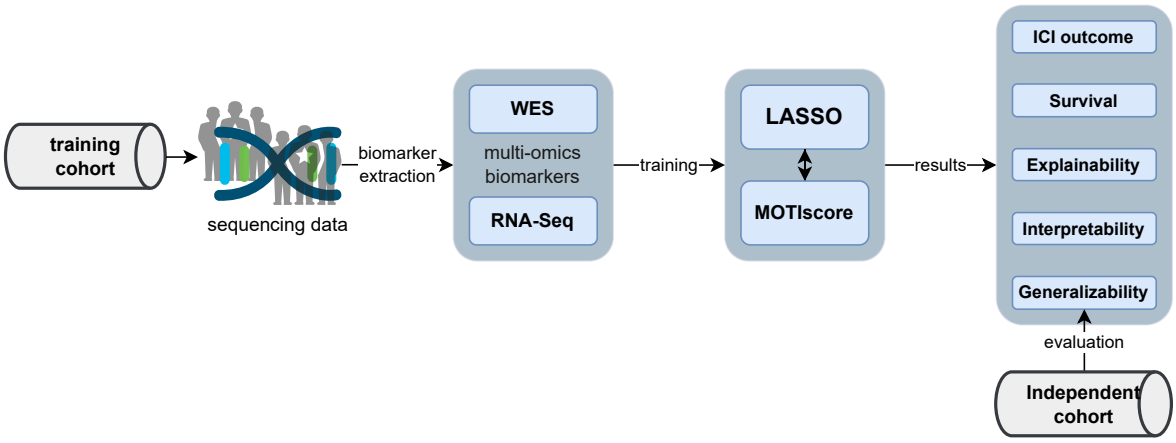

Figure 2.1: Flowchart of the overall goals and objectives of this cumulative thesis. After the curation of a training cohort, multi-omics biomarkers will be extracted from cancer sequencing data, that is, WES and RNA-seq. Using these biomarkers, we will train and develop models for the publications constituting this thesis, namely a LASSO regression model and the MOTIscore model. The results will be evaluated using an independent cohort and according to the objectives described in Chapter 2.

Figure 2.1 shows a flowchart of our research objectives. After obtaining annotated sequencing data, we will use bioinformatics pipelines and tools to extract genomic and transcriptomic biomarkers. Important sources of sequencing data are the database of Genotypes and Phenotypes (dbGaP), the Sequence Read Archive (SRA), and the local MTB[75], [82], [83]. The biomarkers extracted from those data sets will then be used for model training or definition, respectively. Subsequently, the model predictions as primary results will be evaluated using independent cohorts and from various perspectives, as described in the following

sections of this chapter.

2.1 ICI Outcome Prediction

The primary objective of this thesis is to improve the prediction of ICI outcomes by integrating transcriptomic and genomic biomarkers. The predictive accuracy of our models will be compared with that of already established individual biomarkers, such as TMB and *PDL1* expression. To achieve these goals, a consistent categorical ICI outcome classification system must be established. Given the available data annotations, this outcome classification will be defined in terms of clinical RECIST criteria[84]. The output of most ML and scoring models is usually a continuous probability. Thus, we need to find thresholds for the models, defined as an optimal trade-off between sensitivity and specificity. Furthermore, appropriate model performance measures are required to evaluate and compare the predictive accuracies of our models with those of the individual biomarkers.

2.2 Survival Analysis

Categorical response criteria cannot fully capture the clinical outcomes of ICI treatment. For instance, patients whose RECIST ICI responses were classified as stable disease (SD) may experience long term survival benefits because the target lesions do not show any progress for a long time. Conversely, patients with partial response (PR) may not show any clinical benefit if there is an initial response that turns into tumor progression shortly after[85]. Thus, a further objective of this thesis is to evaluate multi-omics biomarker models in terms of survival. Kaplan-Meier estimators will be used to inspect the model predictions using PFS and OS times. This survival analysis includes significance testing and estimation of hazard ratios (HRs) using the Cox proportional hazards model, thereby complementing the analysis of the categorical model outcome predictions.

2.3 Models

Several modeling strategies can be applied to integrate biomarkers into a single predictive score. In this thesis, we aim to investigate at least one ML algorithm in models that combine genomics, transcriptomics, and multi-omics biomarkers. The ML model should be an algorithm that has not yet been published for the prediction of ICI outcomes using NGS-derived biomarkers, thereby filling a research gap. As biological and medical features are often highly correlated, model selection and training must account for biomarker redundancy and multicollinearity. Another objective of this work is to develop at least one more straightforward model that is interpretable by design, such as weighted sum or weighted product scoring models. For this second approach, it is neccessary to find a statistical method to determine appropriate weights assigned to each biomarker.

2.4 Explainability and Interpretability

It is often difficult or even impossible to understand how ML or AI models make predictions. However, explainability and interpretability are crucial prerequisites for the potential clinical applications of a model. Therefore, we will establish and evaluate techniques that provide explanations for the model predictions in this cumulative thesis. For the ML models, we will apply both local and global post hoc explanation techniques. This includes feature permutation importance sampling, which provides the importance of any model biomarker at the global level. At the local level, we will apply techniques that provide per-sample biomarker contributions, such as SHAP and Local Interpretable Model-agnostic Explanations (LIME)[78], [86]. In addition to these explainability methods for ML, we aim to develop scoring models that are interpretable by design and that do not require explainability techniques. For binary classifiers, a cutoff of the predictions must be defined and the definition of this threshold should be comprehensible to clinicians.

2.5 Generalizability

It is of particular interest whether a model is predictive of ICI outcomes in distinct cancer types. If a model generalizes well to different entities, it may describe the general molecular mechanisms underlying tumor immunogenicity. Thus, we will test the predictive accuracy of the models developed in this work as predictors of ICI outcomes in different cancer types and cohorts. Additionally, it is crucial to test ML models using an independent validation cohort to ensure that they do not overfit. We will achieve this by randomly splitting the data into training and validation cohorts.

By analyzing DEGs and performing gene set enrichment analysis (GSEA) using a model cutoff as a group discriminator, we can identify the underlying molecular mechanisms in a cohort[87]. If we find the same DEGs and pathways enriched in different cancer types, this will provide further evidence for the generalizability of the model.

Chapter 3

List of Scientific Contributions

In this chapter, we list all scientific contributions of the candidate that are relevant to this work and the bioinformatics field. The candidate not only wrote the two core publications of this cumulative thesis but also contributed to more than ten scientific publications as a co-author. Further scientific contributions included talks, conference posters, peer reviews, and teaching.

3.1 List of Main Publications

This cumulative dissertation is based on two scientific publications. The candidate is the first and main author of the following peer-reviewed manuscripts.

1. A. Gschwind and S. Ossowski, "AI Model for Predicting Anti-PD1 Response in Melanoma Using Multi-Omics Biomarkers", *Cancers*, vol. 17, no. 5, p. 714, Feb. 20, 2025. DOI: 10.3390/cancers17050714[88]

2. A. Gschwind et al., "Multi-Omics Tumor Immunogenicity Score Predicts Immunotherapy Outcome and Survival", *Biology*, vol. 14, no. 12, p. 1698, Dec. 2025. DOI: 10.3390/biology14121698[89]

Both papers are integral part of this thesis and aim to predict ICI outcomes by combining multi-omics biomarkers. We refer to [88] as the "first" paper and to [89] as the "second" paper in the remainder of this thesis. Full copies and a detailed description of the candidate's contributions to each paper are provided in Appendix A and Appendix B.

Of note, the first paper was selected by the journal as the cover story for the March 2025 issue. We provide a copy of the cover page in Appendix A.2. For the second project, we applied for funding. The corresponding process was organized by the candidate and he wrote the grant application. Applying for grants is a crucial part of a modern scientist's work, but it is not a standard experience for an average PhD candidate. Hence, we have included the grant application in Appendix B.4.

3.2 List of Other Publications

In addition to the two main publications constituting this dissertation, the candidate contributed to the scientific papers listed in this section. He is a co-author of these publications, but they are not integral part of this thesis. However, they cover a wide range of topics in the field of NGS-based cancer diagnostics and some manuscripts investigate ICI treatment and corresponding biomarkers. The relevance of these co-authored publications for the core studies will be discussed in Chapter 5.1.

- A. K. Sommer et al., "Mutational Landscape of Colorectal Tumors From Individuals With Unexplained Adenomatous or Serrated Colorectal Polyposis", *Gastroenterology*, Jan. 12, 2026. DOI: 10.1053/j.gastro.2025.10.011[90]
- J. Forschner et al., "Adjuvant anti-PD-1 therapy improves melanoma-specific survival in stage IIIC-IV melanoma patients with high tumor mutation burden and BRAF V600 mutation", *Frontiers in Oncology*, vol. 15, Aug. 12, 2025. DOI: 10.3389/fonc.2025.1618596[91]
- G. M. H. Abdel-Salam et al., "Biallelic *MAD2L1BP* (p31^{comet}) mutation is associated with mosaic aneuploidy and juvenile granulosa cell tumors", *JCI Insight*, vol. 8, no. 22, Nov. 22, 2023. DOI: 10.1172/jci.insight.170079[92]
- A. Liebmann et al., "UV-radiation and *MC1R* germline mutations are risk factors for the development of conventional and spitzoid melanomas in children and adolescents", *eBioMedicine*, vol. 96, Oct. 1, 2023. DOI: 10.1016/j.ebiom.2023.104797[93]
- M. Menzel et al., "Multicentric pilot study to standardize clinical whole exome sequencing (WES) for cancer patients", *npj Precision Oncology*, vol. 7, no. 1, p. 106, Oct. 20, 2023. DOI: 10.1038/s41698-023-00457-x[94]
- S. Mittelstadt et al., "Detection of circulating cell-free HPV DNA of 13 HPV types for patients with cervical cancer as potential biomarker to monitor therapy response and to detect relapse", *British Journal of Cancer*, vol. 128, no. 11, pp. 2097–2103, Jun. 2023. DOI: 10.1038/s41416-023-02233-x[95]
- J. Eckardt et al., "TMB and BRAF mutation status are independent predictive factors in high-risk melanoma patients with adjuvant anti-PD-1 therapy", *Journal of Cancer Research and Clinical Oncology*, vol. 149, no. 2, pp. 833–840, Feb. 1, 2023. DOI: 10.1007/s00432-022-03939-w[96]
- M. Renovanz et al., "Clinical outcome of biomarker-guided therapies in adult patients with tumors of the nervous system", *Neuro-Oncology Advances*, vol. 5, no. 1, vdad012, Jan. 1, 2023. DOI: 10.1093/noajnl/vdad012[97]
- C. Roggia et al., "Germline findings in patients with advanced malignancies screened with paired blood–tumour testing for personalised treatment approaches", *European*

Journal of Cancer, vol. 179, pp. 48–55, Jan. 1, 2023. DOI: 10.1016/j.ejca.2022.11.003[98]

- F. J. Hilke et al., "Distinct Mutation Patterns Reveal Melanoma Subtypes and Influence Immunotherapy Response in Advanced Melanoma Patients", *Cancers*, vol. 12, no. 9, p. 2359, Sep. 2020. DOI: 10.3390/cancers12092359[99]

- A. Forschner et al., "MDM2, MDM4 and EGFR Amplifications and Hyperprogression in Metastatic Acral and Mucosal Melanoma", *Cancers*, vol. 12, no. 3, p. 540, Mar. 2020. DOI: 10.3390/cancers12030540[100]

Note that Hilke et al.[99] and Forschner et al.[100] were published before the candidate enrolled as a PhD student. The candidate is a co-author of the following preprint. The manuscript was submitted to a scientific journal, but the peer-review process has not yet been completed.

- D. Boceck et al. "aiDIVA – Diagnostics of Rare Genetic Diseases Using Large Language Models", Accessed: Dec. 15, 2025. [Online]. Available: https://www.medrxiv.org/content/10.1101/2025.09.04.25335099v1 pre-published[101]

Notably, the candidate is the first author of a preliminary publication he has written as part of his Master thesis in computational soft matter physics. The manuscript was written years before starting the PhD project, and the topic of that paper is not directly related to the bioinformatics field.

- A. Gschwind et al., "Isotropic-nematic transition for hard rods on a three-dimensional cubic lattice", *Physical Review E*, vol. 96, no. 1, p. 012 104, Jul. 5, 2017. DOI: 10.1103/PhysRevE.96.012104[102]

3.3 Conference Contributions

The candidate contributed the following poster presentations at international conferences. The posters covered early results of the same studies as they were later published in the core publication of this thesis.

- FOG 2026 in London, United Kingdom: *Integration of Multi-Omics Tumor Immunogenicity Biomarkers for Predicting Immunotherapy Response.*

- ISMB/ECCB 2025 in Liverpool, United Kingdom: *Multi-Omics Tumor Immunogenicity Score.*

- ECCB 2024 in Turku, Finland: *AI model predicts Anti-PD1 response in melanoma using multiomics biomarkers.*

- TüBMI 2024 in Tübingen, Germany: *AI model predicts Anti-PD1 response in melanoma using multiomic biomarkers.*

- ISMB/ECCB 2023 in Lyon, France: *Machine learning models predicting response to immune checkpoint inhibitors (ICI) based on DNA and RNA biomarkers.*

A scientific talk was given at the TüBMI 2025 conference.

- TüBMI 2025 in Tübingen, Germany: *Tumor Immunogenicity Unlocked: Multiomics and AI Join Forces to Predict Immunotherapy Response.*

In 2022 and 2023, the candidate participated in the NGSchool, a summer school covering topics relevant to modern bioinformatics. The NGSchool was funded by the Visegrád Group and took place in the Warsaw metropolitan area. The focuses of both schools were on "Machine Learning in Computational Biology" and "Advances in Computational Biology." The corresponding certificates of participation are provided in Appendix C.1 and Appendix C.2.

3.4 Teaching

The candidate contributed to academic teaching. During his time as a PhD student, he served as mentor for the following master theses. All of them covered ML techniques applied to oncology data.

- *Supervised machine learning based approach to predict relapse-free survival time in melanoma patients.* Tübingen. 2022.
- *MaLiPre – an explorative protoype evaluation of machine-learning based lymphocyte infiltration prediction.* Erfurt. 2023.
- *Comprehensive Neoantigen Annotation and Prioritization for Personalized Cancer Immunotherapy.* Tübingen. 2024.

3.5 Scientific Peer Review

During his doctoral studies, the candidate was asked to review several scientific papers as a peer reviewer. He accepted the review of three scientific manuscripts in various journals. Two of the corresponding reviewer certificates can be inspected in Appendix C.3.

Chapter 4

Results Summary

In this chapter, we briefly summarize the main results of this cumulative work, with respect to our main research objectives defined in Chapter 2. This dissertation resulted in two main publications. The first paper focused on ICI outcome prediction using ML models and their explainability. Thereby, the ML models leveraged genomics, transcriptomics, or multi-omics biomarkers derived from WES and RNA-seq data. All ML models of that study were developed and evaluated using various datasets of melanoma patients. In contrast, the second paper developed an interpretable model using a weighted sum scoring method and multi-omics biomarkers. This publication focused on ICI survival analysis, generalizability across cancer types, and underlying molecular mechanisms of tumor immunogenicity. Both works are listed in Chapter 3.1. Full copies and a list of the candidate's contributions to each paper are provided in Appendix A and Appendix B.

4.1 ICI Outcome Prediction

The RECIST criteria estimate the size changes of malignant target lesions using imaging technologies[84]. Therapy responses are grouped into four RECIST categories, providing a coherent outcome classification: complete response (CR), partial response (PR), stable disease (SD), and progressive disease (PD). The RECIST criteria are often binarized, with patients classified as responders or non-responders. CR and PR are categorized as responders, whereas SD and PD are regarded as non-responders. We used this binary outcome classification as the primary outcome measure in the main publications of this thesis. In both core papers, the continuous model predictions were binarized by maximizing Youden's index. This ensured an ideal trade-off between sensitivity and specificity[103]. Receiver operating characteristic (ROC) area under the curves (AUCs) were used as the main outcome performance measure for the models developed in this work[104]. Using ROC AUCs, the performance of different models can easily be compared.

In the first core paper, three distinct ML models were developed, integrating either genomic, transcriptomic, or multi-omic biomarkers. All three models outperformed the FDA-approved individual biomarker TMB in terms of ROC AUCs, with ICI outcomes defined as

responders and non-responders. The highest ROC AUC was observed in the multi-omics model, whereas the genomic and transcriptomic models outperformed TMB alone but had slightly lower ROC AUCs than the multi-omics model. Surprisingly, using either genomic or transcriptomic biomarkers led to similar predictive performances, although they are usually considered orthogonal data. In summary, the increase in ROC AUCs of all three ML models was moderate compared to that of TMB alone.

In the second core paper, we developed the MOTIscore to predict ICI outcomes in several cancer types and cohorts. Similar to the ML models, the MOTIscore was defined as a multi-omics model that integrates several transcriptomic and genomic biomarkers predictive of ICI outcomes. The results showed an improved predictive accuracy of ICI outcomes compared to individual biomarkers. The overall performance in terms of ROC AUC was comparable to that of an ML model in melanoma and gastric cancer. In a benchmark comparison, our MOTIscore outperformed other models that leveraged single-omic RNA-seq strategies in terms of ROC AUC in a gastric cancer cohort.

In summary, both approaches led to a higher predictive accuracy than that of TMB alone. Since both models outperformed TMB, the primary research objective of outperforming individual biomarkers was met (Chapter 2.1).

4.2 Survival Analysis

In the first paper, we developed an ML model and investigated ICI outcomes in terms of the binary definition we introduced above. However, we did not analyze other possible ICI outcome measures, because the available data were not consistently annotated with survival times. This limitation did not apply to the second paper constituting this thesis, in which we extended the binary outcome definition. The MOTIscore predictions were additionally analyzed in terms of survival times. PFS and OS were annotated for many cancer patients in the available cohorts. Accordingly, we plotted Kaplan–Meier curves for different cancer types and used the MOTIscore model as a group discriminator. We used a Cox proportional hazards model to test the groups for statistically significant differences in survival times. In both gastric cancer and melanoma, the MOTIscore was significantly predictive of PFS and OS. Cancer patients whose tumors had a high MOTIscore exhibited an extended survival following ICI treatment. Using cohorts from the MTB Tübingen, we defined a ICI-specific PFS, which describes the overall duration of ICI, that is, the time from initiation until termination of ICI. The MOTIscore model was predictive of extended ICI-specific PFS in melanoma and a pan-cancer cohort.

4.3 Models

In the first publication, we chose LASSO regression as model algorithm for the integration of genomic, transcriptomic, and multi-omic features. During the training of the model, LASSO can identify correlated features, and keeps only one of both by rejecting the other's coefficient

to zero. The same way, LASSO can shrink coefficients of unimportant features to zero. This way, we addressed the problem of multicollinearity in the input data, a problem that occurs frequently in biological sequencing data. Most biomarkers derived from NGS data are highly correlated due to interconnected biological processes. For example, LASSO reduced the initial feature space of the genomic model from 40 biomarkers to 13 biomarkers by shrinking the coefficient size of the remaining features to zero. To our knowledge, no LASSO regression model has been applied for the integration of NGS-based multi-omics biomarkers or the prediction of ICI outcomes. Hence, we successfully filled a research gap and developed three distinct LASSO models integrating genomics, transcriptomics, and multi-omics biomarkers in the first paper.

In the second publication, we developed a weighted sum scoring model, establishing our own multi-omics MOTIscore. Eight initial transcriptomic and genomic immunogenicity biomarkers were selected through an expert interview and integrated into the MOTIscore model. Using this approach, the model became interpretable by design, making it more suitable for potential clinical use cases. The MOTIscores were highly correlated to the predictions of a LASSO model using the same set of biomarkers, and the predictive performance was comparable to that of the LASSO model. The weights of the MOTIscore were determined by statistical tests (Fisher's exact test and Mann-Whitney U test) in the input cohort. Thereby, we removed insignificant biomarkers. We accounted for multicollinearities in the feature space by removing correlated features, further reducing the biomarker count. The final MOTIscore model resulted in four biomarkers: TMB, TCR repertoire, mutations in ICI-response pathways, and *PDL1* expression.

4.4 Explainability and Interpretability

We implemented several approaches to explain the predictions of our models. In the first paper, we conducted feature permutation importance analyses to determine the overall statistical impact of the individual biomarkers onto the LASSO model. However, this approach only improves the explainability on a global level and does not provide explanations on a per-sample base. Hence, we conducted a subsequent SHAP value analysis of our LASSO models. Using this approach, we obtained per-sample explanations, extending potential use cases of the models to clinical applications. Since SHAP values are a post-hoc method, these model explanations remain cohort-dependent. In the second paper, we therefore developed the MOTIscore model, a weighted sum scoring approach that is interpretable by design. The MOTIscore model explicitly specifies how individual biomarkers contribute to the final score, ensuring model interpretability.

The models of both studies resulted in continuous predictions and scores, respectively. The results were binarized using a cutoff determined by maximizing Youden's index, an approach that regards specificity and sensitivity with equal importance. Using this technique, the determination of the cutoffs remained comprehensible.

4.5 Generalizability

In the first publication, we tested the generalizability of the LASSO model using only melanoma data, that is, the same cancer entity as we used for model training. However, the data set was randomly split into training and test cohorts. The comparison showed that the LASSO models were also predictive of ICI outcomes in the validation cohort, that is, the model generalized well to previously unseen data and did not overfit. The test data set of the first paper comprised only 46 samples, underscoring the need for larger datasets in future studies.

In the second paper, we extended this data analysis to additional cancer entities, mainly a gastric cancer cohort. The MOTIscore was developed using a melanoma cohort but also showed good predictive performance in gastric cancer, both in terms of ROC AUC and survival. Using pan-cancer dataset from the local MTB, we could also show a good predictive performance of the MOTIscore in terms of ICI-specific survival using this independent cohort. Notably, an extended analysis of DEGs revealed the same set of up-regulated immune system-related genes in both melanoma and gastric cancer. In particular, *CXCL9*, *CXCL10*, and *CXCL11* were up-regulated in patients with high MOTIscore. These genes are part of the C-X-C chemokine ligand pathway, which plays an important role in immune-cell activation. Similarly, GSEA revealed a common set of immune response-related gene sets in both melanoma and gastric cancer. Both findings give evidence that the MOTIscore captured underlying molecular mechanisms that generalized well across cancer types.

Chapter 5

Discussion

Taken together, the findings of this cumulative dissertation showed that integrating multi-omics biomarkers can improve the accuracy of ICI outcome predictions. In the first core publication, we demonstrated this for melanoma using a LASSO model predictive of ICI outcomes according to the RECIST criteria. In the second paper, we confirmed these findings using the interpretable MOTIscore, which was also predictive of ICI outcomes in terms of PFS and OS. Both models outperformed established individual biomarkers, particularly TMB, in terms of ROC AUCs. Moreover, the MOTIscore outperformed RNA-seq-based models in gastric cancer in a benchmark comparison. For the MOTIscore, we demonstrated a good generalizability of the score from melanoma to various cancer types. In the second paper, this was also shown for a multi-omics LASSO model using the same set of biomarkers as the MOTIscore. Our benchmark showed that it generalized well from melanoma to gastric cancer. To a lesser extent, we showed the generalizability of the LASSO models in the first paper. The model predictions generalized well to an independent test cohort, showing that the LASSO models did not overfit.

In the first paper, we developed two LASSO models predictive of ICI outcomes that used either genomic or transcriptomic biomarkers. Interestingly, the performance of both models was comparable, and both models outperformed TMB, although the transcriptomic model was based exclusively on RNA-seq and did not include TMB. Genomic biomarkers primarily capture the mutational landscape of tumors, whereas transcriptomic biomarkers reflect information about the TME. Hence, the similar performance may indicate that both types of biomarkers capture complementary but converging information about tumor immunogenicity, eventually reflecting the same immune-related processes relevant for ICI success. This finding underscores the potential of RNA-seq-based biomarkers in predicting ICI outcomes. This idea is supported by the identification of the expression of C-X-C motif chemokine ligand pathway genes as independent predictive factors in the second paper.

To our knowledge, no previous study has used LASSO regression to predict ICI outcomes using NGS-derived biomarkers. The corresponding literature review was presented in the introduction, Chapter 1.4. Similarly, the MOTIscore is a new approach for the integration of multi-omics biomarkers into a single interpretable score to predict ICI responses and sur-

vival. Thus, both studies contributed important and significant new findings to the field of computational oncology by introducing new methodologies. In the second paper, another novel finding was the enrichment of genes of the C-X-C motif chemokine ligand pathway as an independent predictive factor for ICI outcomes in several cancer types.

An important focus of this thesis was to provide explanations for the model predictions and, alternatively, to design a model that is inherently interpretable. For clinical applications, these are crucial prerequisites because physicians need to comprehend how the predictions are made. In the first paper, we achieved explainability by applying SHAP values to the LASSO predictions. However, the SHAP methodology is cohort-dependent and provides post-hoc explanations, potentially limiting the clinical usability of these explanations[105]. Therefore, we developed the MOTIscore in the second core publication of this thesis. The MOTIscore was designed as a tool that is interpretable through design. This way, we provided a methodology that can be more easily transferred to clinical applications.

5.1 Co-Authored Publications

All studies to which the candidate contributed as a co-author covered important oncogenetic topics and most of the research was usually performed using NGS data. These contributions provided important methodological and scientific experience for the candidate, although the co-authored publications are not integral part of this cumulative thesis. Some findings of the papers were directly relevant for the core studies of this cumulative thesis. Insights gained from the publications helped to refine the selection of biomarkers for our models. For example, Forschner et al. revealed the role of *MDM2*, *MDM4*, and *EGFR* amplifications as negative prognostic markers in ICI-treated metastatic melanoma[100]. Patients with amplifications in these genes were more likely to experience hyperprogression under ICI treatment. Hence, these alterations can be considered as ICI resistance mutations. Subsequently, we used amplifications of these three genes as biomarkers for the LASSO model in the first main paper[88]. Surprisingly, mutations in ICI resistance pathways were not important for the predictions of the LASSO model in the first publication.

5.2 Limitations

Both studies of the two main publications have several limitations. In this section, we briefly summarize the main restrictions, see both papers for a more detailed discussion. An important limitation of our study was that our models only incorporated transcriptomic and genomic data, whereas we did not include data from other omics layers, such as proteomics or metabolomics. Likewise, our models did not include non-NGS data, such as serum albumin, age, or smoker status, even though many of these clinical variables have been described as strong predictors of ICI outcomes[106].

The overall cohort sizes were limited and the patient cohorts were heterogeneous, that is, many patients were not treatment-naïve at the start of ICI. However, ICIs are known

to perform better when given as first-line therapy compared to later treatment lines[107]. Hence, these prior therapies may have affected both treatment efficacy and survival, thereby introducing a potential bias to the models we have developed as part of this dissertation. In addition, our cohorts were assembled using data from different sequencing centers, platforms and library preparation kits. Although we applied several strategies to minimize batch effects, these factors are a potential source of bias and error[108]. This may limit the reproducibility of our findings. In particular, gene expression derived from RNA-seq is prone to biases introduced by such batch effects.

All studies that were included in the patient cohorts used for our models had a retrospective design, which limits causal inferences[109]. For instance, there could be selection biases, inconsistent annotation of RECIST outcomes, and confounders that were not measured by the authors of the original studies. Such sources of bias could affect both model training and evaluation, thereby limiting the generalizability of our findings.

5.3 Future Directions

Therefore, all findings presented in the publications of this cumulative thesis should be validated in independent prospective studies in the future. This is particularly important for the potential clinical applications of our models. Future work may extend the existing models by incorporating additional biomarkers and omics layers, such as proteomics, methylation data, and spatial transcriptomics. Recent studies suggest that the immune response to ICI treatment may be driven by a single or few high-quality neoantigens[110]. As a consequence, identifying such neoantigens using an appropriate prioritization algorithm is a promising direction for future ICI biomarker discovery. Such neoantigen-based biomarkers could be integrated into models that predict ICI outcomes.

5.4 Conclusion

Both core studies of this cumulative work demonstrated that integrating multi-omics biomarkers can improve ICI outcome predictions. We applied two different methods, a LASSO model and a weighted sum scoring scheme, to predict ICI outcomes. Using explainability and interpretability techniques, our models may serve as a clinically applicable tools. Particularly, if our findings can be validated in prospective studies. Together, our results support the use of integrative multi-omics models as a promising direction for decision-making in personalized oncology.

Bibliography

[1] J. A. Marin-Acevedo, E. O. Kimbrough, and Y. Lou, "Next generation of immune checkpoint inhibitors and beyond", *Journal of Hematology & Oncology*, vol. 14, no. 1, p. 45, Mar. 19, 2021. DOI: 10.1186/s13045-021-01056-8

[2] S. Das and D. B. Johnson, "Immune-related adverse events and anti-tumor efficacy of immune checkpoint inhibitors", *Journal for ImmunoTherapy of Cancer*, vol. 7, no. 1, p. 306, Nov. 15, 2019. DOI: 10.1186/s40425-019-0805-8

[3] C. Jolly and P. Van Loo, "Timing somatic events in the evolution of cancer", *Genome Biology*, vol. 19, no. 1, p. 95, Jul. 24, 2018. DOI: 10.1186/s13059-018-1476-3

[4] S. Zhang et al., "Tumor initiation and early tumorigenesis: Molecular mechanisms and interventional targets", *Signal Transduction and Targeted Therapy*, vol. 9, no. 1, p. 149, Jun. 19, 2024. DOI: 10.1038/s41392-024-01848-7

[5] B. Vogelstein, N. Papadopoulos, V. E. Velculescu, S. Zhou, L. A. Diaz, and K. W. Kinzler, "Cancer Genome Landscapes", *Science*, vol. 339, no. 6127, pp. 1546–1558, Mar. 29, 2013. DOI: 10.1126/science.1235122

[6] A. Marusyk, M. Janiszewska, and K. Polyak, "Intratumor Heterogeneity: The Rosetta Stone of Therapy Resistance", *Cancer Cell*, vol. 37, no. 4, pp. 471–484, Apr. 13, 2020. DOI: 10.1016/j.ccell.2020.03.007

[7] Y. Wolf and Y. Sameuls, "Neoantigens in cancer immunotherapy: Quantity vs. quality", *Molecular Oncology*, vol. 17, no. 8, pp. 1457–1459, 2023. DOI: 10.1002/1878-0261.13483

[8] T. N. Schumacher and R. D. Schreiber, "Neoantigens in cancer immunotherapy", *Science*, vol. 348, no. 6230, pp. 69–74, Apr. 3, 2015. DOI: 10.1126/science.aaa4971

[9] J. Nemunaitis et al., "Clonal Neoantigen: Emerging "Mechanism-based" Biomarker of Immunotherapy Response", *Cancers*, vol. 15, no. 23, p. 5616, Nov. 28, 2023. DOI: 10.3390/cancers15235616

[10] D. Mittal, M. M. Gubin, R. D. Schreiber, and M. J. Smyth, "New insights into cancer immunoediting and its three component phases — elimination, equilibrium and escape", *Current Opinion in Immunology*, vol. 27, pp. 16–25, Apr. 1, 2014. DOI: 10.1016/j.coi.2014.01.004

[11] M. Roerden and S. Spranger, "Cancer immune evasion, immunoediting and intratumour heterogeneity", *Nature Reviews Immunology*, vol. 25, no. 5, pp. 353–369, May 2025. DOI: 10.1038/s41577-024-01111-8

[12] W. H. Fridman, L. Zitvogel, C. Sautès–Fridman, and G. Kroemer, "The immune contexture in cancer prognosis and treatment", *Nature Reviews Clinical Oncology*, 2017. DOI: 10.1038/nrclinonc.2017.101

[13] J. Galon and D. Bruni, "Approaches to treat immune hot, altered and cold tumours with combination immunotherapies", *Nature Reviews Drug Discovery*, vol. 18, no. 3, pp. 197–218, Mar. 2019. DOI: 10.1038/s41573-018-0007-y

[14] C. U. Blank et al., "Defining 'T cell exhaustion'", *Nature Reviews Immunology*, vol. 19, no. 11, pp. 665–674, Nov. 2019. DOI: 10.1038/s41577-019-0221-9

[15] G. Plitas and A. Y. Rudensky, "Regulatory T Cells in Cancer", *Annual Review of Cancer Biology*, vol. 4, pp. 459–477, Volume 4, 2020 Mar. 4, 2020. DOI: 10.1146/annurev-cancerbio-030419-033428

[16] D. F. Quail and J. A. Joyce, "The Microenvironmental Landscape of Brain Tumors", *Cancer Cell*, vol. 31, no. 3, pp. 326–341, Mar. 13, 2017. DOI: 10.1016/j.ccell.2017.02.009

[17] S. Mariathasan et al., "TGF attenuates tumour response to PD-L1 blockade by contributing to exclusion of T cells", *Nature*, vol. 554, no. 7693, pp. 544–548, Feb. 2018. DOI: 10.1038/nature25501

[18] C. Robert, "A decade of immune-checkpoint inhibitors in cancer therapy", *Nature Communications*, vol. 11, no. 1, p. 3801, Jul. 30, 2020. DOI: 10.1038/s41467-020-17670-y

[19] D. Chowell and T. A. Chan, "The immunogenicity of cancer mutations and implications for T cell therapy", *Translational Cancer Research*, vol. 5, Suppl 4 Oct. 2016. DOI: 10.21037/tcr.2016.10.26

[20] M. Soltani, M. Abbaszadeh, H. Fouladseresht, M. J. M. Sullman, and N. Eskandari, "PD-L1 importance in malignancies comprehensive insights into the role of PD-L1 in malignancies: From molecular mechanisms to therapeutic opportunities", *Clinical and Experimental Medicine*, vol. 25, no. 1, p. 106, Apr. 3, 2025. DOI: 10.1007/s10238-025-01641-y

[21] L. Marcus et al., "FDA Approval Summary: Pembrolizumab for the Treatment of Tumor Mutational Burden–High Solid Tumors", *Clinical Cancer Research*, vol. 27, no. 17, pp. 4685–4689, Sep. 1, 2021. DOI: 10.1158/1078-0432.CCR-21-0327

[22] A. Gunturi and D. F. McDermott, "Nivolumab for the treatment of cancer", *Expert Opinion on Investigational Drugs*, vol. 24, no. 2, pp. 253–260, Feb. 1, 2015. DOI: 10.1517/13543784.2015.991819

[23] S. Gandini, D. Massi, and M. Mandalà, "PD-L1 expression in cancer patients receiving anti PD-1/PD-L1 antibodies: A systematic review and meta-analysis", *Critical Reviews in Oncology/Hematology*, vol. 100, pp. 88–98, Apr. 1, 2016. DOI: 10.1016/j.critrevonc.2016.02.001

[24] A. Marabelle et al., "Association of tumour mutational burden with outcomes in patients with advanced solid tumours treated with pembrolizumab: Prospective biomarker analysis of the multicohort, open-label, phase 2 KEYNOTE-158 study", *The Lancet Oncology*, vol. 21, no. 10, pp. 1353–1365, Oct. 1, 2020. DOI: 10.1016/S1470-2045(20)30445-9

[25] E. L. van Dijk, H. Auger, Y. Jaszczyszyn, and C. Thermes, "Ten years of next-generation sequencing technology", *Trends in Genetics*, vol. 30, no. 9, pp. 418–426, Sep. 1, 2014. DOI: 10.1016/j.tig.2014.07.001

[26] K. Polonis, J. H. Blommel, A. E. O. Hughes, D. Spencer, J. A. Thompson, and M. C. Schroeder, "Innovations in Short-Read Sequencing Technologies and Their Applications to Clinical Genomics", *Clinical Chemistry*, vol. 71, no. 1, pp. 97–108, Jan. 1, 2025. DOI: 10.1093/clinchem/hvae173

[27] S. B. Ng et al., "Targeted capture and massively parallel sequencing of 12 human exomes", *Nature*, vol. 461, no. 7261, pp. 272–276, Sep. 2009. DOI: 10.1038/nature08250

[28] A. Mortazavi, B. A. Williams, K. McCue, L. Schaeffer, and B. Wold, "Mapping and quantifying mammalian transcriptomes by RNA-Seq", *Nature Methods*, vol. 5, no. 7, pp. 621–628, Jul. 2008. DOI: 10.1038/nmeth.1226

[29] A. Isaic et al., "Next-Generation Sequencing: A Review of Its Transformative Impact on Cancer Diagnosis, Treatment, and Resistance Management", *Diagnostics*, vol. 15, no. 19, p. 2425, Jan. 2025. DOI: 10.3390/diagnostics15192425

[30] R. K. Patel and M. Jain, "NGS QC Toolkit: A Toolkit for Quality Control of Next Generation Sequencing Data", *PLOS ONE*, vol. 7, no. 2, e30619, Feb. 1, 2012. DOI: 10.1371/journal.pone.0030619

[31] H. Li and R. Durbin, "Fast and accurate short read alignment with Burrows–Wheeler transform", *Bioinformatics*, vol. 25, no. 14, pp. 1754–1760, Jul. 15, 2009. DOI: 10.1093/bioinformatics/btp324

[32] A. Dobin et al., "STAR: Ultrafast universal RNA-seq aligner", *Bioinformatics*, vol. 29, no. 1, pp. 15–21, Jan. 1, 2013. DOI: 10.1093/bioinformatics/bts635

[33] E. Garrison and G. Marth. "Haplotype-based variant detection from short-read sequencing". arXiv: 1207.3907 [q-bio], Accessed: Feb. 4, 2026. [Online]. Available: http://arxiv.org/abs/1207.3907 pre-published.

[34] S. Kim et al., "Strelka2: Fast and accurate calling of germline and somatic variants", *Nature Methods*, vol. 15, no. 8, pp. 591–594, Aug. 2018. DOI: 10.1038/s41592-018-0051-x

[35] A. Conesa et al., "A survey of best practices for RNA-seq data analysis", *Genome Biology*, vol. 17, no. 1, p. 13, Jan. 26, 2016. DOI: 10.1186/s13059-016-0881-8

[36] W. McLaren et al., "The Ensembl Variant Effect Predictor", *Genome Biology*, vol. 17, no. 1, p. 122, Jun. 6, 2016. DOI: 10.1186/s13059-016-0974-4

[37] J. G. Tate et al., "COSMIC: The Catalogue Of Somatic Mutations In Cancer", *Nucleic Acids Research*, vol. 47, no. D1, pp. D941–D947, Jan. 8, 2019. DOI: 10.1093/nar/gky1015

[38] T. I. Zack et al., "Pan-cancer patterns of somatic copy number alteration", *Nature Genetics*, vol. 45, no. 10, pp. 1134–1140, Oct. 2013. DOI: 10.1038/ng.2760

[39] A. M. Newman et al., "Robust enumeration of cell subsets from tissue expression profiles", *Nature Methods*, vol. 12, no. 5, pp. 453–457, May 2015. DOI: 10.1038/nmeth.3337

[40] L. Song, D. Cohen, Z. Ouyang, Y. Cao, X. Hu, and X. S. Liu, "TRUST4: Immune repertoire reconstruction from bulk and single-cell RNA-seq data", *Nature Methods*, vol. 18, no. 6, pp. 627–630, Jun. 2021. DOI: 10.1038/s41592-021-01142-2

[41] K. Yoshihara et al., "The landscape and therapeutic relevance of cancer-associated transcript fusions", *Oncogene*, vol. 34, no. 37, pp. 4845–4854, Sep. 2015. DOI: 10.1038/onc.2014.406

[42] S. Uhrig et al., "Accurate and efficient detection of gene fusions from RNA sequencing data", *Genome Research*, vol. 31, no. 3, pp. 448–460, Jan. 3, 2021. DOI: 10.1101/gr.257246.119

[43] H. Chen et al., "A unified DNA- and RNA-based NGS strategy for the analysis of multiple types of variants at the dual nucleic acid level in solid tumors", *Journal of Clinical Laboratory Analysis*, vol. 37, no. 19–20, e24977, 2023. DOI: 10.1002/jcla.24977

[44] M. Menzel et al., "Benchmarking whole exome sequencing in the German network for personalized medicine", *European Journal of Cancer*, vol. 211, p. 114 306, Nov. 1, 2024. DOI: 10.1016/j.ejca.2024.114306

[45] M. Langouo Fontsa, F. Padonou, and K. Willard-Gallo, "Biomarkers and immunotherapy: Where are we?", *Current Opinion in Oncology*, vol. 34, no. 5, p. 579, Sep. 2022. DOI: 10.1097/CCO.0000000000000891

[46] M. Catalano, L. F. Iannone, G. Nesi, S. Nobili, E. Mini, and G. Roviello, "Immunotherapy-related biomarkers: Confirmations and uncertainties", *Critical Reviews in Oncology / Hematology*, vol. 192, p. 104 135, Dec. 1, 2023. DOI: 10.1016/j.critrevonc.2023.104135

[47] C. H. Cheng and S.-s. Shi, "Artificial intelligence in cancer: Applications, challenges, and future perspectives", *Molecular Cancer*, vol. 24, no. 1, p. 274, Oct. 30, 2025. DOI: 10.1186/s12943-025-02450-3

[48] S.-K. Yoo et al., "Prediction of checkpoint inhibitor immunotherapy efficacy for cancer using routine blood tests and clinical data", *Nature Medicine*, vol. 31, no. 3, pp. 869–880, Mar. 2025. DOI: 10.1038/s41591-024-03398-5

[49] S. Benzekry et al., "Machine Learning for Prediction of Immunotherapy Efficacy in Non-Small Cell Lung Cancer from Simple Clinical and Biological Data", *Cancers*, vol. 13, no. 24, p. 6210, Jan. 2021. DOI: 10.3390/cancers13246210

[50] P. Johannet et al., "Using Machine Learning Algorithms to Predict Immunotherapy Response in Patients with Advanced Melanoma", *Clinical Cancer Research*, vol. 27, no. 1, pp. 131–140, Jan. 4, 2021. DOI: 10.1158/1078-0432.CCR-20-2415

[51] V. Seebacher et al., "The value of serum albumin as a novel independent marker for prognosis in patients with endometrial cancer", *European Journal of Obstetrics & Gynecology and Reproductive Biology*, vol. 171, no. 1, pp. 101–106, Nov. 1, 2013. DOI: 10.1016/j.ejogrb.2013.07.044

[52] K. Sehgal et al., "Association of Performance Status With Survival in Patients With Advanced Non–Small Cell Lung Cancer Treated With Pembrolizumab Monotherapy", *JAMA Network Open*, vol. 4, no. 2, e2037120, Feb. 11, 2021. DOI: 10.1001/jamanetworkopen.2020.37120

[53] E. Bigelow et al., "A Random Forest Genomic Classifier for Tumor Agnostic Prediction of Response to Anti-PD1 Immunotherapy", *Cancer Informatics*, vol. 21, Jan. 1, 2022. DOI: 10.1177/11769351221136081

[54] A. Schina, Z. Sztupinszki, I. M. Svane, Z. Szallasi, G. Jönsson, and M. Donia, "Intratumoral T-cell and B-cell receptor architecture associates with distinct immune tumor microenvironment features and clinical outcomes of anti-PD-1/L1 immunotherapy", *Journal for ImmunoTherapy of Cancer*, vol. 11, no. 8, Aug. 21, 2023. DOI: 10.1136/jitc-2023-006941

[55] K. Litchfield et al., "Meta-analysis of tumor- and T cell-intrinsic mechanisms of sensitization to checkpoint inhibition", *Cell*, vol. 184, no. 3, 596–614.e14, Feb. 4, 2021. DOI: 10.1016/j.cell.2021.01.002

[56] D. M. A. S. Elkahwagy, C. J. Kiriacos, and M. Mansour, "Logistic regression and other statistical tools in diagnostic biomarker studies", *Clinical and Translational Oncology*, vol. 26, no. 9, pp. 2172–2180, Sep. 1, 2024. DOI: 10.1007/s12094-024-03413-8

[57] L. Breiman, "Random Forests", *Machine Learning*, vol. 45, no. 1, pp. 5–32, Oct. 1, 2001. DOI: 10.1023/A:1010933404324

[58] C. Cortes and V. Vapnik, "Support-vector networks", *Machine Learning*, vol. 20, no. 3, pp. 273–297, Sep. 1, 1995. DOI: 10.1007/BF00994018

[59] T. Chen and C. Guestrin, "XGBoost: A Scalable Tree Boosting System", in *Proceedings of the 22nd ACM SIGKDD International Conference on Knowledge Discovery and Data Mining*, ser. KDD '16, New York, NY, USA: Association for Computing Machinery, Aug. 13, 2016, pp. 785–794. DOI: 10.1145/2939672.2939785

[60] S. W. Choi, T. S.-H. Mak, and P. F. O'Reilly, "Tutorial: A guide to performing polygenic risk score analyses", *Nature Protocols*, vol. 15, no. 9, pp. 2759–2772, Sep. 2020. DOI: 10.1038/s41596-020-0353-1

[61] P. S. Kamath and R. W. Kim, "The model for end-stage liver disease (MELD)", *Hepatology*, vol. 45, no. 3, p. 797, Mar. 2007. DOI: 10.1002/hep.21563

[62] D. Feldner-Busztin et al., "Dealing with dimensionality: The application of machine learning to multi-omics data", *Bioinformatics*, vol. 39, no. 2, btad021, Feb. 1, 2023. DOI: 10.1093/bioinformatics/btad021

[63] L. Pestarino et al., "Recommendations for Validating Omics Prediction Models: Insights from a Lung Cancer RNA Biomarker Study", *Cancer Epidemiology, Biomarkers & Prevention*, vol. 34, no. 10, pp. 1852–1860, Oct. 3, 2025. DOI: 10.1158/1055-9965.EPI-25-0787

[64] A. Morabito, G. De Simone, R. Pastorelli, L. Brunelli, and M. Ferrario, "Algorithms and tools for data-driven omics integration to achieve multilayer biological insights: A narrative review", *Journal of Translational Medicine*, vol. 23, no. 1, p. 425, Apr. 10, 2025. DOI: 10.1186/s12967-025-06446-x

[65] T. Łukaszuk, J. Krawczuk, K. Żyła, and J. Kęsik, "Stability of Feature Selection in Multi-Omics Data Analysis", *Applied Sciences*, vol. 14, no. 23, p. 11 103, Jan. 2024. DOI: 10.3390/app142311103

[66] J. L. Sztepanacz and D. Houle, "Regularized regression can improve estimates of multivariate selection in the face of multicollinearity and limited data", *Evolution Letters*, vol. 8, no. 3, pp. 361–373, Jun. 1, 2024. DOI: 10.1093/evlett/qrad064

[67] B. B. Misra, C. Langefeld, M. Olivier, and L. A. Cox, "Integrated omics: Tools, advances and future approaches", *Journal of Molecular Endocrinology*, vol. 62, no. 1, R21–R45, Jan. 1, 2019. DOI: 10.1530/JME-18-0055

[68] T. Hastie, R. Tibshirani, and J. Friedman, *The Elements of Statistical Learning* (Springer Series in Statistics). New York, NY: Springer, 2009. DOI: 10.1007/978-0-387-84858-7

[69] R. Argelaguet et al., "Multi-Omics Factor Analysis—a framework for unsupervised integration of multi-omics data sets", *Molecular Systems Biology*, vol. 14, no. 6, MSB178124, Jun. 20, 2018. DOI: 10.15252/msb.20178124

[70] J. T. Leek et al., "Tackling the widespread and critical impact of batch effects in high-throughput data", *Nature Reviews Genetics*, vol. 11, no. 10, pp. 733–739, Oct. 2010. DOI: 10.1038/nrg2825

[71] C. S. R. Chilamakuri et al., "Performance comparison of four exome capture systems for deep sequencing", *BMC Genomics*, vol. 15, no. 1, p. 449, Jun. 9, 2014. DOI: 10.1186/1471-2164-15-449

[72] K. Haresamudram, S. Larsson, and F. Heintz, "Three Levels of AI Transparency", *Computer*, vol. 56, no. 2, pp. 93–100, Feb. 2023. DOI: 10.1109/MC.2022.3213181

[73] C. Rudin, "Stop explaining black box machine learning models for high stakes decisions and use interpretable models instead", *Nature Machine Intelligence*, vol. 1, no. 5, pp. 206–215, May 2019. DOI: 10.1038/s42256-019-0048-x

[74] S.-C. Lu, C. L. Swisher, C. Chung, D. Jaffray, and C. Sidey-Gibbons, "On the importance of interpretable machine learning predictions to inform clinical decision making in oncology", *Frontiers in Oncology*, vol. 13, Feb. 28, 2023. DOI: 10.3389/fonc.2023.1129380

[75] P. Missios, J. Beha, M. Bitzer, and N. P. Malek, "The molecular tumor board", *Der Onkologe*, vol. 26, no. 8, pp. 679–684, Aug. 1, 2020. DOI: 10.1007/s00761-020-00775-w

[76] R. Tibshirani, "Regression Shrinkage and Selection Via the Lasso", *Journal of the Royal Statistical Society: Series B (Methodological)*, vol. 58, no. 1, pp. 267–288, Jan. 1, 1996. DOI: 10.1111/j.2517-6161.1996.tb02080.x

[77] A. Altmann, L. Toloşi, O. Sander, and T. Lengauer, "Permutation importance: A corrected feature importance measure", *Bioinformatics*, vol. 26, no. 10, pp. 1340–1347, May 15, 2010. DOI: 10.1093/bioinformatics/btq134

[78] S. M. Lundberg and S.-I. Lee, "A Unified Approach to Interpreting Model Predictions", in *Advances in Neural Information Processing Systems*, vol. 30, Curran Associates, Inc., 2017.

[79] C. Tofallis. "Objective Weights for Scoring: The Automatic Democratic Method". Social Science Research Network: 4465402, Accessed: Nov. 6, 2025. [Online]. Available: https://papers.ssrn.com/abstract=4465402 pre-published.

[80] E. L. Kaplan and P. Meier, "Nonparametric Estimation from Incomplete Observations", *Journal of the American Statistical Association*, vol. 53, no. 282, pp. 457–481, Jun. 1, 1958. DOI: 10.1080/01621459.1958.10501452

[81] M. I. Love, W. Huber, and S. Anders, "Moderated estimation of fold change and dispersion for RNA-seq data with DESeq2", *Genome Biology*, vol. 15, no. 12, p. 550, Dec. 5, 2014. DOI: 10.1186/s13059-014-0550-8

[82] M. D. Mailman et al., "The NCBI dbGaP database of genotypes and phenotypes", *Nature Genetics*, vol. 39, no. 10, pp. 1181–1186, Oct. 2007. DOI: 10.1038/ng1007-1181

[83] R. Leinonen, H. Sugawara, M. Shumway, and on behalf of the International Nucleotide Sequence Database Collaboration, "The Sequence Read Archive", *Nucleic Acids Research*, vol. 39, pp. D19–D21, suppl_1 Jan. 1, 2011. DOI: 10.1093/nar/gkq1019

[84] E. A. Eisenhauer et al., "New response evaluation criteria in solid tumours: Revised RECIST guideline (version 1.1)", *European Journal of Cancer*, vol. 45, no. 2, pp. 228–247, Jan. 1, 2009. DOI: 10.1016/j.ejca.2008.10.026

[85] I. M. Noringriis et al., "Long-term clinical outcome of patients with metastatic melanoma and initial stable disease during anti-PD-1 checkpoint inhibitor immunotherapy with pembrolizumab", *British Journal of Cancer*, vol. 133, no. 3, pp. 337–345, Aug. 2025. DOI: 10.1038/s41416-025-03048-8

[86] M. T. Ribeiro, S. Singh, and C. Guestrin, ""Why Should I Trust You?": Explaining the Predictions of Any Classifier", in *Proceedings of the 22nd ACM SIGKDD International Conference on Knowledge Discovery and Data Mining*, San Francisco California USA: ACM, Aug. 13, 2016, pp. 1135–1144. DOI: 10.1145/2939672.2939778

[87] A. Subramanian et al., "Gene set enrichment analysis: A knowledge-based approach for interpreting genome-wide expression profiles", *Proceedings of the National Academy of Sciences*, vol. 102, no. 43, pp. 15 545–15 550, Oct. 25, 2005. DOI: 10.1073/pnas.0506580102

[88] A. Gschwind and S. Ossowski, "AI Model for Predicting Anti-PD1 Response in Melanoma Using Multi-Omics Biomarkers", *Cancers*, vol. 17, no. 5, p. 714, Feb. 20, 2025. DOI: 10.3390/cancers17050714

[89] A. Gschwind et al., "Multi-Omics Tumor Immunogenicity Score Predicts Immunotherapy Outcome and Survival", *Biology*, vol. 14, no. 12, p. 1698, Dec. 2025. DOI: 10.3390/biology14121698

[90] A. K. Sommer et al., "Mutational Landscape of Colorectal Tumors From Individuals With Unexplained Adenomatous or Serrated Colorectal Polyposis", *Gastroenterology*, Jan. 12, 2026. DOI: 10.1053/j.gastro.2025.10.011

[91] J. Forschner et al., "Adjuvant anti-PD-1 therapy improves melanoma-specific survival in stage IIIC-IV melanoma patients with high tumor mutation burden and BRAF V600 mutation", *Frontiers in Oncology*, vol. 15, Aug. 12, 2025. DOI: 10.3389/fonc.2025.1618596

[92] G. M. H. Abdel-Salam et al., "Biallelic *MAD2L1BP* ($p31^{comet}$) mutation is associated with mosaic aneuploidy and juvenile granulosa cell tumors", *JCI Insight*, vol. 8, no. 22, Nov. 22, 2023. DOI: 10.1172/jci.insight.170079

[93] A. Liebmann et al., "UV-radiation and *MC1R* germline mutations are risk factors for the development of conventional and spitzoid melanomas in children and adolescents", *eBioMedicine*, vol. 96, Oct. 1, 2023. DOI: 10.1016/j.ebiom.2023.104797

[94] M. Menzel et al., "Multicentric pilot study to standardize clinical whole exome sequencing (WES) for cancer patients", *npj Precision Oncology*, vol. 7, no. 1, p. 106, Oct. 20, 2023. DOI: 10.1038/s41698-023-00457-x

[95] S. Mittelstadt et al., "Detection of circulating cell-free HPV DNA of 13 HPV types for patients with cervical cancer as potential biomarker to monitor therapy response and to detect relapse", *British Journal of Cancer*, vol. 128, no. 11, pp. 2097–2103, Jun. 2023. DOI: 10.1038/s41416-023-02233-x

[96] J. Eckardt et al., "TMB and BRAF mutation status are independent predictive factors in high-risk melanoma patients with adjuvant anti-PD-1 therapy", *Journal of Cancer Research and Clinical Oncology*, vol. 149, no. 2, pp. 833–840, Feb. 1, 2023. DOI: 10.1007/s00432-022-03939-w

[97] M. Renovanz et al., "Clinical outcome of biomarker-guided therapies in adult patients with tumors of the nervous system", *Neuro-Oncology Advances*, vol. 5, no. 1, vdad012, Jan. 1, 2023. DOI: 10.1093/noajnl/vdad012

[98] C. Roggia et al., "Germline findings in patients with advanced malignancies screened with paired blood–tumour testing for personalised treatment approaches", *European Journal of Cancer*, vol. 179, pp. 48–55, Jan. 1, 2023. DOI: 10.1016/j.ejca.2022.11.003

[99] F. J. Hilke et al., "Distinct Mutation Patterns Reveal Melanoma Subtypes and Influence Immunotherapy Response in Advanced Melanoma Patients", *Cancers*, vol. 12, no. 9, p. 2359, Sep. 2020. DOI: 10.3390/cancers12092359

[100] A. Forschner et al., "MDM2, MDM4 and EGFR Amplifications and Hyperprogression in Metastatic Acral and Mucosal Melanoma", *Cancers*, vol. 12, no. 3, p. 540, Mar. 2020. DOI: 10.3390/cancers12030540

[101] D. Boceck et al. "aiDIVA – Diagnostics of Rare Genetic Diseases Using Large Language Models", Accessed: Dec. 15, 2025. [Online]. Available: https://www.medrxiv.org/content/10.1101/2025.09.04.25335099v1 pre-published.

[102] A. Gschwind, M. Klopotek, Y. Ai, and M. Oettel, "Isotropic-nematic transition for hard rods on a three-dimensional cubic lattice", *Physical Review E*, vol. 96, no. 1, p. 012 104, Jul. 5, 2017. DOI: 10.1103/PhysRevE.96.012104

[103] M. Hassanzad and K. Hajian-Tilaki, "Methods of determining optimal cut-point of diagnostic biomarkers with application of clinical data in ROC analysis: An update review", *BMC Medical Research Methodology*, vol. 24, no. 1, p. 84, Apr. 8, 2024. DOI: 10.1186/s12874-024-02198-2

[104] A. P. Bradley, "The use of the area under the ROC curve in the evaluation of machine learning algorithms", *Pattern Recognition*, vol. 30, no. 7, pp. 1145–1159, Jul. 1, 1997. DOI: 10.1016/S0031-3203(96)00142-2

[105] Z. C. Lipton, "The mythos of model interpretability", *Commun. ACM*, vol. 61, no. 10, pp. 36–43, Sep. 26, 2018. DOI: 10.1145/3233231

[106] L. V. M. Leek et al., "Multi-omic analysis identifies hypoalbuminemia as independent biomarker of poor outcome upon PD-1 blockade in metastatic melanoma", *Scientific Reports*, vol. 14, p. 11 244, May 16, 2024. DOI: 10.1038/s41598-024-61150-y

[107] N. Lamba, P. A. Ott, and J. B. Iorgulescu, "Use of First-Line Immune Checkpoint Inhibitors and Association With Overall Survival Among Patients With Metastatic Melanoma in the Anti–PD-1 Era", *JAMA Network Open*, vol. 5, no. 8, e2225459–e2225459, Aug. 25, 2022. DOI: 10.1001/jamanetworkopen.2022.25459

[108] Y. Yu, Y. Mai, Y. Zheng, and L. Shi, "Assessing and mitigating batch effects in large-scale omics studies", *Genome Biology*, vol. 25, no. 1, p. 254, Oct. 3, 2024. DOI: 10.1186/s13059-024-03401-9

[109] K. Talari and M. Goyal, "Retrospective Studies – Utility and Caveats", *Journal of the Royal College of Physicians of Edinburgh*, vol. 50, no. 4, pp. 398–402, Dec. 1, 2020. DOI: 10.4997/jrcpe.2020.409

[110] M. Łuksza et al., "A neoantigen fitness model predicts tumour response to checkpoint blockade immunotherapy", *Nature*, vol. 551, no. 7681, pp. 517–520, Nov. 2017. DOI: 10.1038/nature24473

Appendix A

AI Model for Predicting Anti-PD1 Response in Melanoma Using Multi-Omics Biomarkers

This manuscript was submitted to MDPI *Cancers* on January 11, 2025, and was accepted for publication on February 18, 2025. The study investigated three machine learning models using NGS-derived genomics, transcriptomics, and multi-omics biomarkers to predict the outcomes of ICI treatment in melanoma. All models outperformed the current gold-standard TMB, with the multi-omics model achieving the best performance. In-depth analyses of SHAP values revealed post-hoc explanations for the model predictions. This publication was selected as the cover story of the March 2025 issue of MDPI *Cancers*.

A.1 Author Contributions

In this study, the candidate performed all the necessary scientific work independently under the supervision of Prof. Dr. Stephan Ossowski. In detail, the candidate

- Designed the study,
- Wrote a study protocol and applied for approval of the study by the local institutional review board,
- Acquired data from public and access-restricted datasets via the dbGaP[82],
- Wrote research use statements and obtained all necessary permits to access dbGaP datasets,
- Processed the raw sequencing data using various bioinformatics tools and extracted all biomarkers used in the project,
- Wrote the code of the LASSO regression models and analyzed their predictions,
- Wrote the paper,

- Created all the figures,
- Submitted the manuscript to the peer-reviewed journal MDPI *Cancers*,
- Organized the editing of the manuscript during the peer review process, and
- Designed the cover page for the March 2025 issue of MDPI *Cancers*.

A.2 Cover Page

cancers

Impact Factor 4.5
CiteScore 8.0
Indexed in PubMed

ISSN 2072-6694

AI Model Predicts Anti-PD1 Response in Melanoma Using Multi-Omics Biomarkers

Volume 17 · Issue 5 March-1 2025

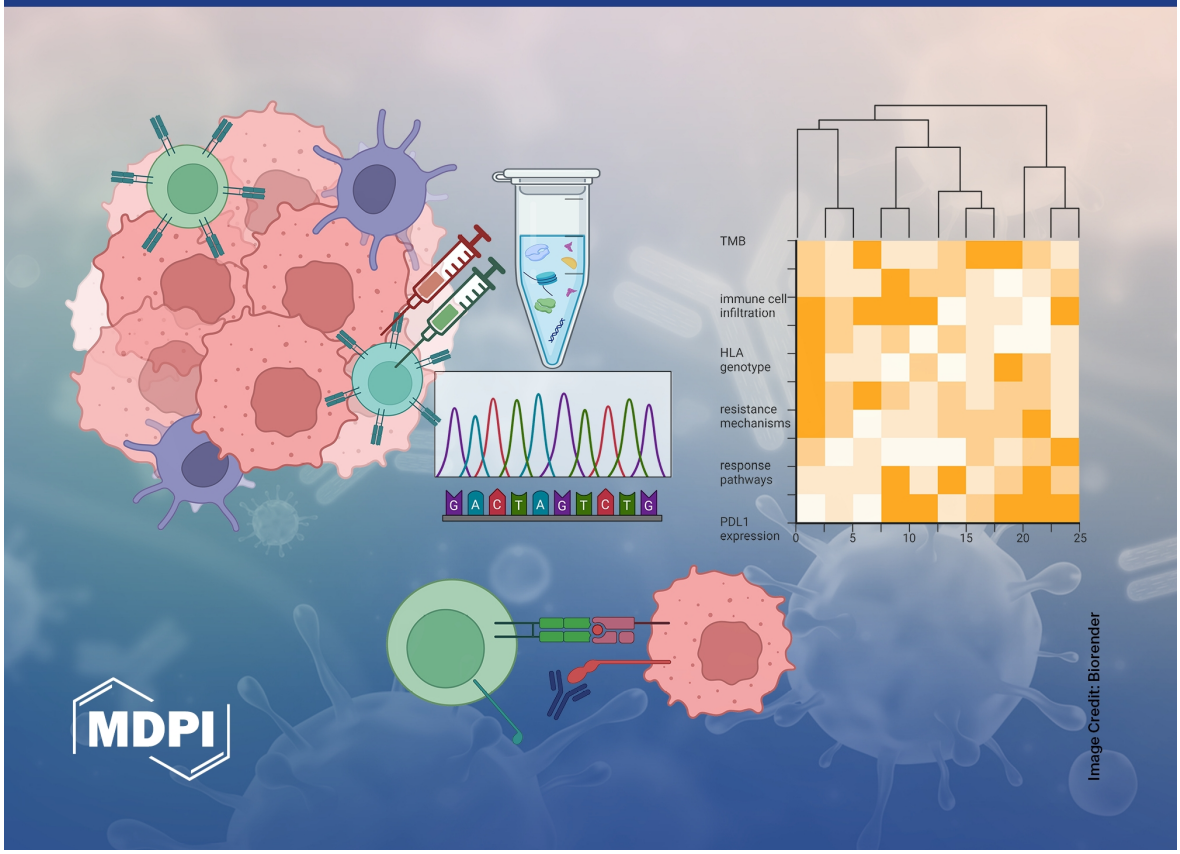

A.3 Main Paper

cancers

MDPI

Article

AI Model for Predicting Anti-PD1 Response in Melanoma Using Multi-Omics Biomarkers

Axel Gschwind [1,2] and Stephan Ossowski [1,2,*]

[1] Institute of Medical Genetics and Applied Genomics, University of Tübingen, 72076 Tübingen, Germany; axel.gschwind@med.uni-tuebingen.de
[2] Institute for Bioinformatics and Medical Informatics, University of Tübingen, 72076 Tübingen, Germany
* Correspondence: stephan.ossowski@med.uni-tuebingen.de

Simple Summary: Many patients with skin cancer are treated with immune checkpoint inhibitors. The treatment can trigger an immune response that attacks cancer cells. This is achieved by inhibiting immune checkpoints, which act as an "off-switch" of the immune system. To date, medical doctors have selected patients with a high number of DNA mutations for this kind of therapy, a biomarker called tumor mutation burden (TMB). Still, only a minority of patients benefit from the treatment, even if they are selected based on high TMB. In our study, we first collected a large cohort of patients with melanoma treated with immune checkpoint inhibitors. We then derived additional tumor biomarkers from the sequencing data of the patients. We combined these new biomarkers into an artificial intelligence model to better predict whether a patient will respond to the therapy. Our results showed that combining multiple biomarkers can improve the treatment selection for patients with melanoma by providing more accurate outcome predictions.

Abstract: Background: Immune checkpoint inhibitors (ICIs) have demonstrated significantly improved clinical efficacy in a minority of patients with advanced melanoma, whereas non-responders potentially suffer from severe side effects and delays in other treatment options. Predicting the response to anti-PD1 treatment in melanoma remains a challenge because the current FDA-approved gold standard, the nonsynonymous tumor mutation burden (nsTMB), offers limited accuracy. Methods: In this study, we developed a multi-omics-based machine learning model that integrates genomic and transcriptomic biomarkers to predict the response to anti-PD1 treatment in patients with advanced melanoma. We employed least absolute shrinkage and selection operator (LASSO) regression with 49 biomarkers extracted from tumor–normal whole-exome and RNA sequencing as input features. The performance of the multi-omics AI model was thoroughly compared to that of nsTMB alone and to models that use only genomic or transcriptomic biomarkers. Results: We used publicly available DNA and RNA-seq datasets of melanoma patients for the training and validation of our model, forming a meta-cohort of 449 patients for which the outcome was recorded as a RECIST score. The model substantially improved the prediction of anti-PD1 outcomes compared to nsTMB alone, with an ROC AUC of 0.7 in the training set and an ROC AUC of 0.64 in the test set. Using SHAP values, we demonstrated the explainability of the model's predictions on a per-sample basis. Conclusions: We demonstrated that models using only RNA-seq or multi-omics biomarkers outperformed nsTMB in predicting the response of melanoma patients to ICI. Furthermore, our machine learning approach improves clinical usability by providing explanations of its predictions on a per-patient basis. Our findings underscore the utility of multi-omics data for selecting patients for treatment with anti-PD1 drugs. However, to train clinical-grade AI models for routine applications, prospective studies collecting larger melanoma cohorts with consistent application of exome and RNA sequencing are required.

check for updates

Academic Editor: David Wong

Received: 11 January 2025
Revised: 10 February 2025
Accepted: 18 February 2025
Published: 20 February 2025

Citation: Gschwind, A.; Ossowski, S. AI Model for Predicting Anti-PD1 Response in Melanoma Using Multi-Omics Biomarkers. *Cancers* **2025**, *17*, 714. https://doi.org/10.3390/cancers17050714

Cancers **2025**, *17*, 714

Keywords: artificial intelligence; immune checkpoint inhibitors; anti-PD1; melanoma; genomics; transcriptomics; multi-omics; least absolute shrinkage and selection operator (LASSO); SHAP values; explainable machine learning

1. Introduction

Immune checkpoint inhibitors (ICIs) have revolutionized the therapy of solid cancers [1]. ICIs targeting the immune checkpoints cytotoxic T-lymphocyte associated protein (*CTLA4*) or programmed cell death protein 1/ligand 1 (*PD1*/*PDL1*) have become an integral part of modern cancer treatment. Anti-PD1 drugs like pembrolizumab or nivolumab have demonstrated clinical efficacy, leading to a substantial clinical benefit for a subset of patients with advanced melanoma [2,3].

Despite these efforts, the majority of patients selected for ICI treatment do not show any benefit from the therapy [4]. There is only one FDA-approved biomarker for the selection of patients for ICI in melanoma: the nonsynonymous tumor mutation burden (nsTMB). A higher nsTMB is associated with better anti-PD1 response rates, with a commonly applied threshold of 10 mutations per megabase [5]. However, nsTMB alone is insufficient to predict therapeutic outcomes accurately. For instance, objective responses to pembrolizumab were observed in only 29% of patients with high nsTMB compared to 6% of patients with low nsTMB in a recent study [6]. Moreover, patients undergoing anti-PD1 treatment could suffer from potentially life-threatening adverse events, highlighting the urgent need for more reliable prediction methods [7]. Many other non-approved genomic and transcriptomic biomarkers have been shown to correlate with ICI outcomes in various cancer types, suggesting a potential avenue for improved outcome prediction [8]. Most of these biomarkers can be derived from next-generation sequencing (NGS) data, particularly whole-exome sequencing (WES) and bulk RNA sequencing (RNA-seq) [9,10].

Given the complex tumor–immune system interactions, we hypothesized that a multi-omics approach might be a more accurate predictor of anti-PD1 response than single biomarkers. Thus, we developed a comprehensive approach that integrates both genomic and transcriptomic biomarkers as features of a multi-omics-based machine learning model.

Several recent studies have developed machine learning (ML) models to enhance the prediction of ICI outcomes. Most models relied on non-NGS features, such as routine clinical biomarkers, serum parameters, or histopathology, to predict ICI outcomes [11–13]. Other studies focused on integrating either genomic or transcriptomic biomarkers [14–16]. Lichtfield et al. [17] developed a multi-omics ML model trained with data from multiple cancer types ("pan-cancer analysis"), using various DNA- and RNA-derived biomarkers. To our knowledge, no multi-omics models specializing in specific cancer types are available yet. The aforementioned models leveraged various ML algorithms, such as random forests, multivariate logistic regression, XGBoost, or neural networks.

Although these developments have improved ICI outcome prediction, most models provide limited clinical explainability of their predictions. To address these challenges, we developed a least absolute shrinkage and selection operator (LASSO) regression model [18] combined with SHAP analysis to enhance the accuracy of anti-PD1 outcome predictions in melanoma, to improve feature selection, and to provide explainable results for specific patients. We utilized WES to generate genomic biomarkers from paired tumor and normal tissues, and RNA-seq to generate transcriptomic biomarkers of the tumor tissue. In total, our LASSO approach initially incorporated 49 multi-omics biomarkers, covering various aspects of tumor biology, including the well-established nsTMB, neoantigens, resistance

Cancers **2025**, *17*, 714

mechanisms, tumor immune microenvironment (immune cell infiltration), germline factors, and additional relevant metrics.

We obtained publicly available datasets of anti-PD1-treated melanoma patients to assemble a meta-cohort combining WES and RNA-seq, which we used to train and test the machine learning model. We classified patients as therapy responders or non-responders according to the well-established Response Evaluation Criteria In Solid Tumors (RECIST) [19]. This binary classification facilitated the comparison of therapeutic outcomes between different studies.

Finally, we thoroughly evaluated our model using several performance metrics to compare our LASSO approach with the current gold standard nsTMB. Our findings showed that the integrated multi-omics approach substantially improved ICI prediction by combining several biomarkers. Notably, a model based on transcriptomic (RNA-seq) biomarkers alone performed at least as good as or better than the genome-based nsTMB. A complementary analysis proved the general explainability of the AI predictions in a clinical context.

2. Materials and Methods

2.1. Patient Collective

We compiled a cohort from several previously published independent studies that investigated the response to anti-PD1 treatment in patients with metastatic melanoma of different stages. Raw sequencing data (paired tumor–normal WES and RNA-seq) were obtained from the Sequence Read Archive (SRA) and from the database of Genotypes and Phenotypes (dbGaP) after approval by the corresponding data access committees [20,21]. We included samples in our meta-cohort both from formalin-fixed paraffin-embedded (FFPE) and fresh frozen tissue. Normal samples are usually derived from peripheral blood. We discarded tumor-only DNA sequencing data and only used samples from pre-treatment biopsies. Patients were classified as responders or non-responders according to the RECIST criteria. Patients with progressive disease, stable disease, or mixed responses were classified as non-responders, whereas those with partial or complete responses were classified as responders.

After quality control, the cohort reached a total size of 449 WES patients, of which 192 were responders and 257 were non-responders. For the RNA-seq samples, we obtained a cohort size of 308, of which 134 were responders and 174 were non-responders. Intersecting WES and RNA-seq data were available for 246 patients, of whom 110 were responders and 136 were non-responders. Figure 1a provides a detailed overview of the cohort. Each sub-cohort is denoted by the name of the first author of its seminal publication: Amato, Cristescu, Gide, Hugo, Liu, Pyke, Riaz, and Wolchok [22–29].

AI models require a test dataset that contains data unseen by the model during training. Thus, we randomly split the data into training and test datasets, resulting in 46 samples in the test dataset. We randomly selected test samples for which both WES and RNA-seq data were available. The split was stratified according to overall response and nsTMB. The final training–test split is illustrated in Figure 1b.

2.2. Machine Learning Model

Here, we used LASSO regression to predict response to anti-PD1 therapy. LASSO performs both regularization and feature selection by setting unimportant features to exactly zero. An important criterion for choosing LASSO as our ML model is its ability to handle multicollinearity in the input features, which is crucial for biological data and specifically for multi-omics data with various dependencies [18]. In contrast, tree-based models, such as XGBoost or RFs, can struggle with highly correlated input features and require extensive hyperparameter tuning. Furthermore, feature selection and interpretability as well as clini-

Cancers **2025**, *17*, 714

cal explainability of the predictions were important criteria in this study. While methods such as XGBoost and RF do not eliminate coefficients of unimportant features [30] and SVMs do not provide feature selection at all, LASSO automatically selects a subset of the most predictive features, thereby improving interpretability. In combination with SHAP analysis (see below), LASSO therefore provided the best clinical explainability of results.

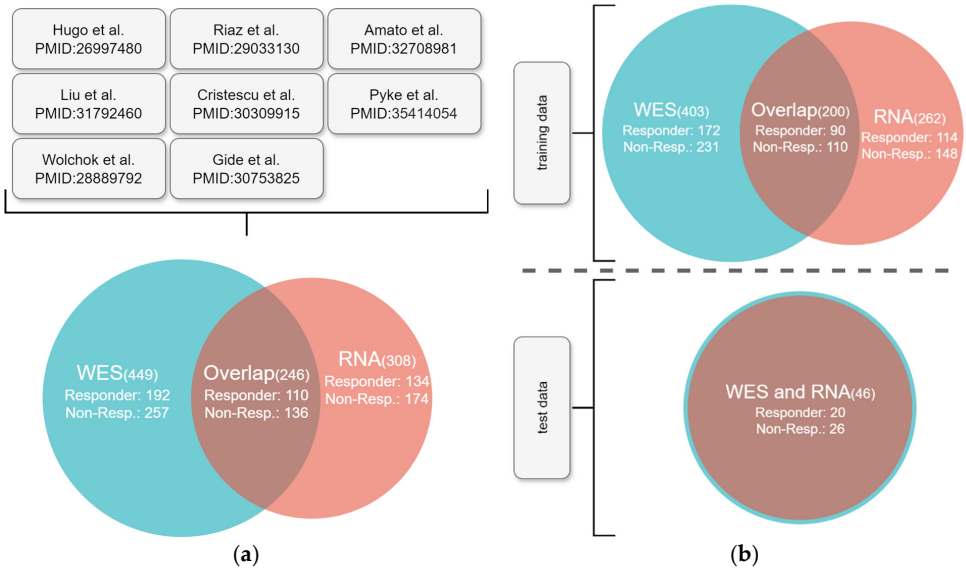

Figure 1. Overview of the overall cohort after quality control. The numbers in brackets denote the corresponding sample counts. (**a**) We integrated sequencing data from eight studies. We denote each study by the name of the first author of its publication [22–29]. RNA-seq data were not available for every WES, and vice versa; however, we achieved an overlap of 246 samples. (**b**) The cohort was randomly split into training and test datasets.

Figure 2 shows an outline of our model design. To exploit the entire training dataset, we created one LASSO model exclusively using DNA biomarkers and another using only RNA-seq features. The contribution of each biomarker was estimated using permutation feature importance [31]. Every feature from the DNA and the RNA model with non-zero coefficients and a feature importance of >0.0055 was then used as an input feature for a multi-omics LASSO model, leading to a total of 10 features for the multi-omics model. This model combined DNA and RNA features and was trained on the overlap of samples for which both DNA and RNA-seq data were available.

We used 40 biomarkers as features of the DNA model. The following WES-derived metrics, describing both somatic and germline properties as well as resistance mechanisms, were used:

- Somatic features: *BRAF*:V600E status, tumor purity, nsTMB, insertion and deletion (indel) burden, frameshift indel (fsIndel) burden, in-frame indel burden, splice burden, missense burden, synonymous burden, multiple amino acid burden, frameshift mutation proportion, nonsynonymous to synonymous substitution ratio (dN/dS ratio), copy number variant (CNV) burden, deletion burden, neoantigen burden, maximum neoantigen-binding affinity, mean differential agretopicity index (DAI), median DAI, maximum DAI, upper decile DAI, maximum recognition potential, maximum HEX alignment score, and maximum dissimilarity score.
- Germline features: mean HLA evolutionary divergence (HED), HLA-B27 supertype, HLA-B44 supertype, HLA-B62 supertype, homozygous HLA-B, and homozygous HLA-C.

Cancers **2025**, *17*, 714

- Mechanisms of ICI resistance (enriched in non-responders): alterations in *B2M*, alterations in *TP53*, alterations in *STK11*, alterations in *PTEN*, alterations in *KRAS*, alterations in *MDM2*, alterations in *MDM4*, and alterations in *EGFR*.
- Mechanisms of ICI response (enriched in responders) were sparse in the training dataset and merged into one biomarker: alterations in *JAK1*/*JAK2*, deletions at chr6p21.3 (this locus contains HLA class I-related genes), and alterations in *CTNNB1*.

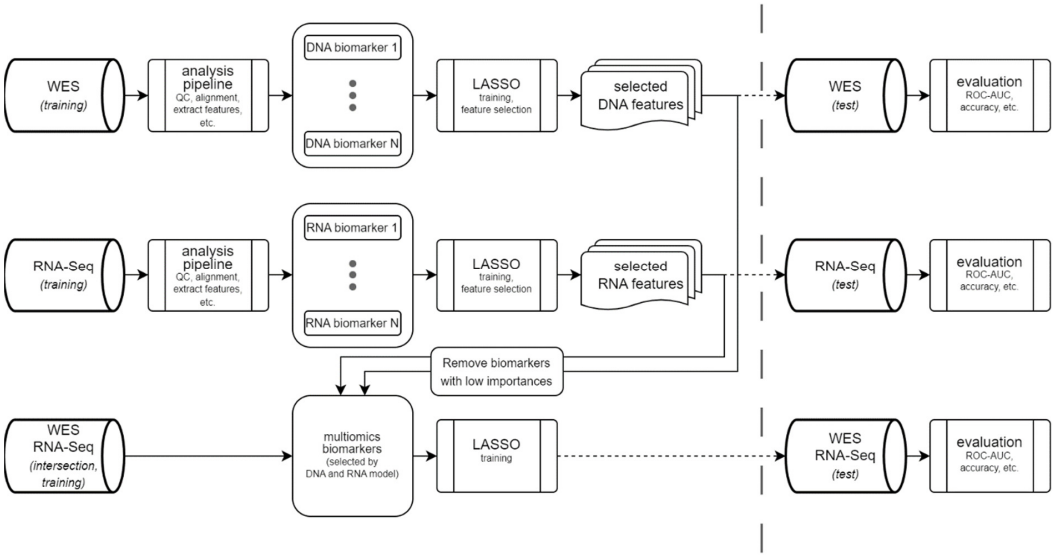

Figure 2. Flowchart of the AI models. First, we trained both the LASSO model using DNA data and the LASSO model using RNA data. The biomarkers selected that way were then used to train a multi-omics model using the overlap between all training samples for which both WES and RNA-seq data were available. We only used biomarkers with a permutation feature importance of >0.0055 for the multi-omics model, resulting in 10 features. All three models were then evaluated in the test set using different performance measures, such as ROC AUC.

The RNA-based ML model was trained using nine input features. We included lymphocyte infiltration, T cell receptor (TCR) α chain entropy, TCR β chain entropy, immunoglobulin heavy chain (IGHG) entropy, interferon-γ to immunosuppression (IFNG-IMS) ratio, in-frame fusion neoepitope count, gene expression profile (GEP) of HLA class I genes, GEP of *PDL1*, and GEP of *B2M*. The implementation details and a thorough discussion of every biomarker used as an input feature in both the DNA and RNA model are provided in Appendix A.

We used LASSO as implemented in LassoCV in the Python library scikit-learn 1.3.2 [32]. We performed z-transformation with StandardScaler and trained each model using five-fold cross-validation. Receiver operating characteristic (ROC) area under the curve (AUC) values were used as the main measures of the predictive power of the DNA, RNA, and multi-omics models. To further analyze model performance, we stratified the predicted probabilities into predicted responders and non-responders. We determined the threshold for these binary predictions by maximizing Youden's index for the training dataset, thereby ensuring an optimal trade-off between specificity and sensitivity [33]. Using this cutoff, we classified the model predictions as true positives (TP), true negatives (TN), false positives (FP), and false negatives (FN).

Cancers 2025, 17, 714

Machine learning models often suffer from a lack of explainability, which makes it difficult to determine the features that influence a specific prediction. Although we calculated permutation feature importance scores for our models, they are not meaningful on a per-sample basis, which is, however, crucial in clinical decision-making. Shapley Additive Explanations (SHAP) is an approach that addresses this issue and provides feature contributions for predictions on a per-sample basis [34]. Therefore, we applied SHAP to evaluate the explainability of the three models and thereby their clinical applicability. This helps clinicians comprehend the model's prediction based on the biomarkers on which the model relied the most for a given case.

2.3. Bioinformatics Pipeline

Basic Analysis Pipeline

We used the megSAP pipeline for the basic analysis of both WES and RNA-seq data. megSAP (commit 2023_04-8-g6e28b110) is publicly available on GitHub https://github.com/imgag/megSAP (accessed on 2 May 2023). Briefly, read alignment against GRCh38 was performed using BWA mem2 for the WES samples. Subsequently, Manta 1.6.0 and Strelka 2.9.10 were used to call somatic variants (structural variants (SVs), single nucleotide variants (SNVs), and small indels) [35]. CNVs were called using ClinCNV 1.18.3 [36]. All variants were annotated using VEP v109 and the COSMIC Cancer Mutation Census (CMC) v99 [37,38]. For the RNA-seq samples, the reads were aligned against GRCh38 using STAR 2.7.10b. The read counts were then quantified using subread featureCounts 2.0.4 and normalized to transcripts per million (TPM) by megSAP [39]. In-frame and frameshift gene fusions were identified using Arriba 2.4.0. HLA genotyping was performed on the germline WES and RNA-seq samples using our in-house Python3 implementation of hla-genotyper [40]. The results were visually inspected using the clinical decision support system GSvar (commit 2023_03-23-g5390f8b), available on GitHub https://github.com/imgag/ngs-bits (accessed on 18 April 2023).

2.4. Target Regions

We constructed intersecting target regions for all studies included in our cohort. In short, we determined the region covered by at least 20× for every normal sample. Based on this information, we included a base in the target region if it was covered in at least half of the samples. The final target region was then constructed by intersecting it with the exonic coordinates ±2 bases obtained from ensemble v109. These target regions were used to calculate the coverage files for the CNV calling by ClinCNV and for quality control. For any other biomarker that required a target region (e.g., TMB calculation), we used the intersection between the target regions of all sub-cohorts to avoid batch effects.

2.5. Quality Control

For paired tumor–normal WES, we discarded all samples that did not meet the minimum coverage requirements of 60× for the tumor sample and 20× for the normal sample. Samples were also excluded if known SNPs found in the tumor and the normal samples did not show a correlation of at least 0.8, indicating that both samples might have originated from different individuals, that is, sample confusion. Multiple sequenced samples from the same tumor were available for a few patients in some studies. In these cases, we excluded all samples except those with the highest SRA number.

On the level of somatic variants (SNVs and small indels), we excluded all variants that did not fulfill the following quality criteria: (i) depth in tumor and normal sample > 20×, (ii) tumor variant allele frequency (VAF) ≥ 5%, (iii) normal VAF < 0.17 × tumor VAF, and (iv) the variant was detected in at least three or more reads. Copy number variants were discarded if ClinCNV reported a log likelihood of <100.

Cancers **2025**, *17*, 714

Gene expression data derived from RNA-seq generated at different sequencing facilities are prone to batch effects. Hence, we conducted a principal component analysis (PCA) of gene expression (in TPM) for all genes and all samples. The results revealed batch effects between samples of different sub-cohorts, as indicated by sub-cohort-based clustering (Figure S1, left). Subsequently, we corrected these batch effects using pyComBat [41]. PCA after batch correction did not show any obvious batch effects (Figure S1, right).

3. Results

3.1. AI Model for Prediction of Anti-PD1 Response

We trained a machine learning model predicting therapy response using a meta-cohort of 449 cases from eight studies, for which response to anti-PD1 was available as a RECIST classification. Our cohort consists of a total of 449 WES samples and 308 RNA-seq samples. However, not every WES sample has a paired RNA-seq sample and vice versa. There are 203 cases with only whole-exome sequencing (WES), 62 cases with only RNA-seq data, and 246 cases with both data types available. Considering this heterogeneity in the OMICs data availability, we trained three models: (1) a DNA biomarker model, (2) an RNA biomarker model, and (3) a multi-omics model. To use the same sub-cohort to evaluate all three models, we only chose cases for the test set that had both WES and RNA-seq data available. This test set consisted of 20% of otherwise randomly selected cases and was not used for model training. An overview of the cohort and the split of the cohort into training and test sets is shown in Figure 1.

An overview of the training and testing procedures is shown in Figure 2. Briefly, 49 DNA- or RNA-based biomarkers (see the Materials and Methods section for a full list) were extracted from short-read NGS data using the NGS analysis platform megSAP (see the Materials and Methods section for details). Next, we trained the DNA model using all cases of the training set with available WES data and the RNA model using all cases of the training set with available RNA data using LASSO. For both models, we performed feature selection (Figure 3a,b) and trained a LASSO model for cases with both WES and RNA-seq data using only features with a feature importance of more than 0.0055 in one of the two single-data models (Figure 3c; see Section 2 for details on model training). Finally, we compared the performance of the three models on the training and the test set and compared them with the well-established nsTMB.

3.2. Feature Selection and Feature Importance

First, we trained the DNA and RNA LASSO models on their corresponding biomarkers and training set using five-fold cross-validation. We obtained moderate LASSO regularization parameters of 0.021 for the DNA model and 0.024 for the RNA model. These parameters indicate that both models discarded some less important features but retained important features. As expected, the coefficients (impact on the model) of several biomarkers shrunk to zero, such as the *BRAF* mutation status for the DNA model or mean HLA expression for the RNA model. Hence, we retained 13 features with non-zero coefficients for the DNA model and four non-zero coefficients for the RNA model. We then evaluated the feature permutation importance scores of the non-zero LASSO coefficients (Figure 3a,b). Every biomarker above the permutation feature importance threshold of 0.0055 was used as an input feature for the multi-omics model. This further reduced the feature count of the multi-omics model to seven DNA and three RNA features. The final multi-omics model incorporated the following 10 initial genomic and transcriptomic biomarkers: response pathway, nsTMB, HED, fsIndel burden, defects in *B2M*, HLA-B27 supertype, tumor purity, TCR α chain entropy, IFNG-IMS ratio, and IGH entropy. The multi-omic model had a small LASSO regularization parameter of 0.002 after five-fold cross-validation, indicating that

Cancers **2025**, *17*, 714

most of the features were retained. Indeed, the multi-omics model selected all the initial input features and resulted in ten non-zero (DNA and RNA) coefficients (Figure 3c).

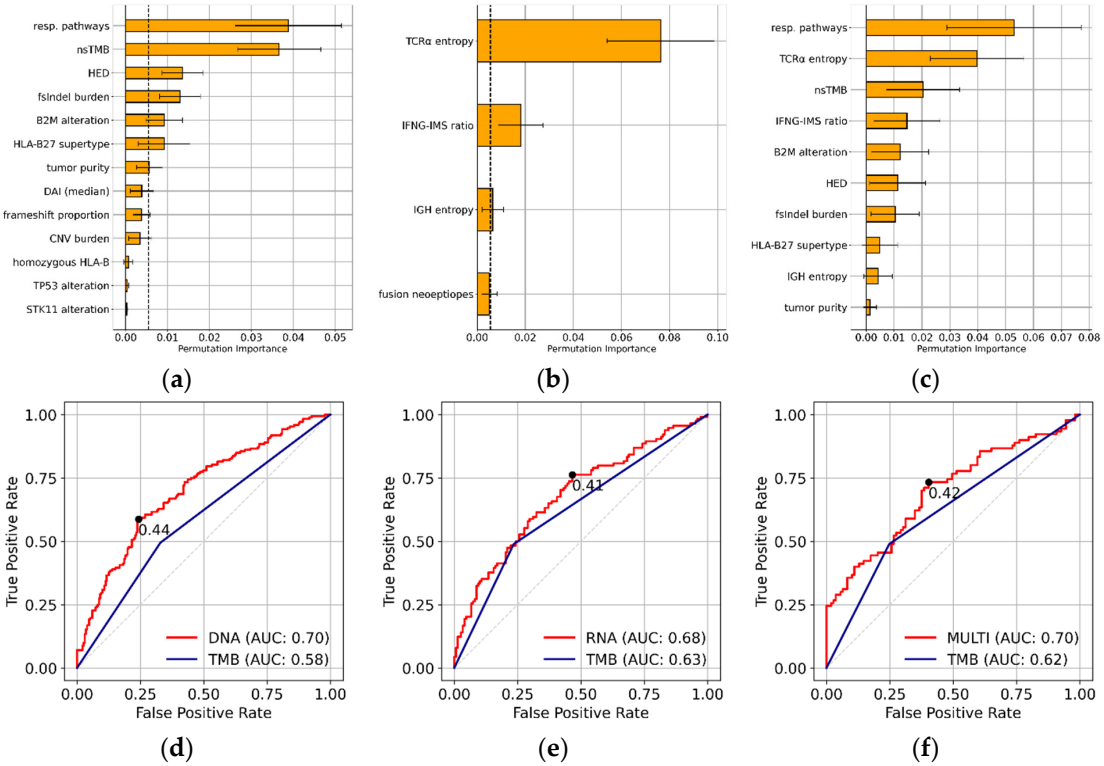

Figure 3. Feature permutation importance scores of the DNA model (**a**), the RNA model (**b**), and the multi-omics model (**c**). The dotted lines at 0.0055 indicate the cutoff used to include a feature in the multi-omics model. The error bars represent the standard deviation for each biomarker. (**d**–**f**) ROC curves for all three models. The red line represents the ROC curve for the LASSO model. The blue line represents the ROC curve for nsTMB using the FDA-approved threshold of 10 mutations per Mb. The black dots denote the optimal probability cutoffs.

3.3. Model Performance on Training and Test Set

Next, we calculated the ROC curves using the response probabilities of the models for the training set, with the actual response data (responders and non-responders) serving as the ground truth. All three models outperformed the gold-standard nsTMB in terms of ROC AUC (Figure 3d–f). The DNA model achieved an ROC AUC of 0.70 versus 0.58 (nsTMB), the RNA model an ROC AUC of 0.68 versus 0.63 (nsTMB), and the multi-omics model an ROC AUC of 0.70 versus 0.62 (nsTMB) on the training dataset. The ROC AUC for the nsTMB of the RNA model was calculated using only the subset of samples for which paired WES data were available. The distribution of the prediction probabilities varied across the three models (Figure S2), emphasizing the necessity of model-specific probability cutoff values. By maximizing Youden's index, we identified optimal probability thresholds of 0.44 for the DNA model, 0.41 for the RNA model, and 0.42 for the multi-omics model. Subsequently, these thresholds were used to classify the model predictions as TP, TN, FP, and FN. Next, we evaluated the DNA, RNA, and multi-omics models using the independent test set. Figure 4a–c show the performance of the models in the form of ROC curves. All three models outperformed nsTMB alone in terms of ROC AUCs: 0.63 versus 0.60 for the DNA

Cancers **2025**, *17*, 714

model, 0.62 versus 0.60 for the RNA model, and 0.64 versus 0.60 for the multi-omics model. These results imply that the model training did not overfit.

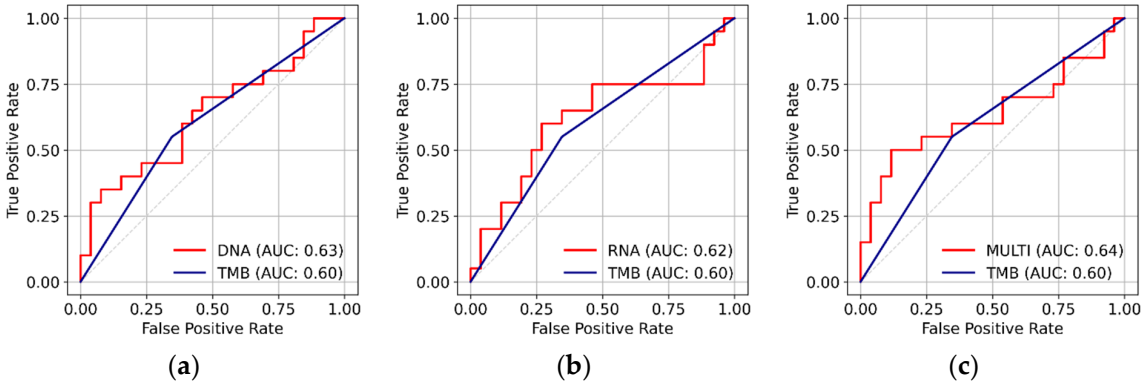

Figure 4. Model performance in the test set. (**a**–**c**) ROC curves of the DNA model (**a**), the RNA model (**b**), and the multi-omics model (**c**). None of the models exhibited overfitting. The ROC AUC of the LASSO models was higher than the ROC AUC of the nsTMB alone.

3.4. SHAP Values

Subsequently, we applied the SHAP methodology to the complete cohort analyzed using the multi-omics model to identify typical biomarkers contributing to the prediction of TP (correctly identified responders) and TN (correctly identified non-responders). SHAP values estimate the impact of each feature on the prediction on a per-sample basis. Figure 5a,b show summary plots ("bee swarm") of the SHAP values for the multi-omics model for true responders and true non-responders. Each dot represents the contribution of a biomarker to a specific model prediction. Positive SHAP values contribute to the prediction of responders, whereas negative SHAP values indicate a negative contribution to the prediction of non-responders. The dot color denotes the original input value of each feature; high input values are plotted in red, and low input values are plotted in blue. This allows us to determine the direction in which the features influence a prediction. For some of the biomarkers, we observed clear differences between the two groups. For instance, true non-responders had very low or zero TCR α chain entropy values that contributed to the prediction of TN. On the other hand, high TCR α chain entropy values contributed to the prediction of TP. To quantify such discriminative biomarkers between TP and TN, we calculated the differences in mean SHAP value for each feature (Figure 5c). We tested the significance of the differences using a two-sided Mann–Whitney U test with Bonferroni correction, resulting in seven statistically significant discriminative biomarkers between true responders and non-responders: TCR α chain entropy, response pathways, nsTMB, IFNG-IMG ratio, fsIndel burden, IGH entropy, and HED.

Figure 6 shows representative plots for two patients, a true responder and a true non-responder, highlighting the model's ability to explain its predictions on a per-sample basis. Both genomic and transcriptomic biomarkers have contributed to these predictions.

Cancers **2025**, *17*, 714

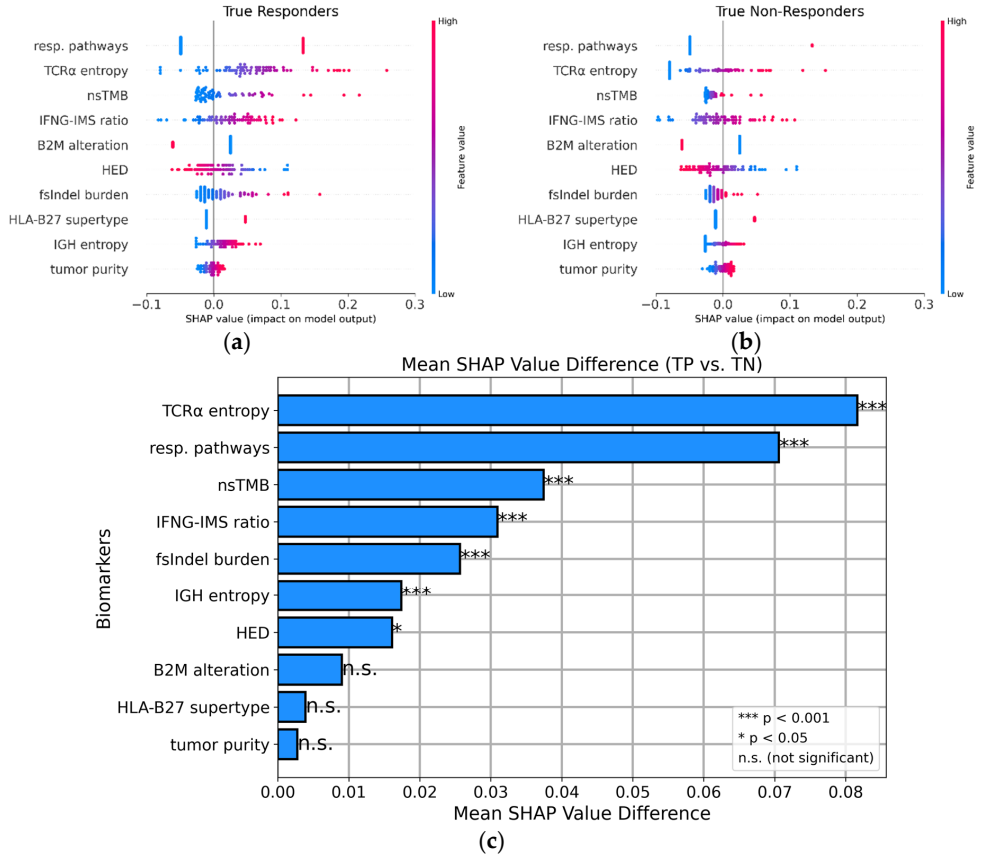

Figure 5. Summary plots ("bee swarm") of the SHAP values for the multi-omics model using the overall cohort. True responders (**a**) were compared with true non-responders (**b**). Each dot represents the contribution of a feature to the prediction for a single sample. The dot color denotes the original feature value: blue, a low value, and red, a high value. (**c**) Differences in mean SHAP values between TP and TN. The asterisks (*) denote the significance level after a two-sided Mann–Whitney U test.

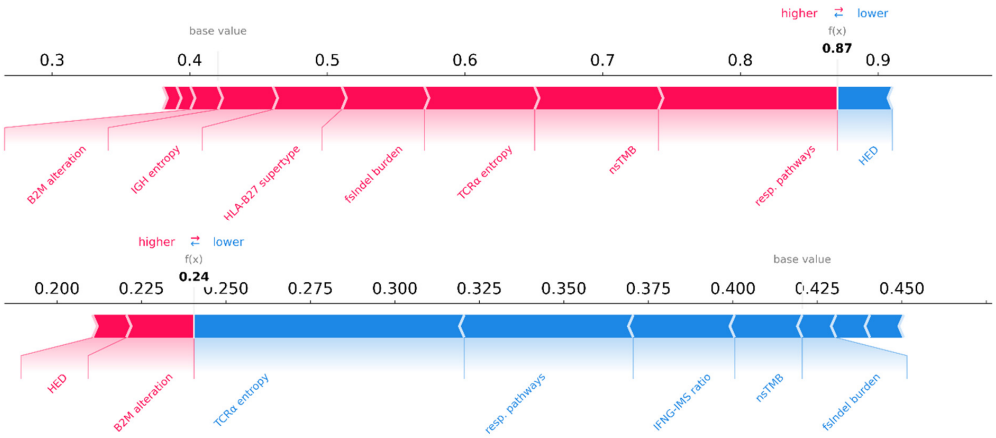

Figure 6. Two representative SHAP force plots of a TP (**top**) and a TN (**bottom**). Using these plots, we can evaluate and visualize the contribution of each feature on a specific sample directly. Both genomic and transcriptomic biomarkers contributed to the correctly identified responder and non-responder.

Cancers **2025**, *17*, 714

4. Discussion

Taken together, our data showed that AI models using multiple DNA- and RNA-seq-based biomarkers improved the prediction of anti-PD1 outcomes compared to the current gold standard, nsTMB. All trained ML models, using only genomic or transcriptomic biomarkers, as well as the multi-omic model, outperformed nsTMB on the training and the test set in terms of the ROC AUC, suggesting that incorporating additional features can provide a more accurate prediction of anti-PD1 responses if sufficient training data are available. However, the availability of homogeneous training data is still unsatisfactory, as even after combining multiple studies into a meta-cohort, the number of samples with both WES and RNA-seq remained limited. Therefore, we expect that larger training datasets will further improve the potential of AI models.

Although the cost of a multi-omics analysis (WES + RNA-seq) is higher than, e.g., a small gene panel, this approach provides not only a comprehensive view on tumor immunogenicity but also various treatment-relevant biomarkers such as fusion gene events, the overexpression of amplified oncogenes, the depletion of deleted tumor suppressor genes, as well as an evaluation of splicing defects. As sequencing costs continue to decline, the wider adoption of combined WES and RNA-seq may become more feasible in routine clinical practice, where even small improvements in prediction accuracy may have clinical benefits, particularly in the selection of patients for ICI.

As anti-PD1 treatment is frequently considered the last treatment option, patients frequently receive ICIs, regardless of the outcome of tumor genome diagnostics. As a result, the identification of discriminative features between responders (true positives) and non-responders (true negatives) is of particular interest to increase the explainability of the results, potentially leading to improved diagnostic interpretation. We achieved patient-specific explainability of the outcome by using SHAP values (Figure 5c). These provide clinicians with a detailed breakdown of the biomarkers that contributed most to the classification of a patient. Patients showing strong indicators of non-respondents could receive another type of therapy, such as *BRAF* inhibitors, or could be spared from the side effects of the treatment.

Surprisingly, the pure RNA model (without DNA-based features) achieved a better overall performance than the well-established gold standard nsTMB alone in both the test and training datasets, although it did not include nsTMB or any other TMB-related metric. This emphasizes the potential of RNA-based features in modeling ICI responses, mostly based on features reflecting immune cell infiltration (quantified as TCR composition) and interferon signatures. Integrating DNA- and RNA-based biomarkers into a multi-omics model resulted in higher overall performance, despite the substantially reduced training dataset for which both WES and RNA-seq were available. Feature selection for the multi-omics model indicated that RNA-derived biomarkers were mostly independent of DNA-derived biomarkers, contributing equally to the top four most influential features. Indeed, we did not detect strong correlations between the genomic and transcriptomic biomarkers in the training dataset (Figure S3). However, we observed correlations between RNA-seq-based biomarkers and tumor purity. Hence, models that include RNA biomarkers may underperform in low-purity samples.

The features preferentially selected by the DNA and RNA models were highly biologically relevant (Figure 3a,b). The DNA model favored, for example, in addition to nsTMB, the related metric fsIndel burden. Frameshift mutations are a rich source of highly immunogenic neoepitopes that are recognized by the immune system [42]. In addition, the DNA model benefitted strongly from information about genetic variants in response pathways and resistance mechanisms, with changes in response pathways (*CTNNB1* alterations, *JAK1*/*JAK2* alterations, and defects at chr6p21.3) being the most important feature.

Cancers **2025**, *17*, 714

Alterations in *B2M* are the most influential feature representing mutated resistance mechanisms. *B2M* alterations can lead to a dysfunctional MHC complex. This mechanism is crucial for antigen presentation by cancer cells [43]. Notably, no biomarker related to the predicted neoantigens exceeded the feature permutation importance threshold of 0.0055. Therefore, we assume that nsTMB is a comprehensive proxy for most neoantigen-related biomarkers. In contrast, the RNA model favored immune-related features, such as TCR α chain entropy, IFNG-IMS ratio, and IGH chain entropy, with TCR α chain entropy being by far the most important biomarker. These features capture many aspects of the tumor immune microenvironment [44]. TCR α and IGH chain entropy reflect information regarding immune cell infiltration and diversity in tumors of both T cells and B cells. With IFNG-IMS, the RNA model also selected an important marker of immune balance because it combines transcriptomic signals of immune response and immunosuppression [45]. All features selected by the DNA and RNA model retained non-zero coefficients in the multi-omics model. However, the permutation feature importance scores differed for some features in the multi-omics models compared with those in the DNA and RNA models. For example, tumor purity had a moderate feature importance score in the DNA model but was almost zero in the multi-omics model. This can be attributed to the correlation between tumor purity and TCR α chain entropy (Figure S3). Tumors with low purity often have higher immune cell infiltration, leading to higher TCR α chain entropy.

The SHAP analysis of true responders and true non-responders in the multi-omics model confirmed the importance of the DNA and RNA features that were originally selected by feature permutation importance (Figure 5a–c). Remarkably, the SHAP methodology allowed us to directly determine the direction in which biomarkers influenced the predictions. For example, it became evident that high TCR α chain entropy or a high nsTMB and fsInDel burden contributed to positive predictions as responders. The SHAP analysis confirmed that patients with mutated response pathways were more likely to respond to immunotherapy, whereas patients with defects in *B2M* were less likely to be classified as responders. More importantly, the application of SHAP values demonstrated the ability of our model to explain the biomarker contribution on a single-sample basis, i.e., the classification of a specific patient. In Figure 6, we showed two representative SHAP examples of single-sample predictions from the multi-omics model, providing further evidence for the per-patient interpretability of our predictions. This is an important step towards the clinical usability of machine learning models because the selection of a patient for anti-PD1 therapy requires individual explainability and assessment of the classification.

Despite showing promising results, the overall improvements in treatment response prediction of the three models over nsTMB are still unsatisfactory. One reason could be the exclusion of non-NGS patient data in our models, such as data on the gut microbiome, comorbidities, age, alcohol consumption, or serum albumin. Some of these factors, such as the gut microbiome [46], or serum albumin level [47], have been shown to correlate with ICI outcomes in various cancer types. Some studies have used AI models to investigate the interplay between clinical non-NGS features and ICI [48]. However, we did not find sufficient data in available melanoma studies capturing a comprehensive selection of such biomarkers together with genomic and transcriptomic data in melanoma. Future studies should aim to collect a broader range of clinical non-NGS biomarkers, in combination with NGS data.

Another limitation of our study is that it combined data from different treatment centers into a meta-cohort. Although we applied several strategies to exclude batch effects (see Figure S1), we cannot rule them out. Moreover, we did not consider information regarding prior treatments or alternative treatment options for the patients, as it was generally not available. Interestingly, only 128 (28%) of the 449 WES samples in our meta-

Cancers **2025**, *17*, 714

cohort had a *BRAF*:V600 alteration, while the expected prevalence of such a mutation is approximately 50% in cutaneous melanoma [49]. This discrepancy suggests that around half the tumors with a *BRAF* alteration may have been treated with *BRAF* inhibitors and not with ICIs, potentially introducing a selection bias. As a result, our findings may not be fully generalizable to the entire melanoma spectrum, particularly for patients harboring *BRAF* mutations (although 128 *BRAF*:V600 cases are a sufficient number to inform model training). Finally, consistent staging information was not available for all studies. As melanoma stage may influence treatment selection and response to anti-PD1 treatment, this limits the assessment of our models regarding specific stages.

The limited size of the meta-cohort, especially the number of samples with both WES and RNA-seq, was the main constraint. Therefore, using a larger cohort would likely improve model training and evaluation. It should also be noted that RECIST, as an outcome measure, is a commonly used but not universally robust metric [50]. Patients with stable disease may have survival benefits, whereas partial responders may progress to a later stage. However, response measures other than the RECIST are often unavailable for public studies. Collecting more comprehensive response data could be a starting point for future trials to address this issue. Despite these limitations, we demonstrated the general usability and interpretability of multi-omics LASSO models for ICI outcome prediction in cancer.

5. Conclusions

In this study, we combined genomic and transcriptomic biomarkers of a large, melanoma-specific meta-cohort to train a multi-omics LASSO model to predict the response to ICI. Multiple biomarkers derived from both whole-exome sequencing and RNA-seq were selected as influential features of the multi-omics model. They showed promising improvements in predicting anti-PD1 outcomes compared with nsTMB alone. The final feature selection revealed that biomarkers describing the tumor immune microenvironment should be considered together with tumor cell-intrinsic mutation-based metrics. By applying the SHAP technique, the model predictions in this study were easier to interpret and explainable on a per-patient basis, making them more applicable in clinical decision-making. Although our study demonstrated the general applicability and explainability of multi-omics LASSO models for ICI outcome prediction, the predictions are not yet fully satisfactory. The main limitations of our study were the limited size of our meta-cohort and limited homogeneity. Future research should therefore aim at collecting large homogeneous ICI cohorts analyzed by WES and RNA-seq for AI model training.

Supplementary Materials: The following supporting information can be downloaded at https://www.mdpi.com/article/10.3390/cancers17050714/s1, Figure S1. Principal Component Analysis (PCA) of the expression of all genes and samples (in TPM). Each dot color represents one sub-cohort constituting our meta-cohort. We plotted the principal components with the highest explained variances. Left: PCA before batch correction. Batch effects were clearly visible. Right: PCA after batch correction using pyComBat. Batch effects were no longer visible. Figure S2. Distribution of the predicted response probabilities of the models in the training datasets. The probability density is different in every model, emphasizing the necessity of model-specific probability cutoff values. The vertical lines represent these thresholds, which were determined by maximizing Youden's indices. Figure S3. Correlation heatmap of the biomarkers in the multi-omics model. We observed only weak correlations between the transcriptomic and genomic biomarkers. However, we can clearly recognize a cluster of transcriptomic biomarkers. We used Pearson's ρ and applied hierarchical clustering to arrange all features into clusters. Only the data from the training set of the multi-omics model were used to generate this plot. Table S1. Resistance mechanisms.

Cancers **2025**, *17*, 714

Author Contributions: A.G. coordinated the project, developed the ML models and visualization, performed the data curation and analysis, and wrote the manuscript. S.O. designed the project together with A.G.; helped with model development, data analysis, and biomarker selection; and revised the manuscript. All authors have read and agreed to the published version of the manuscript.

Funding: A.G. and S.O. received funding from the Deutsche Forschungsgemeinschaft (DFG) as part of the German Human Genome-Phenome Archive (GHGA) under grant number 441914366 (NFDI 1/1).

Institutional Review Board Statement: This study was approved by the independent research ethics committee of the University Hospital Tübingen (project ID 002/2024BO2) and adhered to the ethical principles of the Declaration of Helsinki.

Informed Consent Statement: Informed consent had been obtained from all subjects involved in any of the datasets used in this study. This had been ensured by the submitting authors of the original studies.

Data Availability Statement: The NGS data used for this study were compiled using eight different, publicly available melanoma datasets. These datasets can be obtained from SRA, from the gene expression omnibus, or from dbGaP (after data access request) under the following study accession numbers: Amato et al. [22]: PRJNA639866, GSE15996; Cristescu et al. [23]: phs001572.v1.p1; Gide et al. [24]: PRJEB23709; Hugo et al. [25]: SRP090294, SRP067938, GSE78220; Liu et al. [26]: phs000452.v3.p1; Pyke et al. [27]: phs002388.v1.p1; Riaz et al. [28]: SRP094781, GSE91061; Wolchok et al. [29]: SRP417444.

Conflicts of Interest: There are no known conflicts of interest.

Appendix A.

Appendix A.1. DNA Biomarkers

Tumor Mutational Burden and Related Mutation Count Metrics

To calculate nsTMB, we considered only nonsynonymous variants that occurred in the overlapping target region of all studies. nsTMB was calculated as the number of nonsynonymous variants divided by the size of the target region in megabases. In addition to the classical nsTMB, we derived related burden metrics using different mutation types, normalized by the size of the common target region. We determined the different burdens using the following mutation types: (i) indels, (ii) frameshift indels, (iii) in-frame indels, (iv) splice variants, (v) missense variants, (vi) synonymous variants, and (vii) variants that cause changes in multiple amino acids (i.e., splice and frameshift). The frameshift mutation proportion, another TMB-related biomarker, was also calculated. It is defined as the proportion of frameshift mutations among all the mutation types. Its predictive potential for anti-PD1 therapy has recently been described in a different cancer entity [51]. In addition to these TMB-related metrics, we included the ratio of all nonsynonymous mutations to all synonymous mutations, known as the dN/dS ratio [52].

Appendix A.2. Neoantigen and Neoepitope Analysis

The binding affinities to major histocompatibility complex (MHC) class I molecules were predicted using pVACseq 4.0.1 for all nonsynonymous somatic variants that lie in the common target region [53]. This pipeline was executed for all possible peptides with lengths of 8, 9, and 10, reflecting the most common MHC class I peptide-binding lengths [54]. We executed pVACseq using the neopeptide-binding prediction algorithms MHCflurry, MHCnuggetsI, NNalign, NetMHC, NetMHCpan, and NetMHCpanEL. We used local instances of the IEDB MHC class I-binding prediction tools 3.1.2 and MHCflurry 2.0.6 for the pVACseq predictions. We then filtered neoantigen candidates using a binding affinity cutoff of IC50 < 50 nM. After filtering, neoantigen counts were normalized to the size of the target in megabases, resulting in a TMB-like biomarker called neoantigen burden. To account for neoantigen quality, we used the binding affinity of the biomarker

Cancers **2025**, *17*, 714

with the highest binding affinity as a feature. Another neoantigen metric, the differential agretopicity index (DAI), describes the difference between the predicted binding affinities of wild-type and mutated alleles [55]. Values < 0 indicate a higher binding affinity for the mutated peptide than for the wild-type peptide. We calculated the mean, median, upper decile, and maximum values of all DAIs as biomarkers, reflecting both neoantigen quantity and quality [56].

We passed any neoepitope candidate with a median binding affinity cutoff of IC50 < 500 nM to the neoantigen annotation tool NeoFox 1.1.0 to obtain further neoantigen features [57]. Three metrics predicted by NeoFox were integrated into our model. They describe various properties of the neoepitope candidates:

- HEX alignment score: This score describes the similarity of tumor peptides to known viral-derived peptides [58]. High scores reflect a high similarity of the neopeptide with viral pathogens and could be more likely recognized by the immune system. We used the maximum HEX score in the sample as a biomarker.
- Recognition potential: A fitness model that uses binding affinities and sequence similarity of neoantigens to known pathogens of human infectious diseases to estimate the likelihood of a neoantigen interacting with the immune system [59]. Its maximum value was used as a biomarker for our model.
- Dissimilarity score: This score compares the mutated peptide to the non-mutated self-proteome [60]. Neopeptides with higher dissimilarity scores are more likely to be recognized by the immune system. Therefore, we used the maximum dissimilarity score as the biomarker.

Appendix A.3. Resistance Mechanisms

Resistance mechanisms are those by which cancer cells evade cancer treatment. In ICI, these mechanisms are typical ways in which tumors can escape immune responses. Following a literature review, we included several such biomarkers in our model. Resistance mechanisms are usually described as deleterious mutations in genes of certain pathways.

Frequent mechanisms include defects in the HLA antigen presentation pathway, which prevents T cells from recognizing cancer cells [61]. Most genes that form MHC class I molecules reside at chr6p21.3. Thus, we defined a biomarker that describes deleterious events at this locus: any deletion or loss of heterozygosity (LOH) event at chr6:29941259-33314212. This region contains all HLA class I genes and genes necessary for antigen processing, such as the transporter proteins *TAP1*/*TAP2* and *TAPBP*. Due to the highly polymorphic nature of this locus, we did not include potentially deleterious SNVs and small indels [62]. However, we included deleterious SNVs and indels in *B2M* as independent biomarkers. We assumed a dysfunctional *B2M* protein if we detected LOH events, heterozygous deletions, mutations with a high VEP effect annotation, or variants with an annotation of COSMIC CMC tiers 1, 2, and 3. In addition to these two HLA-related mechanisms, a complete list of all the resistance mechanisms integrated into our models can be found in Table A1.

Some of the mechanisms affected only a small proportion of our training dataset. Thus, we merged the mechanisms affecting less than 20% of the training dataset into one biomarker. This resulted in the union of defects at the HLA locus, CTNNB1 alterations, and JAK/JAK2 alterations as one biomarker. An analysis of odds ratio revealed that these biomarkers were more enriched in responders than in non-responders. That is why we call the resulting merged biomarker a "response pathway". Further details are provided in Supplementary Table S1.

Cancers **2025**, *17*, 714

Table A1. Resistance mechanisms. Each mechanism represents a binary biomarker (true or false). If one of the described alterations was detected, the biomarker was set as true. If none of the described alterations were found, the corresponding biomarker was set as false. Mechanisms marked by an asterisk (*) affected less than 20% of the training cohort and were merged into one biomarker.

Mechanism	Description	Sources
Defects at the HLA locus *	Any deletion or LOH event that overlaps chr6p21.3, chr6:29941259-33314212. This locus contains the majority of HLA class I-related genes.	[61]
Defects in *B2M*	*B2M* is an integral part of both MHC class I and II complexes. Dysfunctional *B2M* proteins lead to the formation of dysfunctional MHC complexes. However, the loss of both functional alleles is uncommon since such cancer clones are eradicated by NK cells. Hence, we counted heterozygous deletions; LOH events; mutations with a high VEP effect; or COSMIC tiers 1, 2, and 3 as defects in *B2M*.	[63]
JAK1/*JAK2* alteration *	Homozygous deletions; VEP-high; or CMC tier 1,2, and 3 somatic variants of *JAK1* and *JAK2*. Other genes of the JAK-STAT pathway were not included because *JAK3* is not expressed in solid tissue and alterations in most STAT genes are difficult to interpret because STATs are, at the same time, both TSG and oncogenes.	[64]
CTNNB1 pathway alteration *	*CTNNB1* is an oncogene. Its pathway includes the negative regulators *APC*, *AXIN1*, and *HNF1A*, which are present in our intersecting target region. Thus, we counted the COSMIC tier 1, 2, and 3 mutations of *CTNNB1*. For its negative regulators, which act as TSG, we considered any somatic mutation with a high VEP effect or COSMIC tiers 1, 2, and 3 as well as homozygous deletions.	[65]
TP53 alteration	*TP53* is frequently mutated in many tumors. Defects in this TSG have manifold effects on cancer cells, including immunosuppression and evasion. Thus, we considered any deletion; LOH; mutation with a high VEP effect; or COSMIC tiers 1, 2, and 3 in *TP53*.	[66]
PTEN alteration	Deleterious events in the TSG *PTEN* were described as a resistance mechanism previously. Thus, we considered any deletion; LOH; mutations with a high VEP effect; or COSMIC tiers 1, 2, and 3 in *PTEN* as deleterious.	[67,68]
STK11 alteration	*STK11* is a tumor suppressor gene. It was predictive of anti-PD1 resistance in a study on another cancer entity. Hence, we counted any deletions; mutations with a high VEP effect; or COSMIC tiers 1, 2, and 3 in *STK11*.	[69]
KRAS alteration	*KRAS* is an oncogene. The predictive potential of *KRAS* mutations in anti-PD1 treatment has been previously described in another cancer entity. Thus, we considered any amplification ≥ 4 and mutations with COSMIC tiers 1, 2, and 3 in *KRAS* deleterious.	[70]
MDM2 alteration	*MDM2* is an oncogene. Activating mutations led to the hyperprogression of melanoma in a previous study. Thus, we counted any amplification ≥ 4 and COSMIC tiers 1, 2, and 3 in *MDM2* as resistance mechanisms.	[71]
MDM4 alteration	*MDM4* is an oncogene. Activating mutations led to the hyperprogression of melanoma in a previous study. Thus, we counted any amplification ≥ 4 and COSMIC tiers 1, 2, and 3 in *MDM4* as resistance mechanisms.	[71]
EGFR alteration	*EGFR* is an oncogene. Activating mutations led to the hyperprogression of melanoma in a previous study. Thus, we counted any amplification ≥ 4 and COSMIC tiers 1, 2, and 3 in *EGFR* as resistance mechanisms.	[71]

Appendix A.4. HLA-Related Biomarkers (Germline)

Carriers of homozygous HLA alleles are thought to be at a considerable disadvantage because their MHC complexes bind to a significantly smaller neopeptide repertoire than that of heterozygous individuals. Indeed, some studies have shown that patients homozygous

for *HLA-B* and *HLA-C* are less likely to respond to ICI [72]. Therefore, we included both *HLA-B* and *HLA-C* homozygosity as binary biomarkers.

HLA evolutionary divergence (HED) is a measure of the evolutionary protein distance between HLA alleles in an individual [73]. It has been described as a predictive biomarker for anti-PD1 therapy outcomes in patients with melanoma [74]. In this study, we used HED, quantified as the Grantham distance between both alleles. We included the mean HED of all three classical HLA loci (*HLA-A*, *HLA-B*, and *HLA-C*) as germline biomarkers in the model. We used an in-house tool to calculate HED, available at GitHub https://github.com/axelgschwind/hlaDivergence (commit 37bd5fc, accessed on 17 April 2023).

HLA alleles can be grouped into several supertypes based on their similar physicochemical properties. The three *HLA-B* supertypes HLA-B27, HLA-B44, and HLA-B62 have been described as predictors of ICI outcomes in melanoma and are thus included as HLA-related binary biomarkers [72,75].

Appendix A.5. Tumor Purity and Heterogeneity

Tumor purity was defined as the percentage of cancer cells in a tumor sample. It has been described as a predictor of ICI outcomes in various types of cancer [76]. In this study, we defined tumor purity as the highest value of tumor clonality determined by ClinCNV. No CNVs were detected in very few samples. In these cases, we used the median VAF of the 15 SNVs with the highest VAF as an estimate of purity.

Appendix A.6. CNV Burden

We defined the CNV burden as the proportion of the genome that carries a CNV to the total size of the genome. We only considered CNVs that passed quality control and autosomal CNVs. The deletion burden is a related biomarker and is defined as the proportion of the genome that carries a heterozygous or homozygous deletion.

Appendix A.7. RNA Biomarkers

TCR and BCR Repertoires

We used TRUST4 to reconstruct TCR and BCR clones from RNA-seq data [77]. We obtained clones of the TCR α, TCR β, and BCR IGH chains. Clones with fewer than two reads were excluded from analysis. We then calculated the Shannon entropy based on the counts of distinct clones for each chain in each sample. This metric integrates both richness (number of distinct clones) and evenness (diversity index and distribution of clone counts) into a single, continuous biomarker.

Appendix A.8. Immune Cell Infiltration

We estimated the composition of immune cell types from RNA-seq expression data using the deconvolution algorithm quanTIseq, as implemented by the wrapper pipeline immunedeconv 2.1.0 [78,79]. Using this approach, we can directly interpret the results as cell proportions in the RNA sample. In our work, we used the sum of the original quanTIseq cell types "B cell", "T cell CD4+ (non-regulatory)", "T cell CD8+", "T cell regulatory (Tregs)", and "NK cell" as a rough estimate for the lymphocyte infiltration of the sample.

Appendix A.9. IFNG-IMS Ratio

We used the ratio of two immune-related gene expression signatures as a biomarker. The impact of this ratio has previously been described as a predictor of ICI outcomes in melanoma [80]. The first signature contained interferon-γ-related genes. The second signature described patterns of immunosuppression, originally obtained by comparing ICI

responders with non-responders. Using the ratio of the signatures, both inflammatory and immunosuppressive elements were combined to predict the ICI outcomes more precisely. Following [80,81], the IFNG signature was calculated as the arithmetic mean of the read counts of *IFNG*, *STAT1*, *IDO1*, *CXCL9*, *CXCL10*, and *HLA-DRA*. The immunosuppression signature was defined as the mean expression values of *ADAM12*, *AXL*, *BCAT1*, *CCL13*, *CCL2*, *CCL8*, *CD163*, *COL6A3*, *FAP*, *IL10*, *INHBA*, *ISG15*, *OLFML2B*, *PDGFRB*, *SIGLEC1*, *STC1*, *TWIST2*, and *VCAN* [80].

Appendix A.10. Gene Expression Profiles

Loss of HLA class I expression is a well-described mechanism of immune evasion and affects anti-PD1 treatment in melanoma [82]. Thus, we calculated the mean gene expression values (in TPM) of the three classical HLA class I loci, *HLA-A*, *HLA-B*, and *HLA-C*, as GEP biomarkers. *B2M* is also crucial for the formation of MHC complexes, and loss of its expression has been associated with anti-PD1 outcomes in a recent study of another cancer entity [83]. For our model, we used the gene expression of *B2M*, which was quantified as TPM. Additionally, the expression of the *PD1* ligand *PDL1* in terms of TPM was utilized as another GEP biomarker. It was included because it serves as an "official" indication for anti-PD1 treatment in other cancer entities.

References

1. Hodi, F.S.; O'Day, S.J.; McDermott, D.F.; Weber, R.W.; Sosman, J.A.; Haanen, J.B.; Gonzalez, R.; Robert, C.; Schadendorf, D.; Hassel, J.C.; et al. Improved Survival with Ipilimumab in Patients with Metastatic Melanoma. *N. Engl. J. Med.* **2010**, *363*, 711–723. [CrossRef] [PubMed]
2. Barone, A.; Hazarika, M.; Theoret, M.R.; Mishra-Kalyani, P.; Chen, H.; He, K.; Sridhara, R.; Subramaniam, S.; Pfuma, E.; Wang, Y.; et al. FDA Approval Summary: Pembrolizumab for the Treatment of Patients with Unresectable or Metastatic Melanoma. *Clin. Cancer Res.* **2017**, *23*, 5661–5665. [CrossRef]
3. Hazarika, M.; Chuk, M.K.; Theoret, M.R.; Mushti, S.; He, K.; Weis, S.L.; Putman, A.H.; Helms, W.S.; Cao, X.; Li, H.; et al. U.S. FDA Approval Summary: Nivolumab for Treatment of Unresectable or Metastatic Melanoma Following Progression on Ipilimumab. *Clin. Cancer Res.* **2017**, *23*, 3484–3488. [CrossRef] [PubMed]
4. Valero, C.; Lee, M.; Hoen, D.; Zehir, A.; Berger, M.F.; Seshan, V.E.; Chan, T.A.; Morris, L.G.T. Response Rates to Anti–PD-1 Immunotherapy in Microsatellite-Stable Solid Tumors With 10 or More Mutations per Megabase. *JAMA Oncol.* **2021**, *7*, 739–743. [CrossRef] [PubMed]
5. Marcus, L.; Fashoyin-Aje, L.A.; Donoghue, M.; Yuan, M.; Rodriguez, L.; Gallagher, P.S.; Philip, R.; Ghosh, S.; Theoret, M.R.; Beaver, J.A.; et al. FDA Approval Summary: Pembrolizumab for the Treatment of Tumor Mutational Burden–High Solid Tumors. *Clin. Cancer Res.* **2021**, *27*, 4685–4689. [CrossRef] [PubMed]
6. Marabelle, A.; Fakih, M.; Lopez, J.; Shah, M.; Shapira-Frommer, R.; Nakagawa, K.; Chung, H.C.; Kindler, H.L.; Lopez-Martin, J.A.; Miller, W.H.; et al. Association of tumour mutational burden with outcomes in patients with advanced solid tumours treated with pembrolizumab: Prospective biomarker analysis of the multicohort, open-label, phase 2 KEYNOTE-158 study. *Lancet Oncol.* **2020**, *21*, 1353–1365. [CrossRef] [PubMed]
7. Martins, F.; Sofiya, L.; Sykiotis, G.P.; Lamine, F.; Maillard, M.; Fraga, M.; Shabafrouz, K.; Ribi, C.; Cairoli, A.; Guex-Crosier, Y.; et al. Adverse effects of immune-checkpoint inhibitors: Epidemiology, management and surveillance. *Nat. Rev. Clin. Oncol.* **2019**, *16*, 563–580. [CrossRef] [PubMed]
8. Baltussen, J.C.; Welters, M.J.P.; Verdegaal, E.M.E.; Kapiteijn, E.; Schrader, A.M.R.; Slingerland, M.; Liefers, G.-J.; van der Burg, S.H.; Portielje, J.E.A.; de Glas, N.A. Predictive Biomarkers for Outcomes of Immune Checkpoint Inhibitors (ICIs) in Melanoma: A Systematic Review. *Cancers* **2021**, *13*, 6366. [CrossRef]
9. Mortazavi, A.; Williams, B.A.; McCue, K.; Schaeffer, L.; Wold, B. Mapping and quantifying mammalian transcriptomes by RNA-Seq. *Nat. Methods* **2008**, *5*, 621–628. [CrossRef]
10. Ng, S.B.; Turner, E.H.; Robertson, P.D.; Flygare, S.D.; Bigham, A.W.; Lee, C.; Shaffer, T.; Wong, M.; Bhattacharjee, A.; Eichler, E.E. Targeted capture and massively parallel sequencing of 12 human exomes. *Nature* **2009**, *461*, 272–276. [CrossRef] [PubMed]
11. Yoo, S.-K.; Fitzgerald, C.W.; Cho, B.A.; Fitzgerald, B.G.; Han, C.; Koh, E.S.; Pandey, A.; Sfreddo, H.; Crowley, F.; Korostin, M.R.; et al. Prediction of checkpoint inhibitor immunotherapy efficacy for cancer using routine blood tests and clinical data. *Nat. Med.* **2025**, 1–12. [CrossRef]

12. Benzekry, S.; Grangeon, M.; Karlsen, M.; Alexa, M.; Bicalho-Frazeto, I.; Chaleat, S.; Tomasini, P.; Barbolosi, D.; Barlesi, F.; Greillier, L. Machine Learning for Prediction of Immunotherapy Efficacy in Non-Small Cell Lung Cancer from Simple Clinical and Biological Data. *Cancers* **2021**, *13*, 6210. [CrossRef] [PubMed]
13. Johannet, P.; Coudray, N.; Donnelly, D.M.; Jour, G.; Illa-Bochaca, I.; Xia, Y.; Johnson, D.B.; Wheless, L.; Patrinely, J.R.; Nomikou, S.; et al. Using Machine Learning Algorithms to Predict Immunotherapy Response in Patients with Advanced Melanoma. *Clin. Cancer Res.* **2021**, *27*, 131–140. [CrossRef]
14. Schina, A.; Sztupinszki, Z.; Marie Svane, I.; Szallasi, Z.; Jönsson, G.; Donia, M. Intratumoral T-cell and B-cell receptor architecture associates with distinct immune tumor microenvironment features and clinical outcomes of anti-PD-1/L1 immunotherapy. *J. ImmunoTherapy Cancer* **2023**, *11*, e006941. [CrossRef] [PubMed]
15. Bigelow, E.; Saria, S.; Piening, B.; Curti, B.; Dowdell, A.; Weerasinghe, R.; Bifulco, C.; Urba, W.; Finkelstein, N.; Fertig, E.J.; et al. A Random Forest Genomic Classifier for Tumor Agnostic Prediction of Response to Anti-PD1 Immunotherapy. *Cancer Inform.* **2022**, *21*, 11769351221136081. [CrossRef]
16. Chowell, D.; Yoo, S.-K.; Valero, C.; Pastore, A.; Krishna, C.; Lee, M.; Hoen, D.; Shi, H.; Kelly, D.W.; Patel, N.; et al. Improved prediction of immune checkpoint blockade efficacy across multiple cancer types. *Nat. Biotechnol.* **2022**, *40*, 499–506. [CrossRef] [PubMed]
17. Litchfield, K.; Reading, J.L.; Puttick, C.; Thakkar, K.; Abbosh, C.; Bentham, R.; Watkins, T.B.K.; Rosenthal, R.; Biswas, D.; Rowan, A.; et al. Meta-analysis of tumor- and T cell-intrinsic mechanisms of sensitization to checkpoint inhibition. *Cell* **2021**, *184*, 596–614.e514. [CrossRef] [PubMed]
18. Tibshirani, R. Regression shrinkage and selection via the lasso. *J. R. Stat. Soc. Ser. B Stat. Methodol.* **1996**, *58*, 267–288. [CrossRef]
19. Eisenhauer, E.A.; Therasse, P.; Bogaerts, J.; Schwartz, L.H.; Sargent, D.; Ford, R.; Dancey, J.; Arbuck, S.; Gwyther, S.; Mooney, M.; et al. New response evaluation criteria in solid tumours: Revised RECIST guideline (version 1.1). *Eur. J. Cancer* **2009**, *45*, 228–247. [CrossRef]
20. Katz, K.; Shutov, O.; Lapoint, R.; Kimelman, M.; Brister, J.R.; O'Sullivan, C. The Sequence Read Archive: A decade more of explosive growth. *Nucleic Acids Res.* **2021**, *50*, D387–D390. [CrossRef]
21. Tryka, K.A.; Hao, L.; Sturcke, A.; Jin, Y.; Wang, Z.Y.; Ziyabari, L.; Lee, M.; Popova, N.; Sharopova, N.; Kimura, M. NCBI's Database of Genotypes and Phenotypes: dbGaP. *Nucleic Acids Res.* **2014**, *42*, D975–D979. [CrossRef] [PubMed]
22. Amato, C.M.; Hintzsche, J.D.; Wells, K.; Applegate, A.; Gorden, N.T.; Vorwald, V.M.; Tobin, R.P.; Nassar, K.; Shellman, Y.G.; Kim, J.; et al. Pre-Treatment Mutational and Transcriptomic Landscape of Responding Metastatic Melanoma Patients to Anti-PD1 Immunotherapy. *Cancers* **2020**, *12*, 1943. [CrossRef] [PubMed]
23. Cristescu, R.; Mogg, R.; Ayers, M.; Albright, A.; Murphy, E.; Yearley, J.; Sher, X.; Liu, X.Q.; Lu, H.; Nebozhyn, M.; et al. Pan-tumor genomic biomarkers for PD-1 checkpoint blockade-based immunotherapy. *Science* **2018**, *362*, eaar3593. [CrossRef] [PubMed]
24. Gide, T.N.; Quek, C.; Menzies, A.M.; Tasker, A.T.; Shang, P.; Holst, J.; Madore, J.; Lim, S.Y.; Velickovic, R.; Wongchenko, M.; et al. Distinct Immune Cell Populations Define Response to Anti-PD-1 Monotherapy and Anti-PD-1/Anti-CTLA-4 Combined Therapy. *Cancer Cell* **2019**, *35*, 238–255.e236. [CrossRef] [PubMed]
25. Hugo, W.; Zaretsky, J.M.; Sun, L.; Song, C.; Moreno, B.H.; Hu-Lieskovan, S.; Berent-Maoz, B.; Pang, J.; Chmielowski, B.; Cherry, G.; et al. Genomic and Transcriptomic Features of Response to Anti-PD-1 Therapy in Metastatic Melanoma. *Cell* **2016**, *165*, 35–44. [CrossRef]
26. Liu, D.; Schilling, B.; Liu, D.; Sucker, A.; Livingstone, E.; Jerby-Arnon, L.; Zimmer, L.; Gutzmer, R.; Satzger, I.; Loquai, C.; et al. Integrative molecular and clinical modeling of clinical outcomes to PD1 blockade in patients with metastatic melanoma. *Nat. Med.* **2019**, *25*, 1916–1927. [CrossRef] [PubMed]
27. Pyke, R.M.; Mellacheruvu, D.; Dea, S.; Abbott, C.W.; McDaniel, L.; Bhave, D.P.; Zhang, S.V.; Levy, E.; Bartha, G.; West, J.; et al. A machine learning algorithm with subclonal sensitivity reveals widespread pan-cancer human leukocyte antigen loss of heterozygosity. *Nat. Commun.* **2022**, *13*, 1925. [CrossRef]
28. Riaz, N.; Havel, J.J.; Makarov, V.; Desrichard, A.; Urba, W.J.; Sims, J.S.; Hodi, F.S.; Martín-Algarra, S.; Mandal, R.; Sharfman, W.H.; et al. Tumor and Microenvironment Evolution during Immunotherapy with Nivolumab. *Cell* **2017**, *171*, 934–949.e916. [CrossRef] [PubMed]
29. Wolchok, J.D.; Chiarion-Sileni, V.; Gonzalez, R.; Rutkowski, P.; Grob, J.J.; Cowey, C.L.; Lao, C.D.; Wagstaff, J.; Schadendorf, D.; Ferrucci, P.F.; et al. Overall Survival with Combined Nivolumab and Ipilimumab in Advanced Melanoma. *N. Engl. J. Med.* **2017**, *377*, 1345–1356. [CrossRef]
30. Gregorutti, B.; Michel, B.; Saint-Pierre, P. Correlation and variable importance in random forests. *Stat. Comput.* **2017**, *27*, 659–678. [CrossRef]
31. Breiman, L. Random Forests. *Mach. Learn.* **2001**, *45*, 5–32. [CrossRef]
32. Pedregosa, F.; Varoquaux, G.; Gramfort, A.; Michel, V.; Thirion, B.; Grisel, O.; Blondel, M.; Prettenhofer, P.; Weiss, R.; Dubourg, V. Scikit-learn: Machine learning in Python. *J. Mach. Learn. Res.* **2011**, *12*, 2825–2830.

33. Martínez-Camblor, P.; Pardo-Fernández, J.C. The Youden Index in the Generalized Receiver Operating Characteristic Curve Context. *Int. J. Biostat.* **2019**, *15*, 20180060. [CrossRef] [PubMed]
34. Lundberg, S.M.; Lee, S.-I. A unified approach to interpreting model predictions. In Proceedings of the 31st International Conference on Neural Information Processing Systems, Long Beach, CA, USA, 4–9 December 2017; pp. 4768–4777.
35. Kim, S.; Scheffler, K.; Halpern, A.L.; Bekritsky, M.A.; Noh, E.; Källberg, M.; Chen, X.; Kim, Y.; Beyter, D.; Krusche, P.; et al. Strelka2: Fast and accurate calling of germline and somatic variants. *Nat. Methods* **2018**, *15*, 591–594. [CrossRef]
36. Demidov, G.; Ossowski, S. ClinCNV: Novel method for allele-specific somatic copy-number alterations detection. *BioRxiv* **2019**, 837971. [CrossRef]
37. Tate, J.G.; Bamford, S.; Jubb, H.C.; Sondka, Z.; Beare, D.M.; Bindal, N.; Boutselakis, H.; Cole, C.G.; Creatore, C.; Dawson, E.; et al. COSMIC: The Catalogue Of Somatic Mutations In Cancer. *Nucleic Acids Res.* **2018**, *47*, D941–D947. [CrossRef]
38. McLaren, W.; Gil, L.; Hunt, S.E.; Riat, H.S.; Ritchie, G.R.S.; Thormann, A.; Flicek, P.; Cunningham, F. The Ensembl Variant Effect Predictor. *Genome Biol.* **2016**, *17*, 122. [CrossRef] [PubMed]
39. Liao, Y.; Smyth, G.K.; Shi, W. featureCounts: An efficient general purpose program for assigning sequence reads to genomic features. *Bioinformatics* **2014**, *30*, 923–930. [CrossRef] [PubMed]
40. Farrell, J.J. The Prediction of HLA Genotypes from Next Generation Sequencing and Genome Scan Data. Doctoral Dissertation, Boston University, Boston, MA, USA, 2014.
41. Behdenna, A.; Colange, M.; Haziza, J.; Gema, A.; Appé, G.; Azencott, C.-A.; Nordor, A. pyComBat, a Python tool for batch effects correction in high-throughput molecular data using empirical Bayes methods. *BMC Bioinform.* **2023**, *24*, 459. [CrossRef]
42. Florou, V.; Floudas, C.S.; Maoz, A.; Naqash, A.R.; Norton, C.; Tan, A.C.; Sokol, E.S.; Frampton, G.; Soares, H.P.; Puri, S.; et al. Real-world pan-cancer landscape of frameshift mutations and their role in predicting responses to immune checkpoint inhibitors in cancers with low tumor mutational burden. *J. ImmunoTherapy Cancer* **2023**, *11*, e007440. [CrossRef] [PubMed]
43. Cai, L.; Michelakos, T.; Yamada, T.; Fan, S.; Wang, X.; Schwab, J.H.; Ferrone, C.R.; Ferrone, S. Defective HLA class I antigen processing machinery in cancer. *Cancer Immunol. Immunother.* **2018**, *67*, 999–1009. [CrossRef] [PubMed]
44. Binnewies, M.; Roberts, E.W.; Kersten, K.; Chan, V.; Fearon, D.F.; Merad, M.; Coussens, L.M.; Gabrilovich, D.I.; Ostrand-Rosenberg, S.; Hedrick, C.C.; et al. Understanding the tumor immune microenvironment (TIME) for effective therapy. *Nat. Med.* **2018**, *24*, 541–550. [CrossRef] [PubMed]
45. Munn, D.H.; Bronte, V. Immune suppressive mechanisms in the tumor microenvironment. *Curr. Opin. Immunol.* **2016**, *39*, 1–6. [CrossRef]
46. Lee, K.A.; Thomas, A.M.; Bolte, L.A.; Björk, J.R.; de Ruijter, L.K.; Armanini, F.; Asnicar, F.; Blanco-Miguez, A.; Board, R.; Calbet-Llopart, N.; et al. Cross-cohort gut microbiome associations with immune checkpoint inhibitor response in advanced melanoma. *Nat. Med.* **2022**, *28*, 535–544. [CrossRef] [PubMed]
47. Saal, J.; Ellinger, J.; Ritter, M.; Brossart, P.; Hölzel, M.; Klümper, N.; Bald, T. Pretreatment albumin is a prognostic and predictive biomarker for response to atezolizumab across solid tumors. *Clin. Transl. Immunol.* **2023**, *12*, e1472. [CrossRef]
48. Abuhelwa, A.Y.; Kichenadasse, G.; McKinnon, R.A.; Rowland, A.; Hopkins, A.M.; Sorich, M.J. Machine Learning for Prediction of Survival Outcomes with Immune-Checkpoint Inhibitors in Urothelial Cancer. *Cancers* **2021**, *13*, 2001. [CrossRef]
49. Ascierto, P.A.; Kirkwood, J.M.; Grob, J.-J.; Simeone, E.; Grimaldi, A.M.; Maio, M.; Palmieri, G.; Testori, A.; Marincola, F.M.; Mozzillo, N. The role of BRAF V600 mutation in melanoma. *J. Transl. Med.* **2012**, *10*, 85. [CrossRef] [PubMed]
50. Kilickap, S.; Demirci, U.; Karadurmus, N.; Dogan, M.; Akinci, B.; Sendur, M.A.N. Endpoints in oncology clinical trials. *JBUON* **2018**, *23*, S1–S6.
51. Sena, L.A.; Fountain, J.; Isaacsson Velho, P.; Lim, S.J.; Wang, H.; Nizialek, E.; Rathi, N.; Nussenzveig, R.; Maughan, B.L.; Velez, M.G.; et al. Tumor Frameshift Mutation Proportion Predicts Response to Immunotherapy in Mismatch Repair-Deficient Prostate Cancer. *Oncologist* **2020**, *26*, e270–e278. [CrossRef]
52. Martincorena, I.; Raine, K.M.; Gerstung, M.; Dawson, K.J.; Haase, K.; Van Loo, P.; Davies, H.; Stratton, M.R.; Campbell, P.J. Universal Patterns of Selection in Cancer and Somatic Tissues. *Cell* **2017**, *171*, 1029–1041.e1021. [CrossRef] [PubMed]
53. Hundal, J.; Kiwala, S.; McMichael, J.; Miller, C.A.; Xia, H.; Wollam, A.T.; Liu, C.J.; Zhao, S.; Feng, Y.-Y.; Graubert, A.P.; et al. pVACtools: A Computational Toolkit to Identify and Visualize Cancer Neoantigens. *Cancer Immunol. Res.* **2020**, *8*, 409–420. [CrossRef]
54. Trolle, T.; McMurtrey, C.P.; Sidney, J.; Bardet, W.; Osborn, S.C.; Kaever, T.; Sette, A.; Hildebrand, W.H.; Nielsen, M.; Peters, B. The Length Distribution of Class I–Restricted T Cell Epitopes Is Determined by Both Peptide Supply and MHC Allele–Specific Binding Preference. *J. Immunol.* **2016**, *196*, 1480–1487. [CrossRef] [PubMed]
55. Duan, F.; Duitama, J.; Al Seesi, S.; Ayres, C.M.; Corcelli, S.A.; Pawashe, A.P.; Blanchard, T.; McMahon, D.; Sidney, J.; Sette, A.; et al. Genomic and bioinformatic profiling of mutational neoepitopes reveals new rules to predict anticancer immunogenicity. *J. Exp. Med.* **2014**, *211*, 2231–2248. [CrossRef] [PubMed]

56. Ghorani, E.; Rosenthal, R.; McGranahan, N.; Reading, J.L.; Lynch, M.; Peggs, K.S.; Swanton, C.; Quezada, S.A. Differential binding affinity of mutated peptides for MHC class I is a predictor of survival in advanced lung cancer and melanoma. *Ann. Oncol.* **2018**, *29*, 271–279. [CrossRef] [PubMed]
57. Lang, F.; Riesgo-Ferreiro, P.; Löwer, M.; Sahin, U.; Schrörs, B. NeoFox: Annotating neoantigen candidates with neoantigen features. *Bioinformatics* **2021**, *37*, 4246–4247. [CrossRef] [PubMed]
58. Chiaro, J.; Kasanen, H.H.E.; Whalley, T.; Capasso, C.; Grönholm, M.; Feola, S.; Peltonen, K.; Hamdan, F.; Hernberg, M.; Mäkelä, S.; et al. Viral Molecular Mimicry Influences the Antitumor Immune Response in Murine and Human Melanoma. *Cancer Immunol. Res.* **2021**, *9*, 981–993. [CrossRef] [PubMed]
59. Łuksza, M.; Riaz, N.; Makarov, V.; Balachandran, V.P.; Hellmann, M.D.; Solovyov, A.; Rizvi, N.A.; Merghoub, T.; Levine, A.J.; Chan, T.A.; et al. A neoantigen fitness model predicts tumour response to checkpoint blockade immunotherapy. *Nature* **2017**, *551*, 517–520. [CrossRef]
60. Richman, L.P.; Vonderheide, R.H.; Rech, A.J. Neoantigen Dissimilarity to the Self-Proteome Predicts Immunogenicity and Response to Immune Checkpoint Blockade. *Cell Syst.* **2019**, *9*, 375–382.e374. [CrossRef]
61. Maggs, L.; Sadagopan, A.; Moghaddam, A.S.; Ferrone, S. HLA class I antigen processing machinery defects in antitumor immunity and immunotherapy. *Trends Cancer* **2021**, *7*, 1089–1101. [CrossRef] [PubMed]
62. Carapito, R.; Radosavljevic, M.; Bahram, S. Next-Generation Sequencing of the HLA locus: Methods and impacts on HLA typing, population genetics and disease association studies. *Hum. Immunol.* **2016**, *77*, 1016–1023. [CrossRef]
63. Wang, H.; Liu, B.; Wei, J. Beta2-microglobulin(B2M) in cancer immunotherapies: Biological function, resistance and remedy. *Cancer Lett.* **2021**, *517*, 96–104. [CrossRef]
64. Shin, D.S.; Zaretsky, J.M.; Escuin-Ordinas, H.; Garcia-Diaz, A.; Hu-Lieskovan, S.; Kalbasi, A.; Grasso, C.S.; Hugo, W.; Sandoval, S.; Torrejon, D.Y.; et al. Primary Resistance to PD-1 Blockade Mediated by JAK1/2 Mutations. *Cancer Discov.* **2017**, *7*, 188–201. [CrossRef] [PubMed]
65. Spranger, S.; Bao, R.; Gajewski, T.F. Melanoma-intrinsic β-catenin signalling prevents anti-tumour immunity. *Nature* **2015**, *523*, 231–235. [CrossRef] [PubMed]
66. Liu, S.; Liu, T.; Jiang, J.; Guo, H.; Yang, R. p53 mutation and deletion contribute to tumor immune evasion. *Front. Genet.* **2023**, *14*, 1088455. [CrossRef]
67. Piro, G.; Carbone, C.; Carbognin, L.; Pilotto, S.; Ciccarese, C.; Iacovelli, R.; Milella, M.; Bria, E.; Tortora, G. Revising PTEN in the Era of Immunotherapy: New Perspectives for an Old Story. *Cancers* **2019**, *11*, 1525. [CrossRef] [PubMed]
68. Roh, W.; Chen, P.-L.; Reuben, A.; Spencer, C.N.; Prieto, P.A.; Miller, J.P.; Gopalakrishnan, V.; Wang, F.; Cooper, Z.A.; Reddy, S.M.; et al. Integrated molecular analysis of tumor biopsies on sequential CTLA-4 and PD-1 blockade reveals markers of response and resistance. *Sci. Transl. Med.* **2017**, *9*, eaah3560. [CrossRef]
69. Pore, N.; Wu, S.; Standifer, N.; Jure-Kunkel, M.; de los Reyes, M.; Shrestha, Y.; Halpin, R.; Rothstein, R.; Mulgrew, K.; Blackmore, S.; et al. Resistance to Durvalumab and Durvalumab plus Tremelimumab Is Associated with Functional STK11 Mutations in Patients with Non–Small Cell Lung Cancer and Is Reversed by STAT3 Knockdown. *Cancer Discov.* **2021**, *11*, 2828–2845. [CrossRef]
70. Dong, Z.-Y.; Zhong, W.-Z.; Zhang, X.-C.; Su, J.; Xie, Z.; Liu, S.-Y.; Tu, H.-Y.; Chen, H.-J.; Sun, Y.-L.; Zhou, Q.; et al. Potential Predictive Value of TP53 and KRAS Mutation Status for Response to PD-1 Blockade Immunotherapy in Lung Adenocarcinoma. *Clin. Cancer Res.* **2017**, *23*, 3012–3024. [CrossRef]
71. Forschner, A.; Hilke, F.J.; Bonzheim, I.; Gschwind, A.; Demidov, G.; Amaral, T.; Ossowski, S.; Riess, O.; Schroeder, C.; Martus, P.; et al. MDM2, MDM4 and EGFR Amplifications and Hyperprogression in Metastatic Acral and Mucosal Melanoma. *Cancers* **2020**, *12*, 540. [CrossRef] [PubMed]
72. Chowell, D.; Morris, L.G.T.; Grigg, C.M.; Weber, J.K.; Samstein, R.M.; Makarov, V.; Kuo, F.; Kendall, S.M.; Requena, D.; Riaz, N.; et al. Patient HLA class I genotype influences cancer response to checkpoint blockade immunotherapy. *Science* **2018**, *359*, 582–587. [CrossRef] [PubMed]
73. Pierini, F.; Lenz, T.L. Divergent Allele Advantage at Human MHC Genes: Signatures of Past and Ongoing Selection. *Mol. Biol. Evol.* **2018**, *35*, 2145–2158. [CrossRef] [PubMed]
74. Chowell, D.; Krishna, C.; Pierini, F.; Makarov, V.; Rizvi, N.A.; Kuo, F.; Morris, L.G.T.; Riaz, N.; Lenz, T.L.; Chan, T.A. Evolutionary divergence of HLA class I genotype impacts efficacy of cancer immunotherapy. *Nat. Med.* **2019**, *25*, 1715–1720. [CrossRef] [PubMed]
75. Oey, O.; Khattak, M.A.; Abed, A.; Meniawy, T.; Reid, A.; Calapre, L.; Millward, M.; Gray, E. Patient human leukocyte antigen (HLA) genotype may predict response to anti-programmed death receptor 1 (anti-PD1) in advanced melanoma. *J. Clin. Oncol.* **2021**, *39*, e21512. [CrossRef]
76. Deng, Y.; Song, Z.; Huang, L.; Guo, Z.; Tong, B.; Sun, M.; Zhao, J.; Zhang, H.; Zhang, Z.; Li, G. Tumor purity as a prognosis and immunotherapy relevant feature in cervical cancer. *Aging* **2021**, *13*, 24768–24785. [CrossRef] [PubMed]
77. Song, L.; Cohen, D.; Ouyang, Z.; Cao, Y.; Hu, X.; Liu, X.S. TRUST4: Immune repertoire reconstruction from bulk and single-cell RNA-seq data. *Nat. Methods* **2021**, *18*, 627–630. [CrossRef]

78. Finotello, F.; Mayer, C.; Plattner, C.; Laschober, G.; Rieder, D.; Hackl, H.; Krogsdam, A.; Loncova, Z.; Posch, W.; Wilflingseder, D.; et al. Molecular and pharmacological modulators of the tumor immune contexture revealed by deconvolution of RNA-seq data. *Genome Med.* **2019**, *11*, 34. [CrossRef] [PubMed]
79. Sturm, G.; Finotello, F.; Petitprez, F.; Zhang, J.D.; Baumbach, J.; Fridman, W.H.; List, M.; Aneichyk, T. Comprehensive evaluation of transcriptome-based cell-type quantification methods for immuno-oncology. *Bioinformatics* **2019**, *35*, i436–i445. [CrossRef]
80. Cui, C.; Xu, C.; Yang, W.; Chi, Z.; Sheng, X.; Si, L.; Xie, Y.; Yu, J.; Wang, S.; Yu, R.; et al. Ratio of the interferon-γ signature to the immunosuppression signature predicts anti-PD-1 therapy response in melanoma. *NPJ Genom. Med.* **2021**, *6*, 7. [CrossRef] [PubMed]
81. Ayers, M.; Lunceford, J.; Nebozhyn, M.; Murphy, E.; Loboda, A.; Kaufman, D.R.; Albright, A.; Cheng, J.D.; Kang, S.P.; Shankaran, V.; et al. IFN-γ–related mRNA profile predicts clinical response to PD-1 blockade. *J. Clin. Investig.* **2017**, *127*, 2930–2940. [CrossRef]
82. Shklovskaya, E.; Lee, J.H.; Lim, S.Y.; Stewart, A.; Pedersen, B.; Ferguson, P.; Saw, R.P.; Thompson, J.F.; Shivalingam, B.; Carlino, M.S.; et al. Tumor MHC Expression Guides First-Line Immunotherapy Selection in Melanoma. *Cancers* **2020**, *12*, 3374. [CrossRef] [PubMed]
83. Zhao, Y.; Cao, Y.; Chen, Y.; Wu, L.; Hang, H.; Jiang, C.; Zhou, X. B2M gene expression shapes the immune landscape of lung adenocarcinoma and determines the response to immunotherapy. *Immunology* **2021**, *164*, 507–523. [CrossRef] [PubMed]

A.4 Supplementary Materials

Supplementary Figures

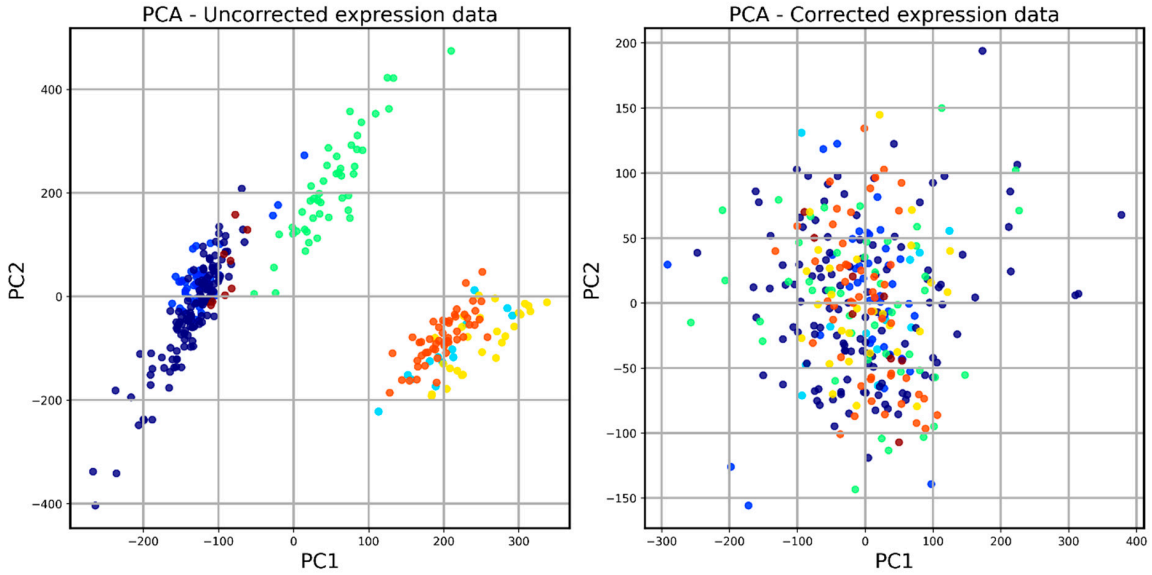

Figure S1. Principal Component Analysis (PCA) of the expression of all genes and samples (in TPM). Each dot color represents one sub-cohort constituting our meta-cohort. We plotted the principal components with the highest explained variances. Left: PCA before batch correction. Batch effects were clearly visible. Right: PCA after batch correction using pyComBat. Batch effects were no longer visible.

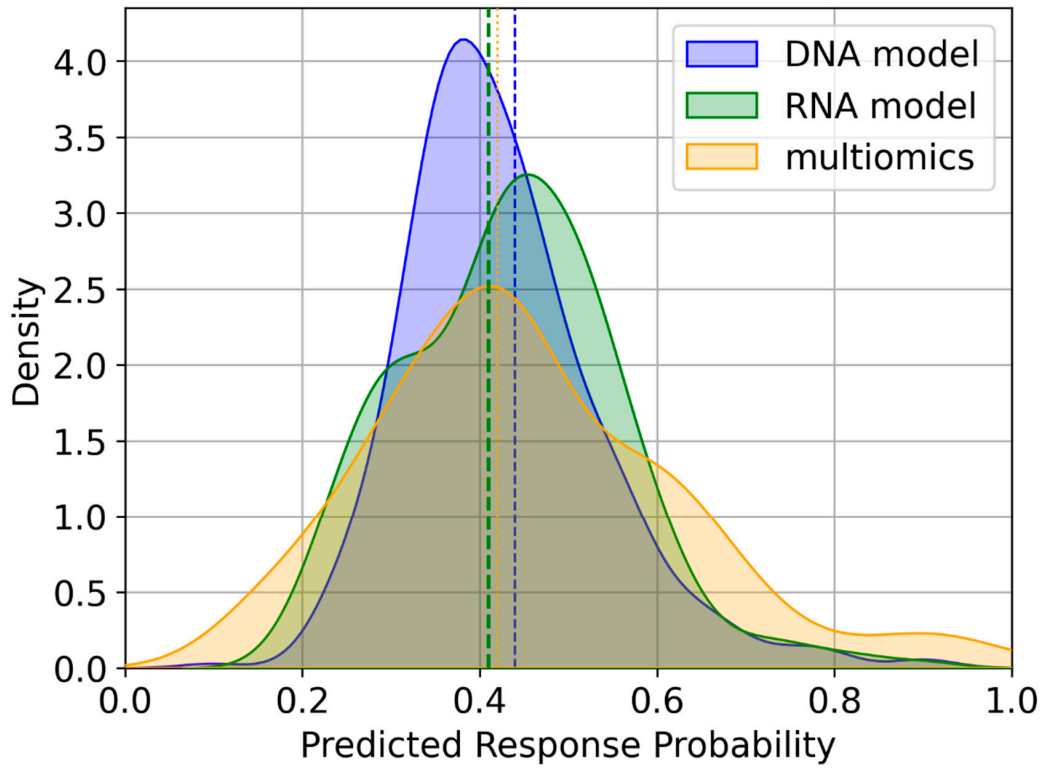

Figure S2. Distribution of the predicted response probabilities of the models in the training datasets. The probability density is different in every model, emphasizing the necessity of model-specific probability cutoff values. The vertical lines represent these thresholds, which were determined by maximizing Youden's indices.

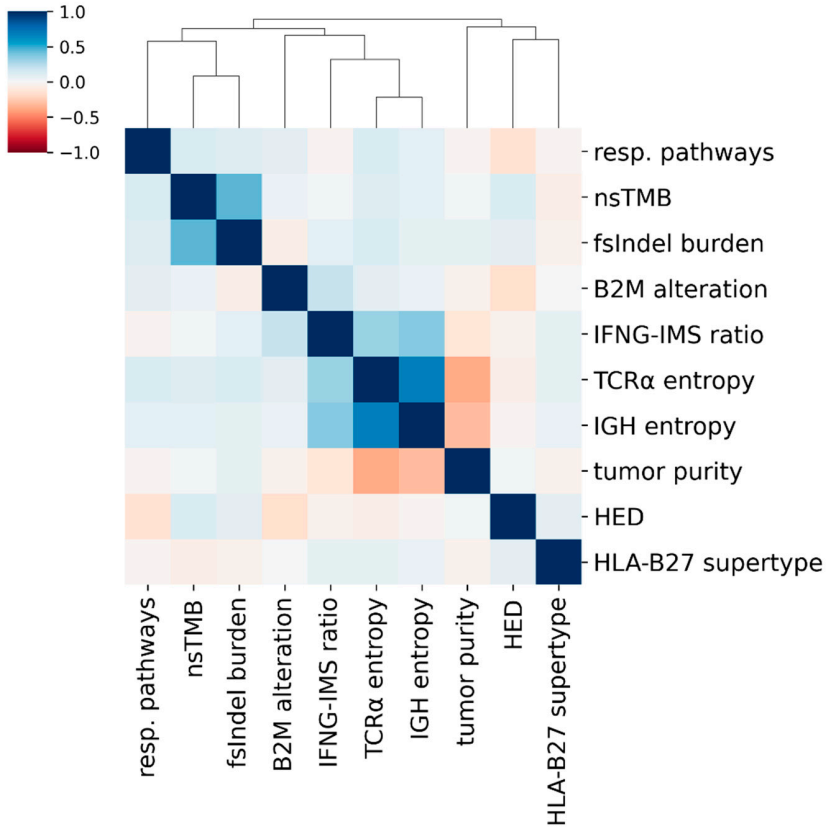

Figure S3. Correlation heatmap of the biomarkers in the multi-omics model. We observed only weak correlations between the transcriptomic and genomic biomarkers. However, we can clearly recognize a cluster of transcriptomic biomarkers. We used Pearson's ρ and applied hierarchical clustering to arrange all features into clusters. Only the data from the training set of the multi-omics model were used to generate this plot.

Supplementary Tables

Resistance Mechanism	Odds Ratio	p-value (Fisher)	total affected	% affected	# responders	# non-responders
defects at the HLA locus*	2.18	0.72%	61	15.14%	36	25
CTNNB1* alteration	2.08	6.15%	32	7.94%	19	13
JAK1/JAK2* alteration	4.86	4.13%	9	2.23%	7	2
***B2M* alteration**	0.70	10.56%	128	31.76%	47	81
***PTEN* alteration**	1.13	58.66%	123	30.52%	55	68
***TP53* alteration**	1.38	13.07%	197	48.88%	92	105
***STK11* alteration**	0.87	57.00%	107	26.55%	43	64
***MDM2* alteration**	0.86	61.87%	83	20.60%	33	50
***MDM4* alteration**	0.81	35.00%	152	37.72%	60	92
***EGFR* alteration**	0.88	60.84%	164	40.69%	67	97
***KRAS* alteration**	1.10	71.94%	92	22.83%	41	51
merged: response pathway	2.34	0.07%	90	22.33%	53	37

Supplementary Table S1. Resistance Mechanisms.

Appendix B

Multi-Omics Tumor Immunogenicity Score Predicts Immunotherapy Outcome and Survival

This paper was submitted to MDPI *Biology* on November 3, 2025, and was accepted for publication on November 27, 2025. In this study, we developed the MOTIscore to predict the outcomes of ICI treatment and survival rates. Similar to the LASSO machine learning model studied in the first paper (Appendix A), the MOTIscore integrates various biomarkers derived from WES and RNA-seq data. It leverages a straightforward weighted sum scoring scheme, the predictions of which are explainable and interpretable by design. This work not only explored ICI predictions in melanoma in terms of ROC AUCs, but also in terms of OS and PFS across various cancer types. Using GSEA, we discovered the role of highly expressed C-X-C motif chemokine ligands as independent predictors of ICI outcomes and survival. Of note, we applied for funding of this project in a similar form at the Bundesministerium für Bildung und Forschung, under the program "Nationale Dekade Gegen Krebs." See Appendix B.4 for the study protocol we used for the application, describing the MOTIscore project in a similar form. However, our funding application was rejected by the Bundesministerium in 2024.

B.1 Author Contributions

Prof. Dr. Sorin Armeanu-Ebinger (co-)supervised this project, curated the initial set of immunogenicity biomarkers, and inspected and corrected the CNVs baselines. Prof. Dr. Stephan Ossowski (co-)supervised this project and helped with data acquisition from the MTB. Dr. Markus Reitmajer and Prof. Dr. Andrea Forschner extracted the PFS of ICI-treated patients with melanoma from the MTB cohort. Amelie Knapp conducted the manual inspection of the clinical data of the false-positive MTB and gastric cancer samples. Alexan-

der Ott developed and maintained parts of the megSAP pipeline. Nadja Ballin and Dr. Christopher Schroeder helped designing the project. Prof. Dr. Michael Bitzer, Prof. Dr. Ghazaleh Tabatabai, Prof. Dr. Andreas Hartkopf, Dr. Thorben Groß provided pan-cancer samples of the MTB Tübingen. Öznur Öner developed and maintained the MTB infrastructure.

The candidate designed the project and performed the vast majority of the scientific research in this study. In detail, the candidate

- Designed the project,
- Managed the project,
- Applied for its funding and wrote the corresponding study protocol,
- Applied for approval of this project by the local institutional review board,
- Organized data acquisition from dbGaP and the local MTB,
- Processed all raw sequencing data, and conducted all necessary bioinformatics steps to extract biomarkers,
- Wrote the code for all data analyses,
- Wrote the manuscript,
- Created all figures in the manuscript,
- Submitted the manuscript, and
- Organized the editing of the paper during the review process.

B.2 Main Paper

biology

MDPI

Article

Multi-Omics Tumor Immunogenicity Score Predicts Immunotherapy Outcome and Survival

Axel Gschwind [1,2,*], Nadja Ballin [1], Alexander Ott [1], Andrea Forschner [3], Amelie Knapp [1], Öznur Öner [4], Michael Bitzer [4], Ghazaleh Tabatabai [5], Andreas Hartkopf [6], Thorben Groß [7], Markus Reitmajer [3], Christopher Schroeder [1], Stephan Ossowski [1,2,4,†] and Sorin Armeanu-Ebinger [1,†]

[1] Institute of Medical Genetics and Applied Genomics, University of Tübingen, 72076 Tübingen, Germany
[2] Institute for Bioinformatics and Medical Informatics, University of Tübingen, 72076 Tübingen, Germany
[3] Center for Dermatooncology, Department of Dermatology, University of Tübingen, 72076 Tübingen, Germany
[4] Center for Personalized Medicine Tübingen, University of Tübingen, 72076 Tübingen, Germany
[5] Center for Neurooncology, University of Tübingen, 72076 Tübingen, Germany
[6] Department of Women's Health, University of Tübingen, 72076 Tübingen, Germany
[7] Department of Medical Oncology and Pneumology, University of Tübingen, 72076 Tübingen, Germany
* Correspondence: axel.gschwind@med.uni-tuebingen.de
† These authors contributed equally to this work.

Simple Summary

Tumor immunogenicity is the ability of cancer cells to evoke an immune response. Several tumor properties have been associated with immunogenicity. However, only a few single biomarkers are used for clinical decision making, providing a fragmented view of the complex tumor-immune interactions. In this study, we propose a multi-omics tumor immunogenicity score (MOTIscore) that combines multiple biomarkers to improve the characterization of tumor immunogenicity. It integrates several biomarkers extracted from DNA and RNA sequencing data and applies weighted sum scoring. The MOTIscore integrates various biomarkers, including tumor mutation burden and immune cell infiltration. We evaluated MOTIscore as a predictor of the outcomes of state-of-the-art cancer immunotherapy. It was predictive of therapeutic success in both skin and gastric cancers, thereby outperforming the well-established tumor mutation burden and a machine learning model. The MOTIscore may help consider immunotherapy approaches for patients discussed in molecular tumor boards.

check for updates

Academic Editor: Ana Paula Silva de Azevedo-Santos

Received: 3 November 2025
Revised: 25 November 2025
Accepted: 27 November 2025
Published: 28 November 2025

Citation: Gschwind, A.; Ballin, N.; Ott, A.; Forschner, A.; Knapp, A.; Öner, Ö.; Bitzer, M.; Tabatabai, G.; Hartkopf, A.; Groß, T.; et al. Multi-Omics Tumor Immunogenicity Score Predicts Immunotherapy Outcome and Survival. *Biology* **2025**, *14*, 1698. https://doi.org/10.3390/biology14121698

Abstract

Background: Tumor immunogenicity is a concept for modeling the susceptibility of tumors to immune checkpoint inhibitors (ICIs) and other immunotherapies. Single biomarkers, such as tumor mutation burden (TMB) or *PDL1* expression, have been shown to correlate with ICI outcomes but are poor predictors of overall and progression-free survival (OS, PFS). Complex machine learning models that integrate multiple biomarkers have shown improved predictions but often lack clear a priori interpretability. In this study, we developed a coherent Multi-Omics Tumor Immunogenicity score (MOTIscore) that combines immunogenicity biomarkers derived from genomic and transcriptomic data and demonstrated its generalizability across multiple cancer types. Methods: Several immunogenicity biomarkers, including TMB, neoantigen burden, T-cell receptor repertoire, *PDL1* expression, *B2M* expression, and variants in pathways of ICI response and resistance, were integrated using a weighted sum scoring scheme. The weights were determined using statistical tests in a large melanoma ICI cohort. We compared the MOTIscore with a machine learning (ML) model trained using the same biomarkers and evaluated the model using melanoma, gastric cancer, and pan-cancer datasets. Results: MOTIscore achieved results similar to those of

Biology **2025**, *14*, 1698

the ML model in predicting ICI in melanoma and gastric cancer, with both outperforming TMB. Gastric cancer and melanoma patients with high MOTIscores had a significantly extended overall and progression-free survival. Gene set enrichment analysis revealed the enrichment of immune-related pathways in patients with high MOTIscores. Differential expression analysis between patients with high and low immunogenicity identified highly expressed C-X-C motif chemokine ligands as important characteristics associated with successful ICI therapy and significantly improved PFS. MOTIscores varied widely across cancers treated in the molecular tumor board at our hospital and showed distinct distributions between non-immunogenic and immunogenic cancer types. Conclusions: MOTIscore demonstrated improved ICI outcome predictions compared to single-omics biomarkers. Patients with higher tumor immunogenicity also show significantly improved OS and PFS in melanoma and gastric cancer. The results demonstrate the potential use of the MOTIscore to prioritize ICI in personalized cancer treatment. However, ICI outcomes and survival should be investigated in prospective studies, and additional cancer types and larger patient cohorts are needed.

Keywords: tumor immunogenicity; immune checkpoint inhibitors; immunotherapy; anti-PD1; multi-omics; next-generation sequencing; whole exome sequencing; bulk RNA sequencing

1. Introduction

Tumor immunogenicity plays an important role in state-of-the-art cancer treatment using immune checkpoint inhibitors (ICIs). Immunogenicity reflects the ability of cancer cells to be recognized and attacked by the immune system [1]. Various biomarkers, such as tumor mutation burden (TMB) and immune cell infiltration, are associated with tumor immunogenicity but provide only a fragmented view of the tumor immune microenvironment. The complex nature of the immune-tumor interface cannot be fully captured by a single biomarker and requires a holistic approach that takes biomarkers from multiple sources into consideration [2]. In line with this, most single-omics biomarkers have shown poor efficacy in predicting ICI treatment outcomes in several cancer types. For example, *PDL1* expression, quantified as Combined Positive Score (CPS) or Tumor Proportion Score (TPS), is an approved and commonly used immunohistochemical biomarker for the selection of patients for ICI. However, neither score is sufficiently selective for ICI [3,4]. Thus, many patients with low CPS or TPS respond well to ICI, whereas many patients with high CPS or TPS do not respond. This underscores the urgent need for the identification of more reliable ICI biomarkers and composite immunogenicity models to predict therapy response with higher accuracy [5].

Next-generation sequencing (NGS) of both tumor DNA and RNA can be employed to extract a diverse set of genomic and transcriptomic biomarkers that characterize immunogenicity [6]. Such biomarkers include, in addition to TMB and immune cell infiltration, several tumor genome-intrinsic factors, such as HLA genotypes or mutations in genes associated with ICI resistance. Biomarkers derived from whole-exome sequencing (WES) and bulk RNA sequencing (RNA-Seq) are thought to provide orthogonal and complementary information [7]. For example, information about mutational processes generating neoantigens can be retrieved from WES data, whereas RNA-Seq captures orthogonal transcriptional data, such as B- and T-cell repertoire and immune cell infiltration. Integrating several such biomarkers into a multi-omics immunogenicity model has the potential to

Biology **2025**, *14*, 1698

improve our understanding of the complex tumor-immune interface, thereby improving ICI outcome prediction [8].

Several methods have been proposed to combine multi-omics biomarkers for a comprehensive description of tumor immunogenicity, including statistical models and machine learning algorithms [9,10]. However, machine learning models often lack explainability and interpretability, which are important criteria for clinical usability [11]. The utilization of advanced algorithms as black boxes makes it difficult for clinicians to trust and understand how these algorithms reach their conclusions. Popular explainability techniques, such as Shapley Additive exPlanations (SHAP) or Local Interpretable Model-Agnostic Explanations (LIME), provide post hoc interpretations of the models [12]. However, these explanations can vary widely among patient cohorts, limiting their reproducibility and potential use in clinical settings.

Here, we propose a straightforward Multi-Omics Tumor Immunogenicity score (MOTIscore) that integrates several biomarkers derived from WES and RNA-Seq data. Both types of sequencing data are becoming increasingly available as part of routine personalized cancer treatment strategies. The MOTIscore model has a transparent design and can be interpreted a priori by providing the exact impact of each feature on the immunogenicity estimate. These are crucial prerequisites for potential clinical applications [13]. The MOTIscore leverages several biologically meaningful immunogenicity biomarkers, the selection of which was manually curated. It includes a comprehensive list of eight initial biomarkers: TMB [14], neoantigen burden [15], T-cell receptor (TCR) repertoire [16], ICI-resistance mechanisms [17,18], ICI-response mechanisms [19], HLA evolutionary divergence (HED) [20], *PDL1* expression [21], and *B2M* expression [18]. The model applies a weighted sum scoring scheme and determines the weights assigned to each biomarker using basic statistical techniques, such as Fisher's exact test or the Mann–Whitney U test [22].

While MOTIscore was designed as an interpretable methodology for integrating multi-omics biomarkers, this work also investigates its practical oncological relevance. We developed and validated the MOTIscore using publicly available cohorts of cancer patients who received ICI treatment, including those with melanoma and gastric cancer. The sequencing and clinical data provided by these studies were well-documented and all cases were annotated with ICI outcomes. An additional validation cohort comprised real-world patients with various cancers from the local molecular tumor board (MTB) of the University Hospital Tübingen in Germany [23]. The MTB patients were treated with various anti-cancer strategies, of which immunotherapy was rare due to a lack of robust biomarkers for the selection of patients for ICI. Hence, by introducing MOTIscore into MTB diagnostics, we aim to identify immunogenic tumors that are likely to benefit from ICI therapy. The use of multiple cohorts for evaluation allowed us to explore the generalizability of the MOTIscore model across various cancer types.

The evaluation of the MOTIscore proved its general ability to discriminate ICI responders from non-responders, thereby outperforming the traditional biomarker TMB. ICI-treated patients with high MOTIscores showed improved survival both in terms of progression-free survival (PFS) and overall survival (OS) in gastric cancer and melanoma. This suggests that the MOTIscore could facilitate improved selection of patients for ICI treatment. To compare the performance of the MOTIscore with a machine learning (ML) approach, we trained a multivariable least absolute shrinkage and selection operator (LASSO) regression model using the same set of input biomarkers. Both models achieved similar predictive performances. Furthermore, a gene set enrichment analysis (GSEA) revealed the role of highly expressed C-X-C motif chemokine ligands as predictive biomarkers for ICI outcomes and survival, thereby increasing the number of impactful features for immunogenicity models.

Biology **2025**, *14*, 1698

2. Materials and Methods

Our multi-omics model integrates multiple immunogenicity biomarkers derived from WES and RNA-Seq data into a weighted sum score. A flowchart of the model is provided in Supplementary Figure S1.

2.1. Initial Biomarkers

We derived genomic and transcriptomic biomarkers from paired tumor-normal WES and corresponding RNA-Seq tumor samples. All biomarkers have been associated with tumor immunogenicity and ICI response in previous studies. In detail, we curated the following initial list of immunogenicity biomarkers:

- Tumor Mutation Burden (TMB) [14]
- Neoantigen burden [15]
- T-cell receptor (TCR) repertoire [16]
- ICI-resistance mechanisms: *B2M* mutations and defects of the antigen processing machinery (APM), which includes the genes *TAP1*, *TAP2*, *TAPBP*, *CIITA*, *CALR*, and *CALX* [17,18]
- ICI-response mechanisms: mutations in *LRP1B* [19]
- HLA evolutionary divergence (HED) [20]
- *PDL1* expression (in counts per million (CPM)) [21]
- *B2M* expression (in CPM) [18]

We provide bioinformatic implementation details for each biomarker in Section 2.5.

2.2. Biomarker Selection and Weight Determination

We selected biomarkers and determined the weights for the MOTIscore using a cohort of melanoma samples for which both ICI treatment outcomes and sequencing data were available. The melanoma discovery cohort was assembled from six previously published melanoma studies. We defined binary outcomes as responders and non-responders according to the Response Evaluation Criteria in Solid Tumors (RECIST) [24]. Patients with complete and partial responses were classified as responders, whereas those with stable and progressive disease were considered non-responders.

To test whether a biomarker was significantly enriched in one of the outcome groups, we used Fisher's exact test for categorical biomarkers, and Mann–Whitney U test for continuous biomarkers. Biomarkers that did not show a significance level of at least $p < 0.05$ were excluded from MOTIscore. We then checked all biomarkers for mutual correlations using Spearman's correlation coefficient ρ. If two biomarkers showed a correlation coefficient of $\rho > 0.5$, the biomarker with the smallest effect size was excluded.

The weights assigned to each biomarker were calculated as $\log_{10}$ p-values, which were normalized by the sum of all weights of the biomarkers that were selected for the MOTIscore. Finally, we calculated the score as the weighted sum of the z-scores of the selected biomarkers.

2.3. Bioinformatics Pipeline

All tumor-normal WES and RNA-Seq samples were analyzed using the megSAP pipeline, available at GitHub https://github.com/imgag/megSAP (commit b148ff9, accessed on 12 September 2024). For the WES samples, the reads were aligned with Illumina DRAGEN 4.2.4 against GRCh38 [25]. Subsequently, DRAGEN was used as a somatic variant caller. All detected somatic variants were annotated using various tools and databases, including ensemble variant effect predictor (VEP) v112 and the Catalogue of Somatic Mutations in Cancer (COSMIC) v99 [26,27]. ClinCNV was used to identify somatic CNVs [28]. For the RNA-Seq samples, megSAP utilized STAR 2.7.11b for the alignment of the reads [29].

Biology 2025, 14, 1698

Read counts were estimated using subread featureCounts 2.0.6 and normalized to CPM [30]. After executing the basic analysis steps of megSAP, we derived additional biomarkers. For Implementation details, see that section.

For subsequent analyses of gene expression, we used the R package DESeq2 1.46.0 to detect differentially expressed genes (DEGs) and clusterProfiler 4.14.6 for gene set enrichment analysis (GSEA) [31,32].

2.4. Quality Control

We excluded every sample in this study that did not meet a minimum coverage of 60× for the tumor and 20× for the normal sample. In addition, we discarded all samples that showed an insufficient correlation of <80% between the SNPs of the tumor and normal samples, indicating potential sample confusion. If more than 70% of a sample's somatic variants appeared in gnomAD, we assumed sample contamination and excluded these samples from the cohort. As an additional quality filter, all samples with a tumor content of <30% were excluded from the study. The tumor content was determined using ClinCNV, and if no CNVs were detected using the median of the 15 highest variant allele frequencies (VAFs). Samples with zero detected somatic variants were visually inspected in IGV and discarded if the tumor content was below 30%.

At the level of SNVs and small indels, we required a minimum read depth of 20× for both the tumor- and normal samples. Only somatic variants with a VAF > 5%, which were present in at least three distinct sequencing reads, were considered. For somatic CNVs, we specified a minimum loglikelihood of >100. All CNV calls were inspected manually and the ClinCNV baselines were corrected if necessary.

2.5. Implementation Details

2.5.1. Target Region

The results presented in this study originated from different sequencing centers and enrichment kits. A common intersecting target region was constructed to avoid batch effects. In short, we determined the region that was covered at least 20× for each normal sample and cohort. We included every base with a coverage of 20× in at least half of the samples in the target region of a specific cohort. This study-specific region was then intersected with the coordinates of all exons (±2 bases). Subsequently, the common target region was obtained by intersecting all study-specific target regions. This intersection was used for the analysis of all samples and subsequent biomarker extraction, with the exception of CNV calling, which required cohort-specific target regions.

2.5.2. Tumor Mutation Burden

We calculated TMB as the total number of nonsynonymous somatic variants, normalized by the size of the target region in megabases. To avoid batch effects, we only considered somatic variants that lied in the intersecting exome target region. All variants with a predicted VEP impact higher than "protein altering variant" were considered as nonsynonymous.

2.5.3. Neoantigen Burden

We used pVACseq 4.4.1, a wrapper pipeline integrating several neoantigen prediction algorithms, for the prediction of neoantigens [33]. The pipeline was executed using three algorithms: NetMHCpan, NetMHC, and MHCflurry. Every predicted neoantigen candidate with a predicted median binding affinity of <500 nM was subsequently considered for the calculation of the neoantigen burden. As an additional filtering step, we excluded all neoantigen candidates that were not expressed in at least one sequencing read of the

Biology **2025**, *14*, 1698

RNA-Seq data. If deletions of HLA alleles were detected in a sample (see Section 2.5.7, we considered only those neoantigen candidates that bound to the remaining allele.

2.5.4. TCR Repertoire

TCR clones were extracted from the RNA-Seq data using TRUST4 v1.1.4 [34]. For further analysis, we included only clones that were detected at least twice in a sample. Subsequently, we used the number of distinct TCR α chain clones to calculate the Shannon entropy H:

$$H = -\sum_{i=1}^{N} p_i \log p_i$$

where p_i represents the relative frequency of the TCR clone i. N is the total count of the detected TCR clones. The TCR Shannon entropy serves as an indicator of TCR diversity in the sample. Therefore, it can be used as a proxy for the TCR repertoire and tumor infiltrating lymphocytes.

2.5.5. ICI-Resistance Mechanisms

We defined a binary biomarker that describes alterations in known ICI resistance genes. This biomarker was set to -1 if any deleterious variant occurred in the resistance mechanisms and 0 otherwise. The negative sign reflects the direction of the mutated resistance mechanism, as it leads to lower immunogenicity. We included any deleterious alterations that affected the antigen processing machinery genes, *TAP1*, *TAP2*, *TAPBP*, *CIITA*, *CALR*, *CALX*. In addition, we considered deleterious alterations of *B2M* [35].

Only homozygous deletions and variants with a high VEP impact or annotated COSMIC Cancer Mutation Census (CMC) levels in any of these seven genes were considered deleterious. For any alterations, we also required that they affected the main clone. For CNVs, we determined this directly from the ClinCNV calls. For the SNVs and indels, this was achieved by filtering out any variant with a variant allele frequency of less than 80% of the tumor clonality.

2.5.6. ICI-Response Mechanisms

LRP1B mutations are associated with higher immune cell infiltration and have recently been shown to improve ICI outcome [19]. We considered any somatic alteration in *LRP1B* with high VEP impact and CMC annotation as deleterious, as well as any homozygous deletion. That is, we excluded variants of unclear significance. We considered all mutations regardless of their clonality. If a mutation was present, this biomarker was set to 1, and 0 otherwise.

2.5.7. HLA Evolutionary Divergence

HLA evolutionary divergence (HED) measures the evolutionary protein distance between two HLA alleles [36]. In this study, we first determined HLA genotypes using our in-house implementation of hla-genotyper, available at GitHub https://github.com/axelgschwind/hla-genotyper (release tag 2022_05, accessed on 24 April 2025) [37]. We then examined whether there was an overlapping CNV that led to the loss of one HLA allele with a CNV clonality of at least 25%. As an additional check, we examined the ratio of assigned hla-genotyper read counts between the tumor and normal samples. We also assumed that an HLA allele was lost if there was a deviation of >40% in the read count ratios of the tumor and normal samples. If one HLA allele was lost, similar to homozygosity, HED was set to 0. HED between the two detected alleles was then measured using Grantham distance, a protein distance measure that integrates several physicochemical properties [38]. We determined HED only for the HLA binding grooves and not for the whole amino acid chain.

Biology **2025**, *14*, 1698

2.5.8. Gene Expression

Read counts were quantified using the RNA-Seq megSAP pipeline. Subsequently, the expression of the immune-related genes *PDL1* and *B2M* was quantified as counts per million (CPM) [18,21]. For the assembled ICI melanoma cohort, we corrected gene expression for batch effects using pyCOMBAT 0.3.3 [39].

3. Results

In this study, we integrated several immunogenicity biomarkers derived from WES and RNA-Seq data into a weighted sum score model. The weights assigned to each biomarker were determined using statistical tests (Fisher's exact test and Mann–Whitney U test) comparing two groups (RECIST responders vs. non-responders) of the melanoma meta-cohort with available ICI outcome data. Biomarkers that did not meet the minimum significance threshold of $p < 0.05$ were excluded. Features with high mutual correlation coefficients were filtered to avoid bias in the score weights. Subsequently, we calculated the MOTIscore using z-standardized biomarkers. The score was then evaluated using three distinct cohorts, two of which had annotated ICI response data. Supplementary Figure S1 shows an outline of the proposed approach. MOTIscore was benchmarked against a LASSO model using the same set of biomarkers. The methodology of the LASSO model has been described elsewhere [9].

3.1. Cohorts

We developed and evaluated MOTIscore using three distinct datasets. Two of these cohorts, melanoma ($n = 225$) and gastric cancer ($n = 33$), were assembled from public studies and evaluated using ICI outcome data. The third, pan-cancer MTB cohort ($n = 559$), had only partially annotated ICI outcome data and represents heterogeneous cancer patients from the local molecular tumor board of the University Hospital Tübingen, Germany. In the MTB cohort, we identified samples with very high MOTIscore to consider patients with highly immunogenic tumors who could potentially benefit from ICI therapy.

In detail, the melanoma cohort ($n = 225$) was assembled from six studies for which pre-ICI-treatment sequencing data (WES and RNA-Seq) were publicly available: Amato et al., Hugo et al., Liu et al., Pyke et al., Riaz et al., and Wolchok et al. [40–45]. A total of 27 samples were excluded based on our quality control criteria. This resulted in a discovery cohort of 225 ICI-treated melanoma patients for whom paired tumor-normal WES and bulk RNA-Seq data were available. According to the RECIST classification, 98 patients were classified as responders and 127 as non-responders, respectively.

The ICI gastric cancer dataset ($n = 45$) was published by Kim et al. with publicly available pre-ICI-treatment sequencing data [46]. After quality control with 12 removed samples, this dataset resulted in 33 ICI-treated patients with gastric cancer, of whom seven were responders and 26 were non-responders.

The MTB cohort consisted of patients who sought medical advice at the MTB in Tübingen between 2020 and 2024 and who provided informed consent to use their sequencing data for clinical research. After quality control, which removed 91 samples, the MTB cohort comprised 559 patients. It contains several cancer types, with brain tumors and melanomas being the most frequent. It comprises sequencing data at various time points, that is, pre- and post-treatment samples. The patients included in the MTB cohort received various anti-cancer drugs, including ICIs. An overview of the MTB cohort and cancer types is provided in Supplementary Table S1.

Biology **2025**, *14*, 1698

3.2. Selection of Biomarkers and Weight Determination

We determined the weights for the MOTIscore weighted sum scoring model using the ICI melanoma cohort of 225 patients, of whom 98 were responders and 127 were non-responders. Five biomarkers remained after filtering out features that did not meet the minimum significance level of $p < 0.05$ for discriminating responders from non-responders. TMB, neoantigen burden, mutations in response pathways, TCR repertoire, and *PDL1* expression were retained as biomarkers for the MOTIscore. A subsequent correlation analysis revealed that TMB and neoantigen burden were highly correlated biomarkers, with a correlation coefficient of $\rho > 0.5$ (Supplementary Figure S2a,b). TMB had a larger effect size than the neoantigen burden. Hence, neoantigen burden was removed as a biomarker from the MOTIscore. Thus, our final list included the following four biomarkers and their corresponding normalized weights:

- TMB: 0.345
- ICI-Response pathways: 0.208
- TCR repertoire: 0.320
- *PDL1* expression: 0.127

3.3. ICI Outcome Prediction and Survival Analysis

We evaluated MOTIscore as a predictor of ICI outcome in the melanoma ($n = 225$) and gastric cancer ($n = 33$) cohorts. First, we determined the performance of MOTIscore using receiver operating characteristic (ROC) curves. In Figure 1a,b, we show the ROCs for both cohorts, with the outcome defined as responders and non-responders. For comparison, we also show the ROC curves of the current gold standard TMB with the FDA-approved cutoff of 10 mutations per megabase [47]. For both cancer types, MOTIscore achieved higher ROC areas under the curve (AUCs) than TMB alone. For melanoma samples, our score achieved an ROC AUC of 0.66 versus 0.63 (TMB), whereas it reached an ROC AUC of 0.93 versus 0.79 (TMB) for gastric cancer patients.

Next, we benchmarked the performance of MOTIscore against a machine learning LASSO model, the methodology of which has recently been described [9]. The LASSO model was trained on the melanoma cohort ($n = 225$) using the same set of biomarkers as used for MOTIscore. The scores of both models were highly correlated in both the ICI melanoma and ICI gastric cancer cohorts (Supplementary Figure S3). The ROC curves of the LASSO model are shown in green in Figure 1a,b for the melanoma ($n = 225$) and gastric cancer ($n = 33$) cohorts, respectively. With ROC AUCs of 0.70 for melanoma and 0.87 for gastric cancer, both the LASSO model and the MOTIscore achieved similar results. However, the MOTIscore achieved a higher ROC AUC in the gastric cancer cohort, indicating good generalizability from melanoma to gastric cancer. It is important to note that the LASSO and MOTIscore ROC AUCs for melanoma were calculated using their training cohorts, likely leading to an overestimation of the ROC AUCs in melanoma due to overfitting.

Next, we determined a cutoff for the MOTIscore in the melanoma cohort by maximizing Youden's index, ensuring an ideal tradeoff between sensitivity and specificity [48]. The cutoff was found to be 0.540, as indicated by the black dot in Figure 1a. Subsequently, we used this threshold to stratify our data for the analysis of PFS and OS. OS data were available for the Liu et al. sub-cohort of melanoma ($n = 111$), and PFS data were available for the Kim et al. gastric cancer cohort ($n = 33$). MOTIscore clearly discriminated responders from non-responders, with a 12-month OS rate of 85% versus 61% in the Liu et al. melanoma cohort, and a 12-month PFS rate of 56% versus 0% in the gastric cancer cohort. The corresponding Kaplan–Meier estimators are shown in Figure 1c,d. A Cox model analysis revealed hazard ratios (HR) of 0.48 ($p = 0.0193$) for melanoma, and of 0.14

Biology **2025**, *14*, 1698

(p = 0.0017) for gastric cancer, indicating a much lower relapse risk for patients with high MOTIscores.

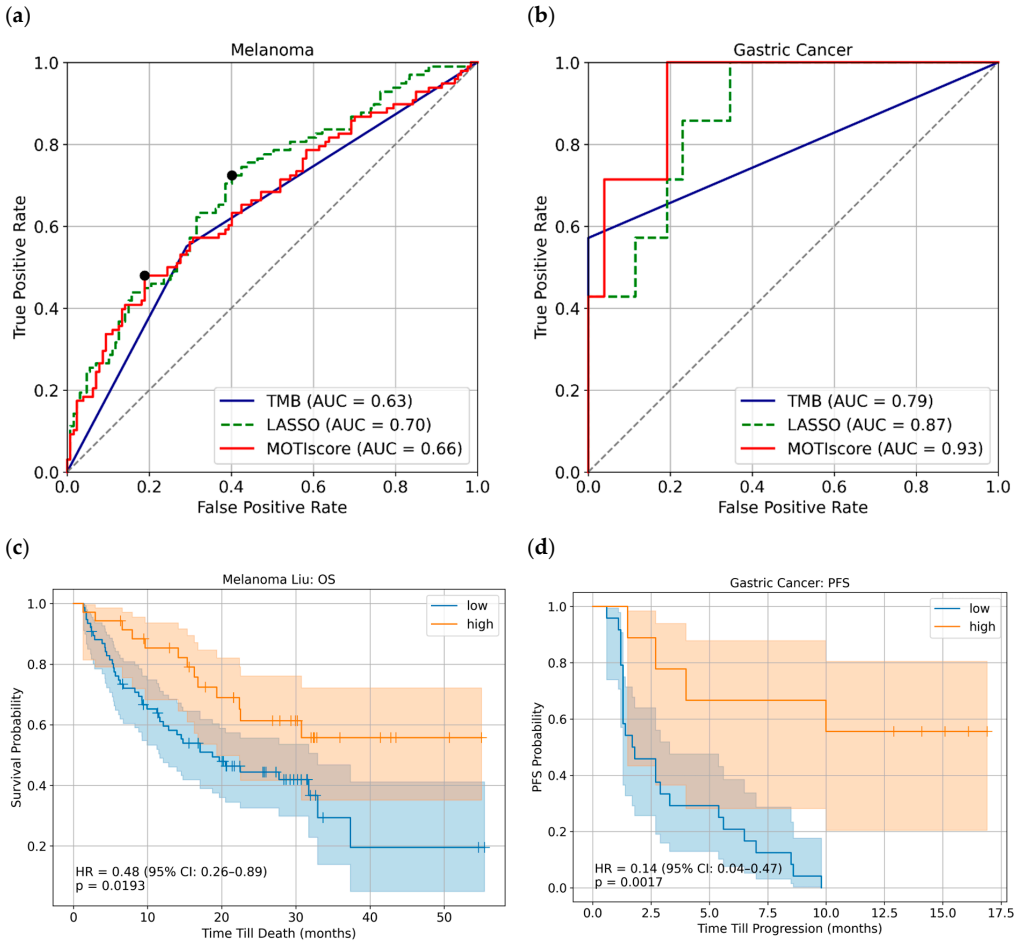

Figure 1. Performance of the MOTIscore and LASSO as predictors of ICI outcomes in (**a**) melanoma and (**b**) gastric cancer. The MOTIscore achieved a higher ROC AUC performance in both groups than TMB alone. The black dot in (**a**) denotes the optimal cutoff, determined using Youden's index. (**c**) Kaplan–Meier curves of OS in the Liu et al. melanoma cohort. Patients with high MOTIscores experienced better OS, with an HR of 0.48 (95% CI: 0.26–0.89, p = 0.0193). (**d**) Kaplan–Meier curves of PFS in the Kim et al. gastric cancer samples. Patients with high MOTIscores clearly exhibited an extended PFS, with an HR of 0.14 (95% CI: 0.04–0.47, p = 0.0017).

A subsequent analysis of the maximum tumor size reduction in gastric cancer patients (n = 33) after treatment showed additional predictive value of the MOTIscore, Figure 2a. MOTIscores and the corresponding molecular and clinical features are provided in Supplementary Table S2 for the Kim et al. gastric cancer cohort. Of the nine gastric cancer patients with high MOTIscores, eight patients experienced a reduction in tumor size, although not all were classified as responders according to the RECIST cutoffs. MOTIscore was significantly inversely correlated with the change in tumor size after treatment, with a Spearman correlation coefficient of $\rho = -0.51$ and p = 0.0026 (Figure 2b). This underscores the predictive power of our score beyond the "official" RECIST cutoffs.

Biology **2025**, *14*, 1698

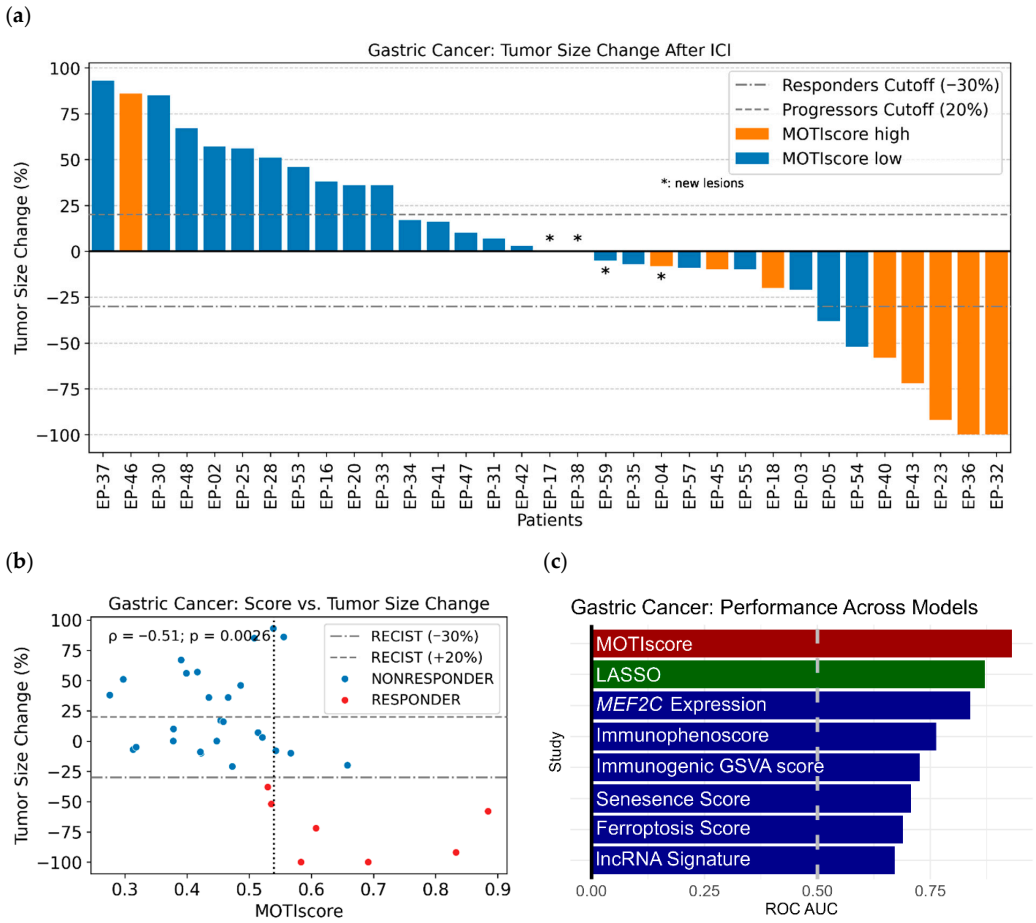

Figure 2. (**a**) Maximal tumor size changes in gastric cancer patients visualized as a waterfall plot. The dotted lines indicate the RECIST classification cutoff values. Bars in orange indicate patients with high MOTIscores whereas blue bars denote patients with low scores. (**b**) Scatter plot of the MOTIscore against the changes in tumor size. The score was inversely correlated with the change in tumor size (Pearson $\rho = -0.51$ and $p = 0.0026$). The data used to generate this figure were extracted from [46]. (**c**) ROC AUCs of different models predicting ICI outcomes in the Kim et al. gastric cancer cohort. The MOTIscore (red) and the LASSO model (green) exhibited a higher performance than the RNA-based single-omics studies we found (blue).

3.4. Benchmarking MOTIscore Against Existing Scores

The gastric cancer cohort (n = 33) was used for method benchmarking in various publications. Several authors have evaluated their models using ROC AUC curves, making their results comparable to those of our MOTIscore benchmark. We conducted a paper search using Google Scholar with the search term '"PRJEB25780" and "ROC"' (http://scholar.google.com, accessed on 12 March 2025) to find existing works. After reviewing the search results, we identified six studies that used the Kim et al. gastric cancer cohort and evaluated their models using ROC AUCs, with the outcome defined in terms of RECIST [49–54]. In contrast to our multi-omics approach, all other models were based on single-omics RNA-Seq data. The methodologies used in the existing studies varied widely. Two models were designed to leverage expression of immunogenicity genes, one model was based on the expression of senescence genes, and one model on the expres-

Biology **2025**, *14*, 1698

sion of ferroptosis genes. One study made predictions based on *MEF2C* expression. Finally, one study made predictions using a long non-coding RNA (lncRNA) signature.

Figure 2c shows a bar plot comparing the ROC AUCs of these studies with MOTIscore. ROC AUCs of RNA-based models ranged from 0.67 to 0.84, with a median value of 0.72. MOTIscore outperformed the RNA-based models with an ROC AUC of 0.93. Note that the effective cohort size of the benchmark tests varies, as the quality control filters of the studies may vary, and because we could only utilize cases having both DNA and RNA-Seq.

3.5. Gene Set Enrichment Analysis

Next, we conducted an analysis using DESeq2 to identify differentially expressed genes (DEGs) and pathways enriched for DEGs in the RNA-Seq samples. We stratified patients into two groups with high and low MOTIscores. Based on the detected DEGs, we performed GSEA for the Kim et al. gastric cancer cohort (n = 33) using the MSigDB Hallmark gene sets [55]. This analysis revealed several enriched immune-related gene sets in the group with high MOTIscores (Figure 3a). After applying significance thresholds (adjusted $p < 0.001$ and normalized enrichment score (NES) ≥ 2), the following six Hallmark gene sets were enriched in gastric cancer: interferon gamma response, interferon alpha response, allograft rejection, inflammatory response, *IL6* JAK *STAT3* signaling, and *TNFA* signaling via NF-κB. All enriched gene sets describe immune system related processes.

For melanoma, we performed another GSEA using the Liu et al. melanoma ICI subcohort (n = 111). Six significantly enriched Hallmark gene sets were identified in the group with high MOTIscores: interferon gamma response, allograft rejection, inflammatory response, interferon alpha response, *IL6* JAK *STAT3* signaling, and complement system (Figure 3b). Similar to gastric cancer, all enriched pathways describe processes of the immune system. The gene sets found in melanoma corresponded to those identified in patients with gastric cancer, with an overlap of four pathways.

3.6. C-X-C Motif Chemokine Ligands Predict ICI Outcome and Survival

Many immune-related genes were significantly up-regulated in the group with high MOTIscores, as indicated by the small triangles in the volcano plots for gastric cancer (n = 33) and the Liu et al. melanoma cohort (n = 111), Figure 3c,d. We defined a gene as immune-related if it occurred in one of the MSigDB Hallmark gene sets describing immune system processes. Importantly, the C-X-C motif chemokine ligands *CXCL9*, *CXCL10*, and *CXCL11* were significantly up-regulated in patients with high MOTIscores in both cancer types, suggesting the presence and activation of immune cells in these tumors. To confirm these findings, we conducted an additional analysis of DEGs in the MTB cohort (n = 559), using the MOTIscore as the group discriminator. At least two-fold upregulation of *CXCL9*, *CXCL10*, and *CXCL11* was observed in all cancer types including melanoma (n = 77), breast cancer (n = 40), brain cancer (n = 198), and lung cancer when comparing samples with high to low MOTIscores (Figure S4), with significance for melanoma and breast cancer. Figure 3f shows box plots of the expression distribution of *CXCL9*, *CXCL10*, and *CXCL11* in MTB brain, lung, breast, and melanoma samples, with the samples stratified into MOTIscore-high and MOTIscore-low groups. The median expression of all three genes was lowest in brain and lung cancers, whereas higher expression values were detected in melanoma and breast cancer. We used the Mann–Whitney U test with Benjamini–Hochberg correction to detect significant differences in the distribution between samples with low and high MOTIscores. Significant differences were observed in melanoma, breast, and brain malignancies, whereas no significant differences were observed in lung cancer.

Biology **2025**, *14*, 1698

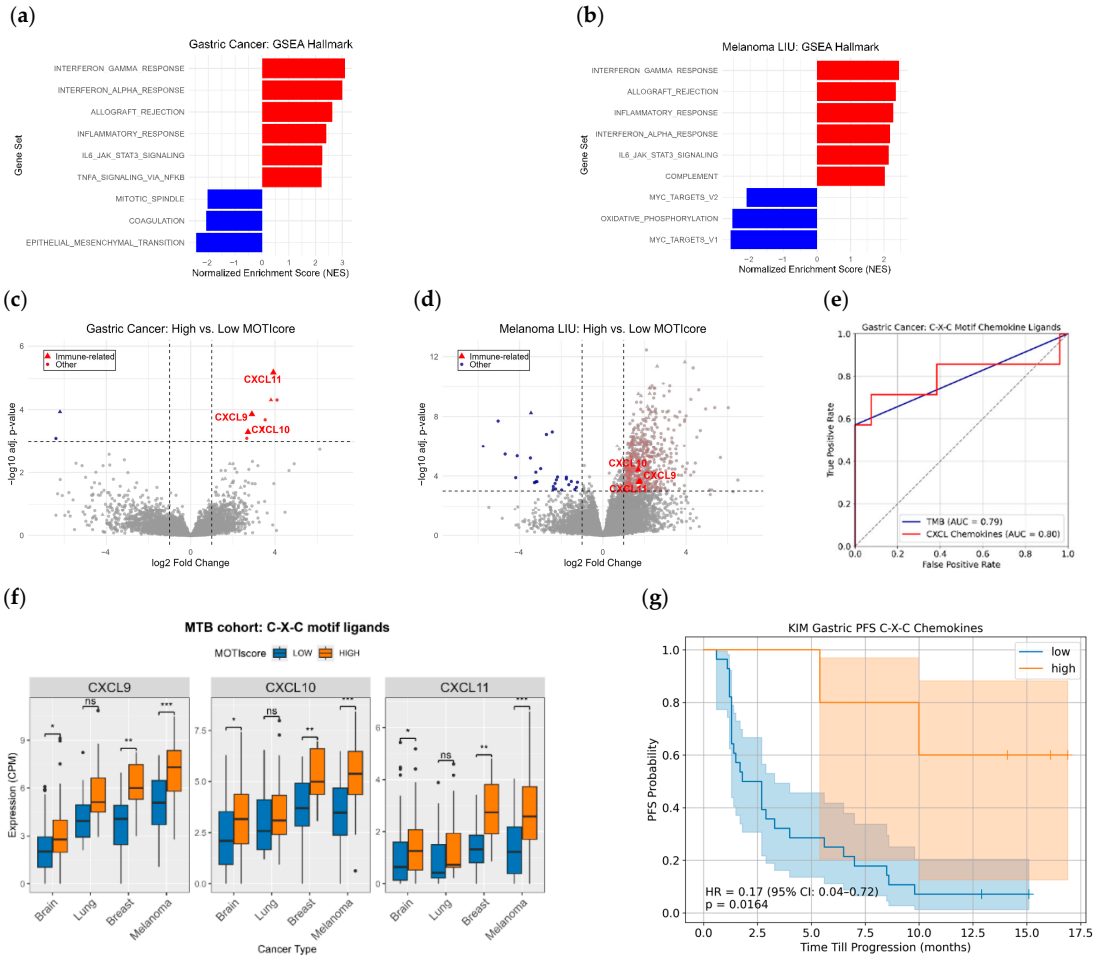

Figure 3. (**a**,**b**) GSEA results for the gastric cancer ($n = 33$) and the Liu et al. melanoma ($n = 111$) cohorts using the Hallmark gene sets. Immune-related pathways were enriched in the MOTIscore-high group, with significance thresholds of NES ≥ 2 and of adjusted $p < 0.001$. Enriched pathways are indicated in red, whereas depleted pathways are blue. (**c**,**d**) Volcano plots of the gastric cancer cohort and the Liu et al. melanoma cohort, with the MOTIscore as the group discriminator. Many immune-related genes (indicated by triangles (▲)) were significantly up-regulated. We used significance cutoffs of $p < 0.001$ and a $\log_2$ fc ≥ 1. Up-regulated genes are denoted in red, down-regulated genes in blue, and non-significant genes in gray. (**e**) The combined expression of *CXCL9*, *CXCL10*, and *CXCL11* was predictive of ICI outcomes in gastric cancer ($n = 33$), with an ROC AUC of 0.80. (**f**) Distribution of the C-X-C motif chemokine ligands expression across cancer types in the MTB cohort. Significance levels are denoted with asterisks (ns: non-significant, *: $p < 0.05$, **: $p < 0.01$, ***: $p < 0.001$), and outliers are represented with black dots. (**g**) Kaplan–Meier curves for this combined biomarker. Patients with high levels exhibited a significantly extended PFS in gastric cancer, with an HR of 0.17 ($p = 0.0164$).

The genes *CXCL9*, *CXCL10*, and *CXCL11* are a crucial components of the C-X-C motif chemokine family, which plays an important role in the attraction and activation of immune cells [56]. Recent studies have suggested predictive relevance of these genes for ICI treatment [57]. Thus, we conducted an exploratory analysis to investigate their effects on treatment outcome in the cohorts used in this study. To investigate the predictive value of *CXCL9*, *CXCL10*, and *CXCL11* for ICI outcomes, we first evaluated each gene individually.

Biology **2025**, *14*, 1698

We found that the expression of each gene was a modest predictor of ICI outcomes in the ICI melanoma (n = 225) and gastric cancer cohorts (n = 33), with ROC AUCs ranging from 0.53 to 0.79 (Supplementary Figure S5a,b). We then merged the genes into a single biomarker using the mean value of their $\log_2$ fc gene expression. This combined C-X-C motif chemokine expression marker was predictive of ICI outcomes in terms of both ROC AUCs and survival. In gastric cancer (n = 33), the combined biomarker achieved an ROC AUC of 0.80, thereby outperforming TMB (Figure 3e). In the ICI melanoma cohort (n = 225), we observed an ROC AUC of 0.57, which was better than random but was outperformed by TMB (Supplementary Figure S5c).

We determined a cutoff value of this combined biomarker by maximizing Youden's index in the melanoma ICI cohort (n = 225). The ICI cohorts were then stratified into two groups based on high and low C-X-C- motif chemokine ligand expression. Figure 3g shows the corresponding Kaplan–Meier curve for the gastric cancer cohort (n = 33). Cox model analysis revealed a significantly (HR = 0.17, p = 0.0164) extended PFS in patients with highly expressed C-X-C motif chemokine ligands. The Kaplan–Meier curves for the Liu et al. melanoma cohort (n = 111) suggest an extended OS in melanoma (HR = 0.72), but this was non-significant (p = 0.2240), Supplementary Figure S5d.

3.7. MOTIscore Distribution Across Cancer Types and Clinical Significance in MTB Cohort

In this section, we investigate the distribution of the MOTIscore within the heterogeneous pan-cancer MTB cohort (n = 559). All patients were sequenced between 2020 and 2024 at the local MTB and received various anti-cancer drugs [23]. This MTB cohort was highly heterogeneous; most tumors were advanced, and patients had received multiple diverse cancer therapies. The most abundant cancer types were malignancies affecting the brain (n = 198, ICD10 C70 and C71), melanoma (n = 77, ICD10 C43), breast (n = 40, ICD10 C50), and lung (n = 29, ICD10 C34). All other cancer types present in the MTB cohort had <25 samples and were summarized as "other" (n = 215). A complete description of the cohort is provided in Supplementary Table S1.

Figure 4a shows boxplots of the MOTIscore for the most abundant cancer types in the MTB cohort. The distribution of the scores varied widely across cancer types. The highest median MOTIscores were found in melanoma and lung cancer, whereas brain and breast cancers showed a very low median score. A Kruskal–Wallis test revealed significant differences in the MOTIscore distributions between melanoma and lung (higher scores) versus brain and breast (lower scores), Figure 4a. Moreover, brain cancer showed the lowest overall distribution of scores (lowest 75% quantile). The median MOTIscores of all cancer types were below Youden's cutoff of 0.540, highlighting the potential use of the MOTIscore in identifying few patients who may benefit from ICI. In both melanoma and lung cancer, approximately 45% of patients had a high MOTIscore, matching previously published estimates of patients potentially responsive to ICI in these cancer types [58]. In breast cancer, less than a quarter of patients showed a high MOTIscore. However, these patients might be of particular interest for the selection of ICIs, even if immunotherapy is not part of the standard treatment for this cancer entity (Figure 4a and Supplementary Table S1). For brain cancer, we only observed a few outliers above the threshold, which was expected, as brain has low immunogenicity. We speculate that in the outlier patients, with sometimes very high MOTIscore, the blood–brain barrier is compromised, allowing immune cells to enter in large amounts. Furthermore, glioblastomas pre-treated with a chemotherapy often exhibit hypermutation, leading to a very high TMB [59].

A total of 52 patients in the MTB cohort received ICI treatment. ICI treatments were usually stopped due to disease progression, but it remains unclear whether these endpoints were censored or whether progression occurred. Thus, we termed this duration the ICI-

Biology **2025**, *14*, 1698

specific PFS. ICI-specific PFS in melanoma (n = 39) and other cancer types (n = 12) was extended in patients with high MOTIscores, Figure 4b. The effect was large, with effect sizes of 0.8 in melanoma and of 1.7 in the other cancer entities, as was determined using Cohen's d. The extended ICI-specific PFS was significant ($p < 0.05$), as proven using the Mann–Whitney U test with Benjamini–Hochberg correction for multiple hypothesis testing.

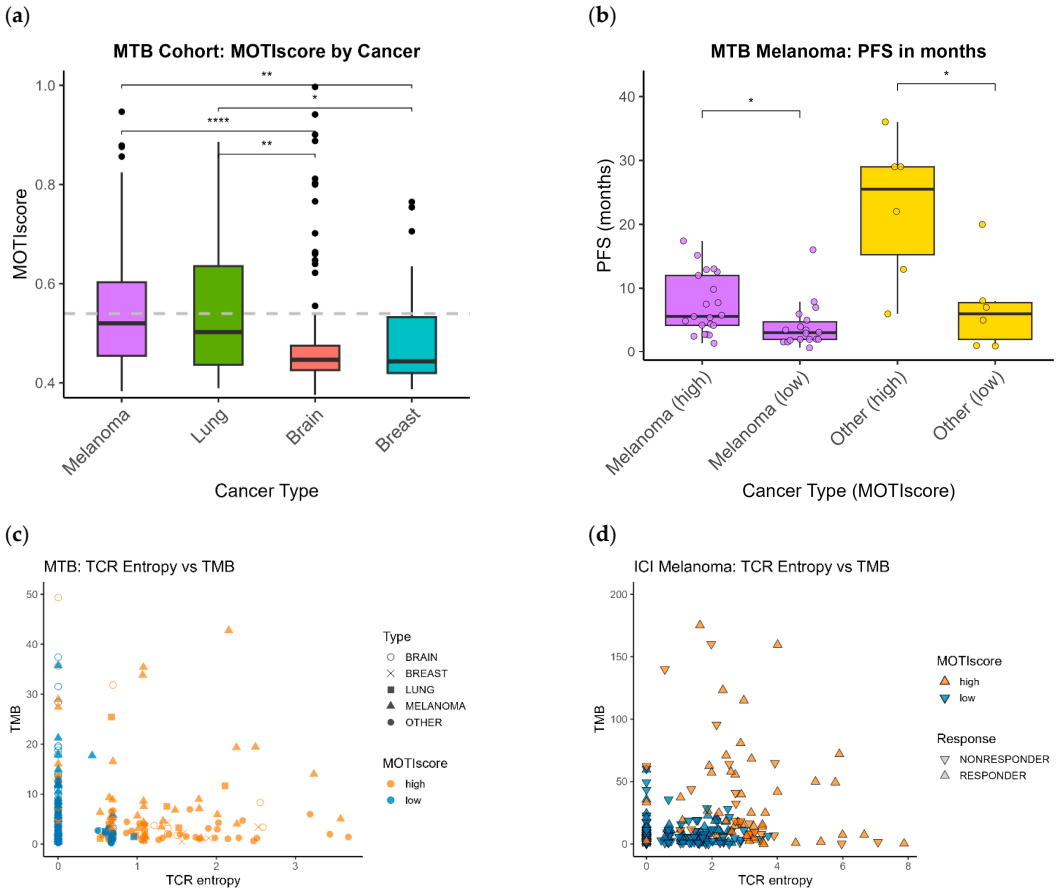

Figure 4. (**a**) Distribution of MOTIscores in cancer entities with more than 25 samples in the MTB cohort. Kruskal–Wallis test followed by Dunn's test with Benjamini–Hochberg correction revealed significant differences in the score distributions. The dashed line depicts the cutoff value of 0.540, which was determined using Youden's index. (**b**) ICI-specific PFS of MTB melanoma (n = 39) and other cancer types (n = 12) for which ICI duration was available. Patients with high MOTIscores exhibited significantly higher ICI-specific PFS than those with low MOTIscores did. The asterisks denote significance levels (*: $p < 0.05$, **: $p < 0.01$, ****: $p < 0.0001$) (**c**) Scatter plot of TCR repertoire versus TMB in the pan-cancer MTB cohort (n = 559). Orange symbols indicate samples with high MOTIscores, whereas blue symbols represent samples with low MOTIscores. The cancer type is denoted by shape. (**d**) TCR repertoire versus TMB in the ICI melanoma cohort (n = 225). Responders are denoted with ▲, and non-responders with ▼.

3.8. Clinical Significance of the TCR Repertoire Biomarker

The two main contributing biomarkers to the MOTIscore (highest weights) were TCR repertoire and TMB. Samples with high TCR repertoire were likely classified as MOTIscore-high. In contrast, high TMB values with low TCR entropy did not necessarily lead to high MOTIscores in the MTB pan-cancer and melanoma cohorts. In Figure 4c,d, we show scatter

Biology 2025, 14, 1698

plots of TMB versus TCR repertoire in the MTB pan-cancer (n = 559) and the ICI melanoma cohorts (n = 225). MOTIscore-high samples are shown in orange, whereas MOTIscore-low samples are denoted in blue. Figure 4c revealed mainly melanoma, but also brain, lung, and other types of tumor samples showing concomitant MOTIscore-high and high TCR repertoire in the MTB cohort (n = 559). These patients may benefit from and should be considered for ICI therapy as part of a personalized treatment strategy. Indeed, most responders in the ICI melanoma cohort (n = 225), Figure 4d, had concomitant high TCR entropy and MOTIscore.

Using the ICI melanoma cohort (n = 225), we analyzed the proportion of responders depending on the TCR repertoire and TMB. The samples were stratified into four groups based on high and low TCR repertoires, and high and low TMB statuses (Table 1). The fewest responders (25.7%) were found in the group with low TCR repertoire and low TMB. Conversely, the highest proportion of responders (67.9%) was found in the group with both high TMB and TCR repertoire. Interestingly, the group with high TCR repertoire but low TMB also showed an increase in responders (41.7% compared to 25.7%), supporting our suggestion to use TCR repertoire as part of the MOTIscore and as an independent biomarker for selecting patients for ICI, even at low TMB status. Hence, our findings provide further evidence that integrating RNA- and DNA biomarkers can help identify patients who may benefit from ICI treatment.

Table 1. We stratified the patients in the ICI melanoma cohort (n = 225) into four groups depending on their TMB and TCR repertoire levels. Both biomarkers were predictive of the outcomes. However, most responders were found in the group with both a high TMB and TCR repertoire. Conversely, the response rate was the lowest in patients with low levels of both biomarkers.

TCR Repertoire	TMB	Non-Responders	Responders	Response Rate
Low	Low	55	19	25.7%
High	Low	35	25	41.7%
Low	High	18	20	52.6%
High	High	17	36	67.9%

4. Discussion

The multi-omics tumor immunogenicity score outperformed TMB in both melanoma and gastric cancers, as demonstrated by better ROC AUCs, Figure 1a,b. Furthermore, we showed that RNA-derived biomarkers, such as TCR repertoire and C-X-C- motif chemokine ligand expression, discriminate between responders and non-responders and are predictive of PFS and OS in some cancer types. These findings confirm the hypothesis that integrating multiple predictive biomarkers derived from both DNA and RNA sequencing can lead to improved overall predictions compared with the use of single biomarkers as predictors. This was also evident in our analysis of the ICI melanoma cohort, in which the proportion of responders was highest in patients with high TMB and TCR repertoire (Table 1). However, MOTIscore only moderately improved predictions in terms of ROC AUCs. Nonetheless, additional analyses (Figures 1c,d and 4b) showed that patients with high MOTIscore had significantly longer PFS and a higher chance of strong shrinkage of the tumor size. Moreover, our analysis demonstrated that MOTIscore generalizes well to different cancer types. In patients with melanoma, those with high MOTIscores exhibited improved OS and ICI-specific PFS. Similarly, in patients with gastric cancer, high MOTIscores were associated with an extended PFS and high probability of tumor shrinkage. These results underscore the potential use of MOTIscore as a decision support tool for ICI therapy in clinical settings.

Biology **2025**, *14*, 1698

The MOTIscore is straightforward to calculate and provides transparent results by design. As WES and RNA-Seq data become increasingly available in routine clinical oncology, our score can be calculated as part of standard genetic tumor diagnostics. No additional diagnostic tests are necessary because the MOTIscore only leverages molecular biomarkers derived from NGS data. However, potential clinical applications will require validation studies in prospective studies with separate cancer entities. The MOTIscore could help to select patients with high chances of success for ICI treatment. Our approach can easily be extended by simply adding and reweighting additional molecular features if additional biomarkers are of interest or are discovered. For instance, the expression of C-X-C chemokine ligands discovered in this study could be added as a feature to the MOTIscore in a prospective study.

The GSEAs of melanoma and gastric cancer revealed intersecting immunogenicity gene sets that were enriched in both cancers, Figure 3a,b. This overlap might indicate that the MOTIscore captures the general underlying molecular tumor properties, leading to the aforementioned good generalizability of the score. The C-X-C motif chemokine ligand genes *CXCL9*, *CXCL10*, and *CXCL11* were up-regulated in patients with high MOTIscores in gastric cancer and melanoma (Figure 3c,d), and we confirmed this finding for different cancer types in the independent MTB cohort (Figure 3f). Consistent with the role of the C-X-C motif pathway in immune cell activation and attraction [56], we showed that the expression of these three genes was a good predictor of ICI outcomes and survival in both melanoma and gastric cancer (Figure 3e,g and Supplementary Figure S4).

For gastric cancer, we compared the predictions of MOTIscore with those of existing models (Figure 2c). All benchmark studies we identified by the literature search applied single-omics models based only on RNA-Seq, whereas MOTIscore and our LASSO model were based on both WES and RNA-Seq. Both multi-omics models outperformed single-omics models in predicting ICI outcomes. This finding suggests that integrating various multi-omics biomarkers provides a more holistic characterization of tumor immunogenicity, thereby leading to better ICI outcome predictions [60,61]. However, we could only compare the outcomes with respect to RECIST, but not survival (PFS or OS), as survival analysis was not available for the other studies.

Our pan-cancer analysis using the local MTB cohort revealed distinct MOTIscore distributions across cancer types, particularly between immunogenic tumors and tumors that are normally considered to have low immunogenicity (Figure 4a). This showed that the MOTIscore also reflects molecular immunogenic properties at the level of cancer types, reflecting cancer type-specific treatment strategies. The variation in the MOTIscore distributions aligns well with the immunologic classification of tumors as "hot" (e.g., melanoma, lung and gastric cancer) and "cold" (e.g., glioblastoma, meningioma, and breast cancer) [62]. MOTIscore may help identify hot tumors, even in typically "cold" cancer types, because it integrates several properties frequently used to distinguish hot and cold tumors, such as TMB and tumor-infiltrating lymphocytes. For instance, 13 of 40 of the MTB breast cancer patients had high MOTIscores (>0.54), suggesting a potential clinical benefit for these patients from ICI, although breast cancer is normally considered a cold tumor type [63].

We conducted a separate analysis of the TCR repertoire and TMB, Figure 4c,d and Table 1, because these two biomarkers contributed the most to the MOTIscore with weights > 0.3. Our in-depth analysis showed that both biomarkers were predictive of ICI outcomes in melanoma, Table 1. The poorest outcomes were observed in patients with both a low TCR repertoire and TMB, but interestingly, the group of patients with low TMB but high TCR repertoire had a strongly increased fraction of responders. Hence, TCR repertoire should be used in addition to TMB as a criterion for selecting patients for ICI

Biology 2025, 14, 1698

therapy. Other recent studies have similarly demonstrated the independent predictive performance of genomic and transcriptomic biomarkers in melanoma [9].

The neoantigen burden was highly correlated with TMB and was subsequently excluded from the MOTIscore (Supplementary Figure S2). This finding confirms that TMB can be used as a proxy for neoantigen burden [64]. However, recent studies have suggested that the immune response is mostly driven by very few or a single high-quality neoantigens [65]. Thus, the contribution of individual neoantigens could be a better predictor of anti-tumor immunogenicity than neoantigen burden or TMB. By focusing only on TMB, we might underestimate the immunogenicity of tumors with low TMB, in which only a few highly potent neoantigens drive anti-tumor immunogenicity. Conversely, we could easily overestimate immunogenicity in tumors with high TMB in which no immunogenic antigens were present. Future studies should include features describing neoantigen quality rather than quantity, with an appropriate neoantigen prioritization algorithm [66].

Our study had several other limitations. First, some biomarkers were sparsely enriched in the melanoma discovery cohort. For instance, we detected only two cases with alterations in the ICI-resistance pathways. These two melanoma cases exhibited homozygous deletions in *B2M*, a strong predictor of ICI-resistance, and both were indeed non-responders with progressive disease. However, ICI-resistance mutations were rejected as biomarkers because they were not significantly associated with ICI outcomes due to their rarity. Hence, a larger discovery cohort would likely lead to a higher number of significant biomarkers that could be included in MOTIscore. An important limitation was our restriction to samples with a tumor purity >30%, although purity is also a molecular tumor property relevant for ICI efficacy [67]. Therefore, this filter may have led to bias. Apart from molecular genetic data, we did not incorporate additional clinical data into MOTIscore, limiting its applicability to certain patients. For example, patients with brain metastases may not benefit from ICI despite high MOTIscores, as we observed in one MTB melanoma patient with brain metastasis. Given the nature of the available data, it remains unclear whether MOTIscore was predictive of ICI treatment or whether it was just a general prognostic marker. However, this problem can only be addressed using a specific prospective study design that involves a non-ICI control group before data acquisition.

5. Conclusions

In summary, we showed that multi-omics biomarkers derived from exome and transcriptome sequencing can be integrated into a unified score, leading to improved characterization of tumor immunogenicity. Comparative analyses of samples with high versus low MOTIscores revealed enrichment of pathways implicated in the immune regulation of tumors, such as the C-X-C chemokine signaling pathway. The predictive performance of the MOTIscore was comparable to that of several other models. MOTIscore demonstrated robust accuracy in forecasting immune checkpoint inhibitor (ICI) responses according to the RECIST criteria, outperforming single-biomarker approaches. High MOTIscores, particularly in cases in which both TCR diversity and TMB were high, were associated with prolonged overall and progression-free survival in patients with melanoma and gastric cancer who were treated with ICIs, as well as with an increased chance of a strongly reduced tumor size in gastric cancer. These findings suggest that the MOTIscore may serve as a clinically useful tool for identifying patients who are likely to benefit from ICI therapy. Hence, it potentially supports treatment prioritization in molecular tumor boards, especially after validating the findings presented here in a prospective study. Thereby, MOTIscore advances personalized oncology.

Biology **2025**, *14*, 1698

Supplementary Materials: The following supporting information can be downloaded at: https://www.mdpi.com/article/10.3390/biology14121698/s1, Figure S1: Outline of the study. First, we determined the weights using a cohort of ICI-treated melanoma patients, who were classified as responders and non-responders. Statistical tests (Mann Whitney U and Fisher's exact test) provided p-values that served as weights for our MOTIscore. Biomarkers that exhibited high mutual correlation coefficients were removed. The MOTIscore was subsequently calculated using z-scores for each biomarker. Finally, the results were evaluated using three distinct cohorts; Figure S2: (a) Heatmap of Spearman's rank correlation coefficients between all biomarkers that were discriminative for ICI outcomes in the melanoma cohort, with significance levels $p < 0.05$. (b) Only TMB and Neoantigen Burden were highly correlated, with a Spearman's rank correlation coefficient of > 0.5. Consequently, we removed the Neoantigen Burden as a biomarker for our score. The correlations were calculated using the melanoma discovery cohort, which was used to determine the weights for the MOTIscore; Figure S3: Correlation of MOTIscore and LASSO regression scores in (a) melanoma (n = 225) and (b) gastric cancer (n = 33). Both scores were highly correlated, with Pearson's correlation coefficients close to 1 in both cohorts; Figure S4: Volcano plots for the (a) MTB melanoma (n = 77), (b) MTB brain cancer (n = 198), (c) MTB lung cancer (n = 29), and (d) MTB breast cancer (n = 40) cohorts. All three C-X-C motif chemokine ligands *CXCL9*, *CXCL10*, and *CXCL11* were significantly enriched in melanoma, and *CXCL9* was up-regulated in brain cancer. However, none of these genes was enriched in lung or breast cancer; Figure S5: ROC AUCs of *CXCL9*, *CXCL10*, and *CXCL11* expression in (a) the ICI melanoma cohort (n = 225) and (b) the gastric cancer cohort (n = 33). All three genes were predictive of ICI outcomes in both cancer types. In gastric cancer, they achieved performance similar to that of TMB. (c) The combination of the log2 fc of these three genes was better than random in the ICI melanoma cohort (n = 225) but was outperformed by TMB. (d) The Kaplan-Meier curves did not show significant differences in terms of OS in the Liu et al. melanoma cohort (n = 111); Table S1: MTB Cohort Overview; Table S2: MOTIscores Gastric Cancer.

Author Contributions: A.G. designed and coordinated the project, developed the models, curated and analyzed the data, generated the figures, and wrote the manuscript. S.A.-E. curated the list of immunogenicity biomarkers, inspected and corrected the CNV baselines, and co-supervised the project. S.O. co-supervised the project and participated in data acquisition for the MTB cohort. M.R. and A.F. extracted the specific PFS of the ICI-treated patients with melanoma in the MTB cohort. Ö.Ö. maintained and provided metadata from the MTB database. A.K. conducted manual inspection of the clinical data of the false-positive MTB and gastric cancer samples. N.B. and C.S. assisted with the project design. A.O. developed the somatic megSAP pipeline. M.B., G.T., A.H., T.G. and A.F. curated samples of the MTB cohort. All authors have read and agreed to the published version of the manuscript.

Funding: A.G. and S.O. received funding from the Deutsche Forschungsgemeinschaft (DFG) as part of the German Human Genome-Phenome Archive (GHGA) under grant number 441914366 (NFDI 1/1). S.O. and C.S. are supported by funding from the European Union's EU4Health program under grant agreement No. 101080009 (Can.Heal).

Institutional Review Board Statement: This study was approved by the institutional review board of the University Hospital Tübingen (project ID 575/2024BO2) and fulfilled the ethical principles of the Declaration of Helsinki.

Informed Consent Statement: Informed consent was obtained from all patients in the MTB cohort at the University Hospital Tübingen to publish this paper. Informed consent was obtained from all patients in the datasets collected from the database of Genotypes and Phenotypes (dbGaP), the Gene Expression Omnibus (GEO), and the European Nucleotide Archive (ENA); as ensured by the submitting authors of the original studies.

Data Availability Statement: Most of the data used in this study were obtained from publicly available NGS datasets. These data can be obtained from the European Nucleotide Archive (ENA), the database of Genotypes and Phenotypes (dbGaP), or the Gene Expression Omnibus (GEO). The melanoma cohort was assembled from six different studies, with the following study accession

numbers: Amato et al.: PRJNA639866, GSE15996 [44]; Hugo et al.: SRP090294, SRP067938 [43]; Liu et al.: phs000452.v3.p1 [42]; Pyke et al.: phs002388.v1.p1 [41]; Riaz et al.: SRP094781, GSE91061 [40]; Wolchok et al.: SRP417444 [45]. The gastric cancer dataset was described by Kim et al. [46] and is available under the study accession number PRJEB25780. The PFS data and the tumor reduction data for the gastric cancer cohort were extracted from Figure 1 of that paper. The data of the local MTB patients cannot be shared in a non-anonymized form owing to broad consent restrictions. A minimal working example for the MOTIscore algorithm can be found on our GitHub repository, https://github.com/axelgschwind/MOTIscore/ (accessed 25 November 2025, commit fbe6101).

Conflicts of Interest: S.O. is cofounder and shareholder of dxOmics GmbH. M.R. received travel support from Almirall Hermal and Pierre Fabre, outside the submitted work. A.H. received consulting fees and travel support from MSD, AstraZeneca, Roche and GSK, outside the submitted work. A.F. received honoraria for advisory boards, and/or honoraria for lectures, and/ot travel/conference support from BMS, MSD, Novartis, Pierre Fabre Immunocore, all outside the submitted work; further research funding was received from BMS Stiftung Immunonkologie and Hiege Stiftung gegen Hautkrebs, all outside the submitted work.

References

1. Blankenstein, T.; Coulie, P.G.; Gilboa, E.; Jaffee, E.M. The determinants of tumour immunogenicity. *Nat. Rev. Cancer* **2012**, *12*, 307–313. [CrossRef]
2. Newnes, H.V.; Armitage, J.D.; Audsley, K.M.; Bosco, A.; Waithman, J. Directing the Future Breakthroughs in Immunotherapy: The Importance of a Holistic Approach to the Tumour Microenvironment. *Cancers* **2021**, *13*, 5911. [CrossRef]
3. Ulas, E.B.; Hashemi, S.M.S.; Houda, I.; Kaynak, A.; Veltman, J.D.; Fransen, M.F.; Radonic, T.; Bahce, I. Predictive Value of Combined Positive Score and Tumor Proportion Score for Immunotherapy Response in Advanced NSCLC. *JTO Clin. Res. Rep.* **2023**, *4*, 100532. [CrossRef]
4. Kuang, X.; Xu, R.; Li, J. Association of PD-L1 expression with survival benefit from PD-1/PD-L1 inhibitors in advanced cancer: Systematic review and meta-analysis of phase III randomized clinical trials. *Crit. Rev. Oncol. Hematol.* **2024**, *198*, 104357. [CrossRef]
5. Pallocca, M.; Angeli, D.; Palombo, F.; Sperati, F.; Milella, M.; Goeman, F.; De Nicola, F.; Fanciulli, M.; Nisticò, P.; Quintarelli, C.; et al. Combinations of immuno-checkpoint inhibitors predictive biomarkers only marginally improve their individual accuracy. *J. Transl. Med.* **2019**, *17*, 131. [CrossRef]
6. Halima, A.; Vuong, W.; Chan, T.A. Next-generation sequencing: Unraveling genetic mechanisms that shape cancer immunotherapy efficacy. *J. Clin. Investig.* **2022**, *132*, e154945. [CrossRef] [PubMed]
7. Chen, H.; Wang, B.; Zhang, Y.; Shu, Y.; Dong, H.; Zhao, Q.; Yang, C.; Li, J.; Duan, X.; Zhou, Q. A unified DNA- and RNA-based NGS strategy for the analysis of multiple types of variants at the dual nucleic acid level in solid tumors. *J. Clin. Lab. Anal.* **2023**, *37*, e24977. [CrossRef] [PubMed]
8. Donisi, C.; Pretta, A.; Pusceddu, V.; Ziranu, P.; Lai, E.; Puzzoni, M.; Mariani, S.; Massa, E.; Madeddu, C.; Scartozzi, M. Immunotherapy and Cancer: The Multi-Omics Perspective. *Int. J. Mol. Sci.* **2024**, *25*, 3563. [CrossRef] [PubMed]
9. Gschwind, A.; Ossowski, S. AI Model for Predicting Anti-PD1 Response in Melanoma Using Multi-Omics Biomarkers. *Cancers* **2025**, *17*, 714. [CrossRef]
10. Li, Y.; Wu, X.; Fang, D.; Luo, Y. Informing immunotherapy with multi-omics driven machine learning. *npj Digit. Med.* **2024**, *7*, 67. [CrossRef]
11. Amann, J.; Blasimme, A.; Vayena, E.; Frey, D.; Madai, V.I.; Precise4Q Consortium. Explainability for artificial intelligence in healthcare: A multidisciplinary perspective. *BMC Med. Inform. Decis. Mak.* **2020**, *20*, 310. [CrossRef]
12. Salih, A.M.; Raisi-Estabragh, Z.; Galazzo, I.B.; Radeva, P.; Petersen, S.E.; Lekadir, K.; Menegaz, G. A Perspective on Explainable Artificial Intelligence Methods: SHAP and LIME. *Adv. Intell. Syst.* **2025**, *7*, 2400304. [CrossRef]
13. Hrinivich, W.T.; Wang, T.; Wang, C. Editorial: Interpretable and explainable machine learning models in oncology. *Front. Oncol.* **2023**, *13*, 1184428. [CrossRef] [PubMed]
14. Marabelle, A.; Fakih, M.; Lopez, J.; Shah, M.; Shapira-Frommer, R.; Nakagawa, K.; Chung, H.C.; Kindler, H.L.; Lopez-Martin, J.A.; Miller, W.H.; et al. Association of tumour mutational burden with outcomes in patients with advanced solid tumours treated with pembrolizumab: Prospective biomarker analysis of the multicohort, open-label, phase 2 KEYNOTE-158 study. *Lancet Oncol.* **2020**, *21*, 1353–1365. [CrossRef]
15. Wang, P.; Chen, Y.; Wang, C. Beyond Tumor Mutation Burden: Tumor Neoantigen Burden as a Biomarker for Immunotherapy and Other Types of Therapy. *Front. Oncol.* **2021**, *11*, 672677. [CrossRef]

16. Joshi, K.; Milighetti, M.; Chain, B.M. Application of T cell receptor (TCR) repertoire analysis for the advancement of cancer immunotherapy. *Curr. Opin. Immunol.* **2022**, *74*, 1–8. [CrossRef]
17. Maggs, L.; Sadagopan, A.; Moghaddam, A.S.; Ferrone, S. HLA class I antigen processing machinery defects in antitumor immunity and immunotherapy. *Trends Cancer* **2021**, *7*, 1089–1101. [CrossRef] [PubMed]
18. Wang, H.; Liu, B.; Wei, J. Beta2-microglobulin(B2M) in cancer immunotherapies: Biological function, resistance and remedy. *Cancer Lett.* **2021**, *517*, 96–104. [CrossRef]
19. Brown, L.C.; Tucker, M.D.; Sedhom, R.; Schwartz, E.B.; Zhu, J.; Kao, C.; Labriola, M.K.; Gupta, R.T.; Marin, D.; Wu, Y.; et al. LRP1B mutations are associated with favorable outcomes to immune checkpoint inhibitors across multiple cancer types. *J. Immunother. Cancer* **2021**, *9*, e001792. [CrossRef]
20. Chowell, D.; Krishna, C.; Pierini, F.; Makarov, V.; Rizvi, N.A.; Kuo, F.; Morris, L.G.T.; Riaz, N.; Lenz, T.L.; Chan, T.A. Evolutionary divergence of HLA class I genotype impacts efficacy of cancer immunotherapy. *Nat. Med.* **2019**, *25*, 1715–1720. [CrossRef]
21. Khunger, M.; Hernandez, A.V.; Pasupuleti, V.; Rakshit, S.; Pennell, N.A.; Stevenson, J.; Mukhopadhyay, S.; Schalper, K.; Velcheti, V. Programmed Cell Death 1 (PD-1) Ligand (PD-L1) Expression in Solid Tumors As a Predictive Biomarker of Benefit From PD-1/PD-L1 Axis Inhibitors: A Systematic Review and Meta-Analysis. *JCO Precis. Oncol.* **2017**, *1*, 1–15. [CrossRef] [PubMed]
22. Fishburn, P.C. Letter to the Editor—Additive Utilities with Incomplete Product Sets: Application to Priorities and Assignments. *Oper. Res.* **1967**, *15*, 537–542. [CrossRef]
23. Missios, P.; Beha, J.; Bitzer, M.; Malek, N.P. The molecular tumor board. *Der Onkol.* **2020**, *26*, 679–684. [CrossRef]
24. Eisenhauer, E.A.; Therasse, P.; Bogaerts, J.; Schwartz, L.H.; Sargent, D.; Ford, R.; Dancey, J.; Arbuck, S.; Gwyther, S.; Mooney, M.; et al. New response evaluation criteria in solid tumours: Revised RECIST guideline (version 1.1). *Eur. J. Cancer* **2009**, *45*, 228–247. [CrossRef]
25. Illumina. *DRAGEN Secondary Analysis*, Version 4.2.4; Illumina: Foster City, CA, USA, 2024.
26. McLaren, W.; Gil, L.; Hunt, S.E.; Riat, H.S.; Ritchie, G.R.S.; Thormann, A.; Flicek, P.; Cunningham, F. The Ensembl Variant Effect Predictor. *Genome Biol.* **2016**, *17*, 122. [CrossRef]
27. Tate, J.G.; Bamford, S.; Jubb, H.C.; Sondka, Z.; Beare, D.M.; Bindal, N.; Boutselakis, H.; Cole, C.G.; Creatore, C.; Dawson, E.; et al. COSMIC: The Catalogue Of Somatic Mutations In Cancer. *Nucleic Acids Res.* **2018**, *47*, D941–D947. [CrossRef]
28. Demidov, G.; Ossowski, S. ClinCNV: Novel method for allele-specific somatic copy-number alterations detection. *bioRxiv* **2019**, 837971. [CrossRef]
29. Dobin, A.; Davis, C.A.; Schlesinger, F.; Drenkow, J.; Zaleski, C.; Jha, S.; Batut, P.; Chaisson, M.; Gingeras, T.R. STAR: Ultrafast universal RNA-seq aligner. *Bioinformatics* **2012**, *29*, 15–21. [CrossRef]
30. Liao, Y.; Smyth, G.K.; Shi, W. featureCounts: An efficient general purpose program for assigning sequence reads to genomic features. *Bioinformatics* **2014**, *30*, 923–930. [CrossRef]
31. Love, M.I.; Huber, W.; Anders, S. Moderated estimation of fold change and dispersion for RNA-seq data with DESeq2. *Genome Biol.* **2014**, *15*, 550. [CrossRef]
32. Xu, S.; Hu, E.; Cai, Y.; Xie, Z.; Luo, X.; Zhan, L.; Tang, W.; Wang, Q.; Liu, B.; Wang, R.; et al. Using clusterProfiler to characterize multiomics data. *Nat. Protoc.* **2024**, *19*, 3292–3320. [CrossRef] [PubMed]
33. Hundal, J.; Kiwala, S.; McMichael, J.; Miller, C.A.; Xia, H.; Wollam, A.T.; Liu, C.J.; Zhao, S.; Feng, Y.-Y.; Graubert, A.P.; et al. pVACtools: A Computational Toolkit to Identify and Visualize Cancer Neoantigens. *Cancer Immunol. Res.* **2020**, *8*, 409–420. [CrossRef]
34. Song, L.; Cohen, D.; Ouyang, Z.; Cao, Y.; Hu, X.; Liu, X.S. TRUST4: Immune repertoire reconstruction from bulk and single-cell RNA-seq data. *Nat. Methods* **2021**, *18*, 627–630. [CrossRef]
35. Sharma, P.; Hu-Lieskovan, S.; Wargo, J.A.; Ribas, A. Primary, Adaptive, and Acquired Resistance to Cancer Immunotherapy. *Cell* **2017**, *168*, 707–723. [CrossRef]
36. Pierini, F.; Lenz, T.L. Divergent Allele Advantage at Human MHC Genes: Signatures of Past and Ongoing Selection. *Mol. Biol. Evol.* **2018**, *35*, 2145–2158. [CrossRef]
37. Farrell, J.J. The Prediction of HLA Genotypes from Next Generation Sequencing and Genome Scan Data. Ph.D. Thesis, Boston University, Boston, MA, USA, 2014.
38. Grantham, R. Amino acid difference formula to help explain protein evolution. *Science* **1974**, *185*, 862–864. [CrossRef] [PubMed]
39. Behdenna, A.; Colange, M.; Haziza, J.; Gema, A.; Appé, G.; Azencott, C.-A.; Nordor, A. pyComBat, a Python tool for batch effects correction in high-throughput molecular data using empirical Bayes methods. *BMC Bioinform.* **2023**, *24*, 459. [CrossRef]
40. Riaz, N.; Havel, J.J.; Makarov, V.; Desrichard, A.; Urba, W.J.; Sims, J.S.; Hodi, F.S.; Martín-Algarra, S.; Mandal, R.; Sharfman, W. H.; et al. Tumor and Microenvironment Evolution during Immunotherapy with Nivolumab. *Cell* **2017**, *171*, 934–949.e916. [CrossRef]
41. Pyke, R.M.; Mellacheruvu, D.; Dea, S.; Abbott, C.W.; McDaniel, L.; Bhave, D.P.; Zhang, S.V.; Levy, E.; Bartha, G.; West, J.; et al. A machine learning algorithm with subclonal sensitivity reveals widespread pan-cancer human leukocyte antigen loss of heterozygosity. *Nat. Commun.* **2022**, *13*, 1925. [CrossRef]

42. Liu, D.; Schilling, B.; Liu, D.; Sucker, A.; Livingstone, E.; Jerby-Arnon, L.; Zimmer, L.; Gutzmer, R.; Satzger, I.; Loquai, C.; et al. Integrative molecular and clinical modeling of clinical outcomes to PD1 blockade in patients with metastatic melanoma. *Nat. Med.* **2019**, *25*, 1916–1927. [CrossRef] [PubMed]
43. Hugo, W.; Zaretsky, J.M.; Sun, L.; Song, C.; Moreno, B.H.; Hu-Lieskovan, S.; Berent-Maoz, B.; Pang, J.; Chmielowski, B.; Cherry, G.; et al. Genomic and Transcriptomic Features of Response to Anti-PD-1 Therapy in Metastatic Melanoma. *Cell* **2016**, *165*, 35–44. [CrossRef]
44. Amato, C.M.; Hintzsche, J.D.; Wells, K.; Applegate, A.; Gorden, N.T.; Vorwald, V.M.; Tobin, R.P.; Nassar, K.; Shellman, Y.G.; Kim, J.; et al. Pre-Treatment Mutational and Transcriptomic Landscape of Responding Metastatic Melanoma Patients to Anti-PD1 Immunotherapy. *Cancers* **2020**, *12*, 1943. [CrossRef]
45. Wolchok, J.D.; Chiarion-Sileni, V.; Gonzalez, R.; Rutkowski, P.; Grob, J.J.; Cowey, C.L.; Lao, C.D.; Wagstaff, J.; Schadendorf, D.; Ferrucci, P.F.; et al. Overall Survival with Combined Nivolumab and Ipilimumab in Advanced Melanoma. *N. Engl. J. Med.* **2017**, *377*, 1345–1356. [CrossRef]
46. Kim, S.T.; Cristescu, R.; Bass, A.J.; Kim, K.-M.; Odegaard, J.I.; Kim, K.; Liu, X.Q.; Sher, X.; Jung, H.; Lee, M.; et al. Comprehensive molecular characterization of clinical responses to PD-1 inhibition in metastatic gastric cancer. *Nat. Med.* **2018**, *24*, 1449–1458. [CrossRef]
47. Marcus, L.; Fashoyin-Aje, L.A.; Donoghue, M.; Yuan, M.; Rodriguez, L.; Gallagher, P.S.; Philip, R.; Ghosh, S.; Theoret, M.R.; Beaver, J.A.; et al. FDA Approval Summary: Pembrolizumab for the Treatment of Tumor Mutational Burden–High Solid Tumors. *Clin. Cancer Res.* **2021**, *27*, 4685–4689. [CrossRef] [PubMed]
48. Martínez-Camblor, P.; Pardo-Fernández, J.C. The Youden Index in the Generalized Receiver Operating Characteristic Curve Context. *Int. J. Biostat.* **2019**, *15*, 20180060. [CrossRef]
49. Wang, S.; Wang, Y.; Guan, L.; Shen, A.; Huang, R.; Yuan, S.; Xiao, Y.; Wang, L.; Lei, D.; Zhao, Y.; et al. Construction of a prognostic model for gastric cancer based on immune infiltration and microenvironment, and exploration of MEF2C gene function. *BMC Med. Genom.* **2025**, *18*, 13. [CrossRef] [PubMed]
50. Chen, M.; Zhu, X.; Zhang, L.; Zhao, D. COL5A2 is a prognostic-related biomarker and correlated with immune infiltrates in gastric cancer based on transcriptomics and single-cell RNA sequencing. *BMC Med. Genom.* **2023**, *16*, 220. [CrossRef]
51. Fu, D.; Weng, X.; Su, Y.; Hong, B.; Zhao, A.; Lin, J. Establishing a model composed of immune-related gene-modules to predict tumor immunotherapy response. *Sci. Rep.* **2024**, *14*, 16630. [CrossRef]
52. Shen, X.; Wang, M.; Chen, W.; Xu, Y.; Zhou, Q.; Zhu, T.; Wang, G.; Cai, S.; Han, Y.; Xu, C.; et al. Senescence-related genes define prognosis, immune contexture, and pharmacological response in gastric cancer. *Aging* **2023**, *15*, 2891–2905. [CrossRef] [PubMed]
53. Dong, X.; Xie, Y.; Chen, W.; He, M.; Liu, H.; Wang, B.; Xu, Y.; Zhou, Q.; Zhu, T.; Wang, G.; et al. Pan-gastrointestinal adenocarcinoma analysis uncovers the prognostic and immune correlates of ferroptosis-related genes. *Transl. Gastroenterol. Hepatol.* **2025**, *10*, 7. [CrossRef]
54. Sun, J.; Guo, H.; Zhang, S.; Nie, Y.; Zhou, S.; Zeng, Y.; Sun, Y. Machine learning-based integration develops an immunogenic cell death-derived lncRNA signature for predicting prognosis and immunotherapy response in lung adenocarcinoma. *Sci. Rep.* **2024**, *14*, 11724. [CrossRef] [PubMed]
55. Liberzon, A.; Birger, C.; Thorvaldsdóttir, H.; Ghandi, M.; Mesirov, J.P.; Tamayo, P. The Molecular Signatures Database Hallmark Gene Set Collection. *Cell Syst.* **2015**, *1*, 417–425. [CrossRef] [PubMed]
56. Tokunaga, R.; Zhang, W.; Naseem, M.; Puccini, A.; Berger, M.D.; Soni, S.; McSkane, M.; Baba, H.; Lenz, H.-J. CXCL9, CXCL10, CXCL11/CXCR3 axis for immune activation—A target for novel cancer therapy. *Cancer Treat. Rev.* **2018**, *63*, 40–47. [CrossRef] [PubMed]
57. Letourneur, D.; Danlos, F.-X.; Marabelle, A. Chemokine biology on immune checkpoint–targeted therapies. *Eur. J. Cancer* **2020**, *137*, 260–271. [CrossRef]
58. Darvin, P.; Toor, S.M.; Sasidharan Nair, V.; Elkord, E. Immune checkpoint inhibitors: Recent progress and potential biomarkers. *Exp. Mol. Med.* **2018**, *50*, 1–11. [CrossRef]
59. Touat, M.; Li, Y.Y.; Boynton, A.N.; Spurr, L.F.; Iorgulescu, J.B.; Bohrson, C.L.; Cortes-Ciriano, I.; Birzu, C.; Geduldig, J.E.; Pelton, K.; et al. Mechanisms and therapeutic implications of hypermutation in gliomas. *Nature* **2020**, *580*, 517–523. [CrossRef]
60. Chen, Y.; Jia, K.; Sun, Y.; Zhang, C.; Li, Y.; Zhang, L.; Chen, Z.; Zhang, J.; Hu, Y.; Yuan, J.; et al. Predicting response to immunotherapy in gastric cancer via multi-dimensional analyses of the tumour immune microenvironment. *Nat. Commun.* **2022**, *13*, 4851. [CrossRef]
61. He, Y.; Wang, X. Identification of molecular features correlating with tumor immunity in gastric cancer by multi-omics data analysis. *Ann. Transl. Med.* **2020**, *8*, 1050. [CrossRef]
62. Wu, B.; Zhang, B.; Li, B.; Wu, H.; Jiang, M. Cold and hot tumors: From molecular mechanisms to targeted therapy. *Signal Transduct. Target. Ther.* **2024**, *9*, 274. [CrossRef]
63. Berger, E.R.; Park, T.; Saridakis, A.; Golshan, M.; Greenup, R.A.; Ahuja, N. Immunotherapy Treatment for Triple Negative Breast Cancer. *Pharmaceuticals* **2021**, *14*, 763. [CrossRef] [PubMed]

64. Jardim, D.L.; Goodman, A.; de Melo Gagliato, D.; Kurzrock, R. The Challenges of Tumor Mutational Burden as an Immunotherapy Biomarker. *Cancer Cell* **2021**, *39*, 154–173. [CrossRef] [PubMed]
65. Wolf, Y.; Sameuls, Y. Neoantigens in cancer immunotherapy: Quantity vs. quality. *Mol. Oncol.* **2023**, *17*, 1457–1459. [CrossRef] [PubMed]
66. Borden, E.S.; Buetow, K.H.; Wilson, M.A.; Hastings, K.T. Cancer Neoantigens: Challenges and Future Directions for Prediction, Prioritization, and Validation. *Front. Oncol.* **2022**, *12*, 836821. [CrossRef]
67. Gong, Z.; Zhang, J.; Guo, W. Tumor purity as a prognosis and immunotherapy relevant feature in gastric cancer. *Cancer Med.* **2020**, *9*, 9052–9063. [CrossRef]

B.3 Supplementary Materials

Supplementary Figures

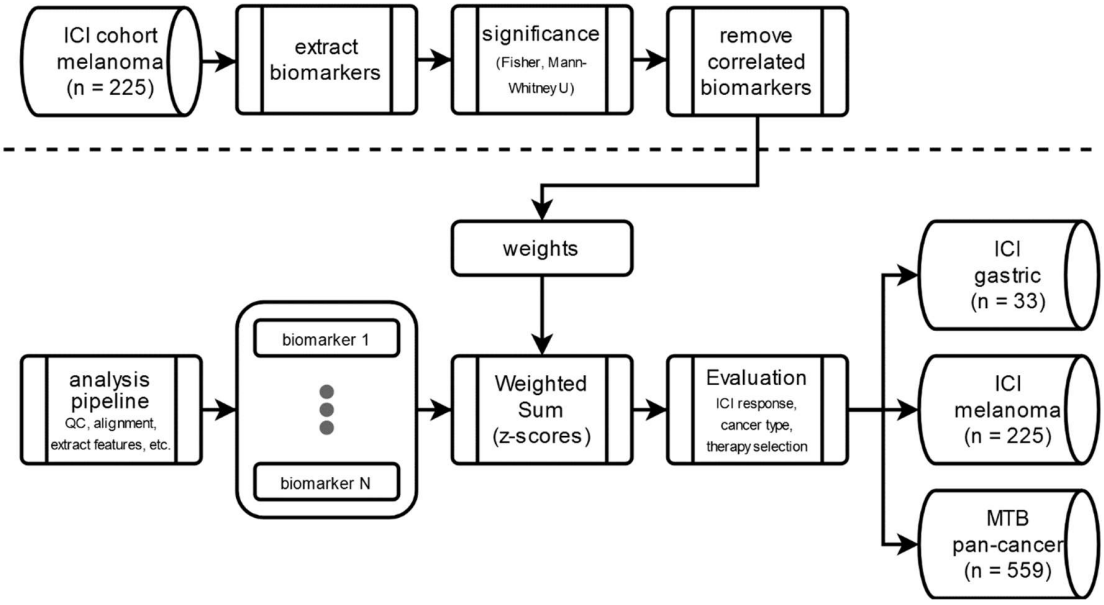

Figure S1. Outline of the study. First, we determined the weights using a cohort of ICI-treated melanoma patients, who were classified as responders and non-responders. Statistical tests (Mann Whitney U and Fisher's exact test) provided p-values that served as weights for our MOTIscore. Biomarkers that exhibited high mutual correlation coefficients were removed. The MOTIscore was subsequently calculated using z-scores for each biomarker. Finally, the results were evaluated using three distinct cohorts.

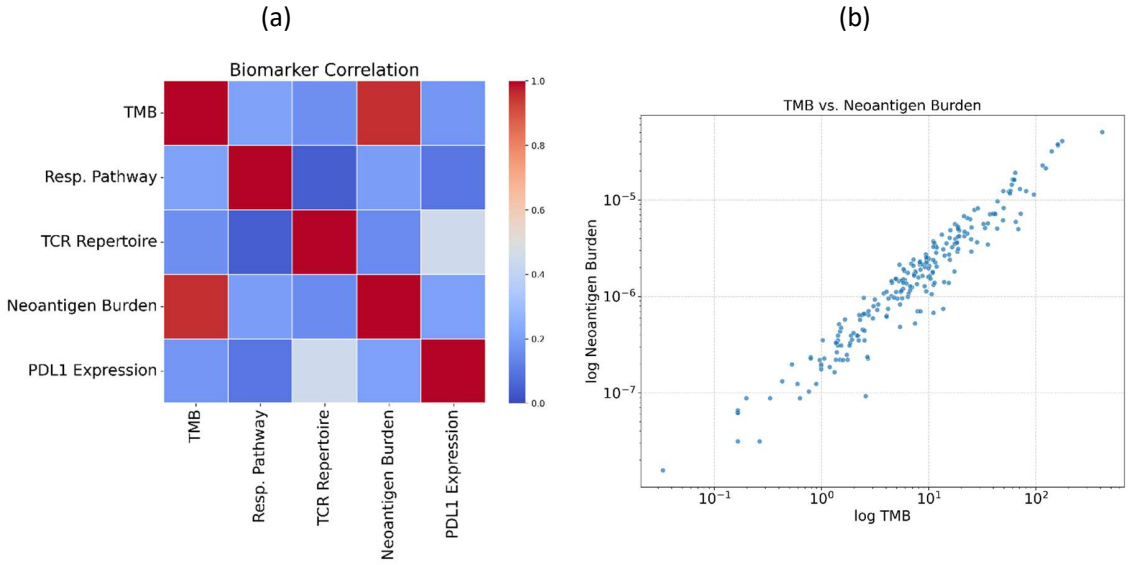

Figure S2. (a) Heatmap of Spearman's rank correlation coefficients between all biomarkers that were discriminative for ICI outcomes in the melanoma cohort, with significance levels $p < 0.05$. (b) Only TMB and Neoantigen Burden were highly correlated, with a Spearman's rank correlation coefficient of > 0.5. Consequently, we removed the Neoantigen Burden as a biomarker for our score. The correlations were calculated using the melanoma discovery cohort, which was used to determine the weights for the MOTIscore.

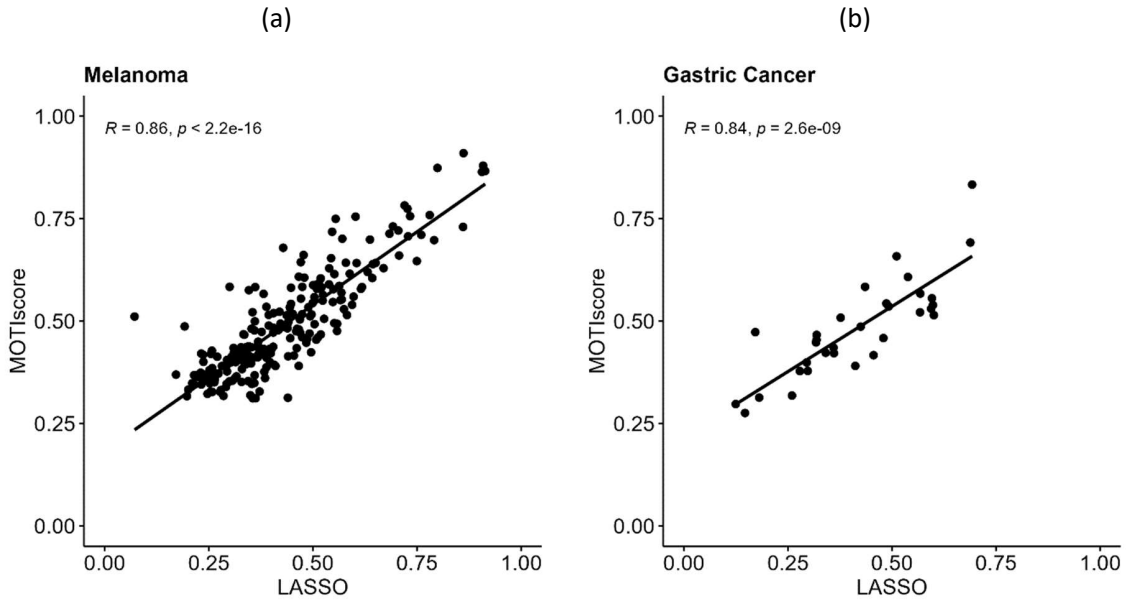

Figure S3. Correlation of MOTIscore and LASSO regression scores in (a) melanoma (n = 225) and (b) gastric cancer (n = 33). Both scores were highly correlated, with Pearson's correlation coefficients close to 1 in both cohorts.

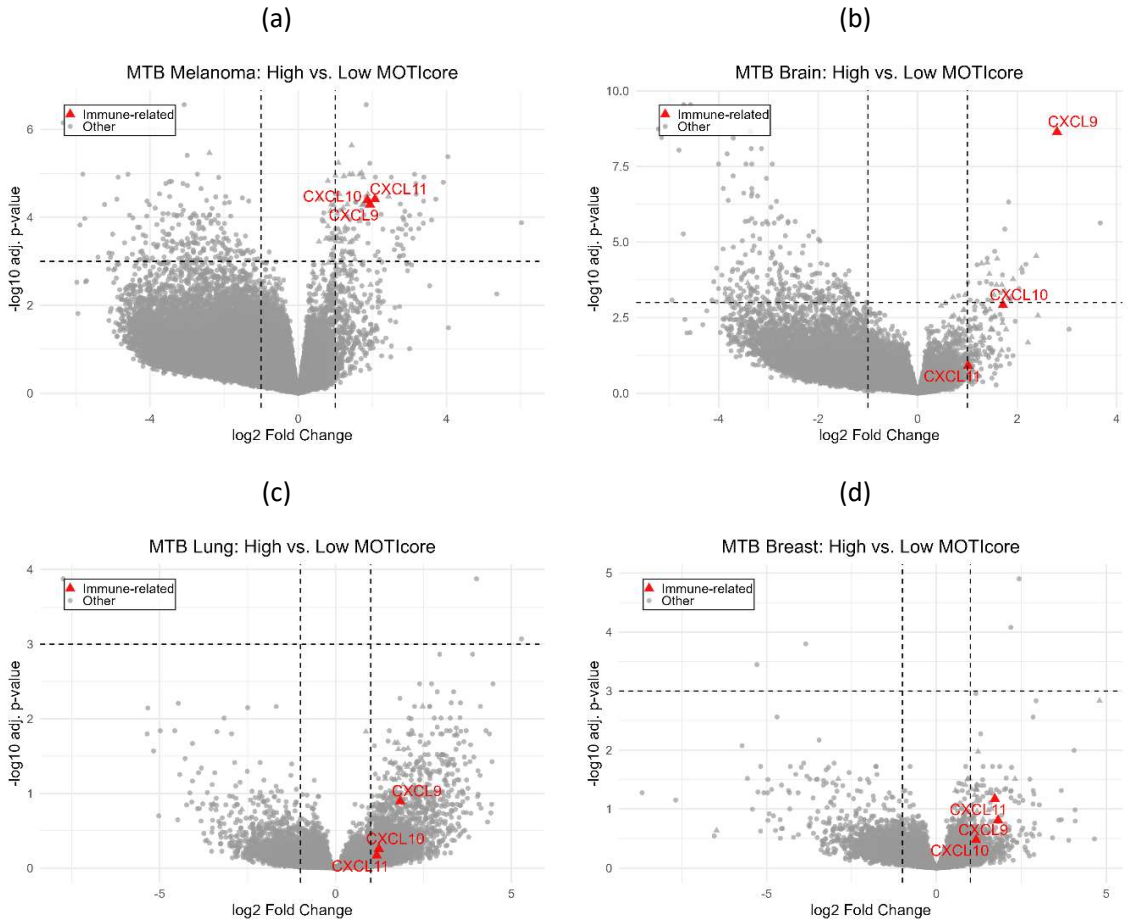

Figure S4. Volcano plots for the (a) MTB melanoma (n = 77), (b) MTB brain cancer (n = 198), (c) MTB lung cancer (n = 29), and (d) MTB breast cancer (n = 40) cohorts. All three C-X-C motif chemokine ligands CXCL9, CXCL10, and CXCL11 were significantly enriched in melanoma, and CXCL9 was up-regulated in brain cancer. However, none of these genes was enriched in lung or breast cancer.

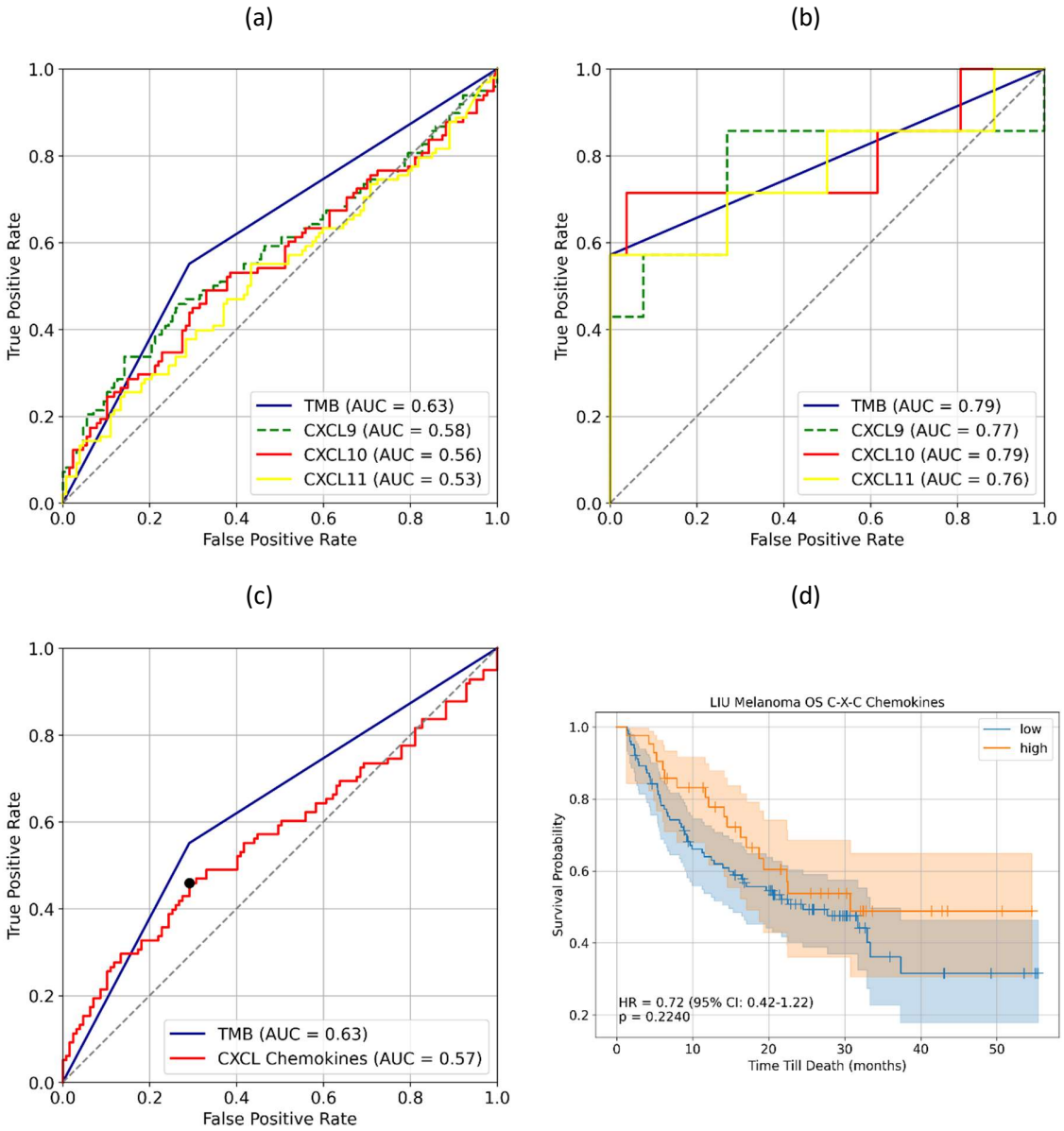

Figure S5. ROC AUCs of CXCL9, CXCL10, and CXCL11 expression in (a) the ICI melanoma cohort (n = 225) and (b) the gastric cancer cohort (n = 33). All three genes were predictive of ICI outcomes in both cancer types. In gastric cancer, they achieved performance similar to that of TMB. (c) The combination of the log2 fc of these three genes was better than random in the ICI melanoma cohort (n = 225) but was outperformed by TMB. (d) The Kaplan-Meier curves did not show significant differences in terms of OS in the Liu et al. melanoma cohort (n = 111).

B.4 MOTIscore Study Protocol

Funding of projects on the topic dataXperiment - Testing innovative feasibility and application scenarios in oncology - National Decade Against Cancer -

Multiomic Immunogenicity Modelling and Rank Sum Scoring of Solid Tumors

ACRONYM: MIMoRScore

PROJECT TITLE: Multiomic Immunogenicity Modelling and Rank Sum Scoring of Solid Tumors

PROJECT DURATION: OCTOBER 1ST 2024 END OF PROJECT: MARCH 31ST 2025

TOTAL REQUESTED BUDGET: 50.000 €

FIVE KEYWORDS: TUMOR IMMUNOGENICITY, MULTIOMICS, MACHINE LEARNING, IMMUNOTHERAPY, PRECISION ONCOLOGY

MIMoRScore

PROJECT DESCRIPTION

1 LAY PROJECT SUMMARY

Modern state-of-the-art cancer therapies include immunotherapies. Such treatments trigger the patient's immune system to attack cancer cells. Clinicians need to know whether tumor cells can cause an immune reaction to select patients for therapy. This property of the tumor is also known as immunogenicity. The current standards to describe the immunogenicity of a tumor are not very comprehensive and are frequently unreliable. Our project aims to design a more accurate score to describe tumor immunogenicity, which would be beneficial for personalized cancer treatment.

To achieve this goal, we will retrieve and combine information about the tumor and the immune system from two different sources: sequencing of the DNA, and sequencing of the RNA of the tumor. DNA sequencing will provide details about molecular mechanisms within the tumor cells, whereas RNA sequencing will inform us not only about certain molecular mechanisms in the tumor cells, but also about the tumor environment, such as immune cells that infiltrated the tumor tissue.

We will then use the information from DNA and RNA to train a machine learning model. In this model, we will use the data of a cohort of skin cancer patients who were previously treated with immunotherapy. The machine learning model will predict the success of the treatment. Then, the results of this model will be used to design a new immunogenicity score, which we termed the MIMoRScore. This MIMoRScore combines RNA and DNA and will describe the immunogenicity of tumors more comprehensively. It will be evaluated in a second, in-house cohort of more than 1100 cancer patients, covering a various range of different cancer types.

2 SCIENTIFIC CONCEPT OF THE PROJECT

Scientific Objectives

Next-generation sequencing (NGS) has revolutionized genetic testing and is one of the central elements of personalized oncology. As of 2024, in general, two different sequencing techniques are the most relevant for tumor profiles: targeted sequencing of panels or whole exomes (WES) and bulk RNA sequencing (RNA-Seq). The information derived from both techniques is usually very distinct. For example, RNA-Seq can be used to obtain transcriptomic data, including gene expression, gene fusions, immune cell infiltration, and other immunological biomarkers. On the other hand, genomic information can be derived from WES, providing tumor-intrinsic biomarkers such as the tumor mutation burden (TMB), neoantigens, deleterious mutations in tumor suppressor genes, or mutated resistance mechanisms. However, in a typical clinical setting, genomic and transcriptomic biomarkers are normally not combined to assess and describe tumor immunogenicity.

Modern anti-cancer drugs, such as immune checkpoint inhibitors (ICIs), require a precise assessment of tumor immunogenicity for the selection of patients for this kind of therapy. Nevertheless, the current gold standards, such as TMB for melanoma or *PDL1* expression for lung cancer, are not satisfactory predictors and descriptors of immunogenicity. Our idea is to integrate both genomic and transcriptomic biomarkers into a score that captures more properties of the tumor to describe its immunogenicity more comprehensively. Therefore, we will apply a combined multiomics approach that uses both transcriptomic and genomic biomarkers. We will combine state-of-the-art machine learning (ML) and weighted rank sum models to generate a reliable immunogenicity score, termed MIMoRScore.

MIMoRScore

Methodological Approach

First, we will train an ML model using a cohort of ICI-treated melanoma patients for which therapy outcome data are available. We will specify a binary target variable (responders and non-responders) using the Response Evaluation Criteria in Solid Tumors (RECIST). Patients with complete or partial responses are classified as responders, whereas patients with mixed responses, stable or progressive disease are considered as non-responders. We will utilize a Least Absolute Shrinkage and Selection Operator (LASSO) regression model using biomarkers derived from both RNA-Seq and WES. LASSO regression has the ability to deal with correlated features as well as the ability to effectively perform feature selection by shrinking coefficients of unimportant features to zero. Following model training, we will estimate the impact of each biomarker by permutation feature importance. The non-zero feature importance scores determined in this way will then be used as weights for a weighted rank sum model. The resulting score is the MIMoRScore, which we will evaluate by estimating tumor immunogenicity in another cohort. This independent pan-cancer clinical cohort contains data on more than 1100 tumors and has been generated for the local molecular tumor board. For every tumor sample, paired tumor-normal WES and RNA-Seq data are available, and the cohort covers a wide range of solid tumor types. ML models often lack the explainability of their predictions, which is, however, crucial in clinical practice. To overcome this problem, we will apply the relatively new technique of Shapley Additive exPlanations (SHAP) values, which provides additional per-sample feature importance estimates for the LASSO model.

We will use various biomarkers for both the ML model and the weighted rank sum scoring. For the transcriptomic biomarkers, we will focus on metrics describing the tumor immune microenvironment (TIME), such as immune cell infiltration or the T cell receptor (TCR) / B cell receptor (BCR) repertoire. These metrics are either already annotated to our cohorts or can be easily computed from RNA-Seq data using tools such as quanTIseq or TRUST4. For the WES data, we will focus on genomic biomarkers that describe tumor-intrinsic properties. Besides the well-established TMB, we are particularly interested in tumor neoantigens, predicted in silico by algorithms like netMHC or netMHCpan. Predicted neoantigens will be filtered for sufficient binding affinities and annotated with NeoFox, a tool that calculates neoantigen features to assess their immunogenicity. Furthermore, variants in ICI-resistance genes and HLA genotypes will be considered. Since our project aims to integrate both WES and RNA-Seq data, we will correlate neoantigen features with transcriptomic biomarkers describing the TIME. In this way, we will assess whether certain neoantigens will lead to an immune response, indicating the immunogenicity of the neoantigen and thus the tumor. It is also of particular interest how strongly neoantigens are expressed, which is another information we can only obtain by combining WES and RNA-Seq.

Quality Assurance, Data Sets and Data Management

We will use two distinct cohorts for our study. For the ML model, we will use a cohort that has been assembled from sequencing data of eight previously published melanoma studies in which patients received anti-PD1 treatment. This meta-cohort includes more than 300 combined WES and RNA-Seq samples. Notably, the therapy outcomes for every sample in this meta-cohort are available in accordance with the RECIST criteria (responder and non-responder). For the weighted rank sum scoring, we will use a large in-house cohort. It contains sequencing data from more than 1100 cancer patients. Each tumor was sequenced using RNA-Seq and tumor-normal WES. This cohort includes various cancer types, such as melanoma, colorectal carcinoma, breast cancer, and glioblastoma.

The basic analysis and annotation of the data sets of both cohorts have already been conducted using an in-house bioinformatics sequence analysis pipeline. The analysis steps for the RNA-Seq

samples included read alignment against GRCh38, read quantification, and fusion detection, among others. For the corresponding tumor-normal WES pairs, the basic analysis included read alignment against GRCh38, somatic variant calling including single nucleotide variants (SNVs), small insertion and deletions (indels) as well as copy number variants (CNVs), and structural variants (SVs). The results from both RNA-Seq and WES were annotated using various tools and databases, such as the variant effect predictor (VEP) and the Catalogue of Somatic Mutations in Cancer (COSMIC). Our bioinformatics system applies several advanced quality control parameters (e.g., read coverage, minimum read count, and contamination detection). This allows discarding all samples that do not meet the minimum quality standards.

The raw sequencing data, as well as the analysis results, have been stored in an organized manner in the high-performance computation cluster of our institution. Our computational infrastructure provides more than 500 computer cores and several petabytes of storage, demonstrating its capability to perform high-throughput analyses of NGS data. Data safety and privacy are ensured by the IT department, e.g., by using a strict firewall. We have applied appropriate clinical safety standards for all samples to prevent unauthorized access. We emphasize that patient credentials (e.g., family name or given name) are stored in a different system to guarantee anonymization.

Every patient included in our in-house cohort signed a broad consent form for research, which allows the use of anonymized patient data for scientific research after approval by the ethical review committee. For the melanoma meta-cohort, patients have given informed consent for research use and publication of their sequencing data. The ethical review committee of our institution ensures that the ethical standards of our study are in accordance with the Declaration of Helsinki. Our analyses will primarily rely on bioinformatics tools, libraries, and databases. As is customary in this field, most computational tools and databases are published as open-source (e.g., VEP was published under the Apache 2.0 license) or are at least free to use for non-commercial research purposes (e.g., COSMIC). Therefore, we do not expect any legal constraints for any of the bioinformatics tools or databases that we will use.

Innovation and Exploitation Strategies, Impact and Output

Here, we presented a new approach that integrates data and biomarkers from different sequencing technologies (RNA-Seq and WES). By integrating genomic and transcriptomic biomarkers, our approach aims to provide a more comprehensive view of tumor immunogenicity. This is highly relevant for the correct selection of the most beneficial treatment options for cancer patients in precision oncology, such as state-of-the-art immunotherapy. Our MIMoRScore score reflects both tumor-intrinsic properties and TIME. This will very likely help improve predictions of the therapeutic outcome for cancer patients treated with ICIs, an urgent need given the poor predictive power of TMB or PDL1 expression alone. For example, the anti-PD1 agent pembrolizumab has an objective response rate of only 29% in TMB-high melanoma patients versus 6% in TMB-low patients, highlighting the necessity of better ICI predictors.

ML models are often not feasible for clinical applications because their predictions cannot be easily explained and interpreted. Applying SHapley Additive exPlanations (SHAP) values is a potential avenue for this problem, with SHAP providing per-sample feature importance scores for all predictions.

Our project will make use of an unpublished cohort of more than 1100 combined RNA-Seq and WES samples, plus a second meta-cohort of more than 300 samples, exploiting a huge transcriptomic and genomic data source across multiple cancer types. As of 2024, we did not find any other published clinical cohort that reached a similarly high count of integrated RNA-Seq and WES tumor samples.

Looking ahead, the results of this project could be used for follow-up research questions after the project ends. With the MIMoRScore describing the immunogenicity of tumors, we could assess its

performance as a predictor in prospective studies. For example, it could be of interest how well the score performs as a predictor for immunotherapy outcome in a future cohort.

3 LIST OF WORK PACKAGES AND DELIVERABLES

We will start with the study on October 1st and will finish by March 31st. All work packages will be performed within this timeframe. Our proposed work packages (WPs) are as follows:

- **WP1 Quality Control:** We will define uniform quality standards. Samples that do not meet the minimum quality requirements will be excluded from the study. **Deliverables:** Quality-controlled cohorts and a statistical report on the quality metrics.
- **WP2 Selection and derivation of biomarkers:** We will define a comprehensive list of biomarkers that will be considered in the models of this study. We will focus on the aforementioned immune system-related biomarkers and neoantigens. We will check whether every sample is annotated with every biomarker and, if necessary, missing biomarkers will be derived. **Deliverables:** Final list of biomarkers and complete derivation of these biomarkers from RNA-Seq and WES for every sample.
- **WP3 Implementation and Training of LASSO:** We will implement and train a LASSO model using the outcome data of the ICI meta-cohort. Permutation feature importance will be performed to obtain weights for the weighted rank sum model. The SHAP values will be determined as a proof of concept for the explainability of the model. **Deliverables:** Feature importance scores as weights and explainable SHAP values.
- **WP4 Weighted Rank Sum Scoring:** Using data of more than 1100 cancer patients, we will use the weights determined in WP3 to conduct a weighted rank sum scoring, resulting in our MIMoRScore score. We will thoroughly examine the resulting score, comparing it with other metrics that describe tumor immunogenicity, such as the TMB or *PDL1* expression. **Deliverables:** MIMoRScore score for every sample, MIMoRScore statistics and a statistical comparison of the score with other already established metrics.
- **WP5 Wrapping up results:** As a last step, we will write a publication manuscript. We will aim for publication in an open-access, peer-reviewed journal. The publication fees can later be covered by the budget of our faculty. **Deliverables:** Draft of a paper and submission of the manuscript after project end.

We request funding of 41.666 € plus 20% project flat rate (“Projektpauschale”), 8.333 €. The requested sum reaches in total 49.999 €, in words forty-nine thousand nine hundred ninety-nine euro. We plan to use this funding as follows:

Expenses	**Description**	**Requested**
Staff	A scientific employee will be released of their other duties at our institute for the duration of the project. They will be assigned full-time to exclusively work on this project. We apply for six months of a TV-L E13/4 position and calculated staff costs using the employer’s gross, including a “VBL Klassik” obligatory company pension.	41.666 €
Project flat rate	We request 20% of the project expenditure.	8.333 €
Sum		49.999 €

4 CONFIRMATION

A request for funding this project has not been submitted to any other addressee. In case I submit such a request, I will inform the Federal Ministry of Education and Research immediately.

Appendix C

Certificates

In this appendix chapter, we provide copies of the certificates the candidate gained during his dissertation process. Namely, he attended two summer schools in Poland in 2022 and in 2023. They covered a wide range of topics in ML in computational biology and multi-modal data integration. In addition, the candidate received certificates for reviewing two papers in Springer Nature *Scientific Reports* and *Archives of Dermatological Research*.

C.1 Participation Certificate NGSchool 2023

C.2 Participation Certificate NGSchool 2022

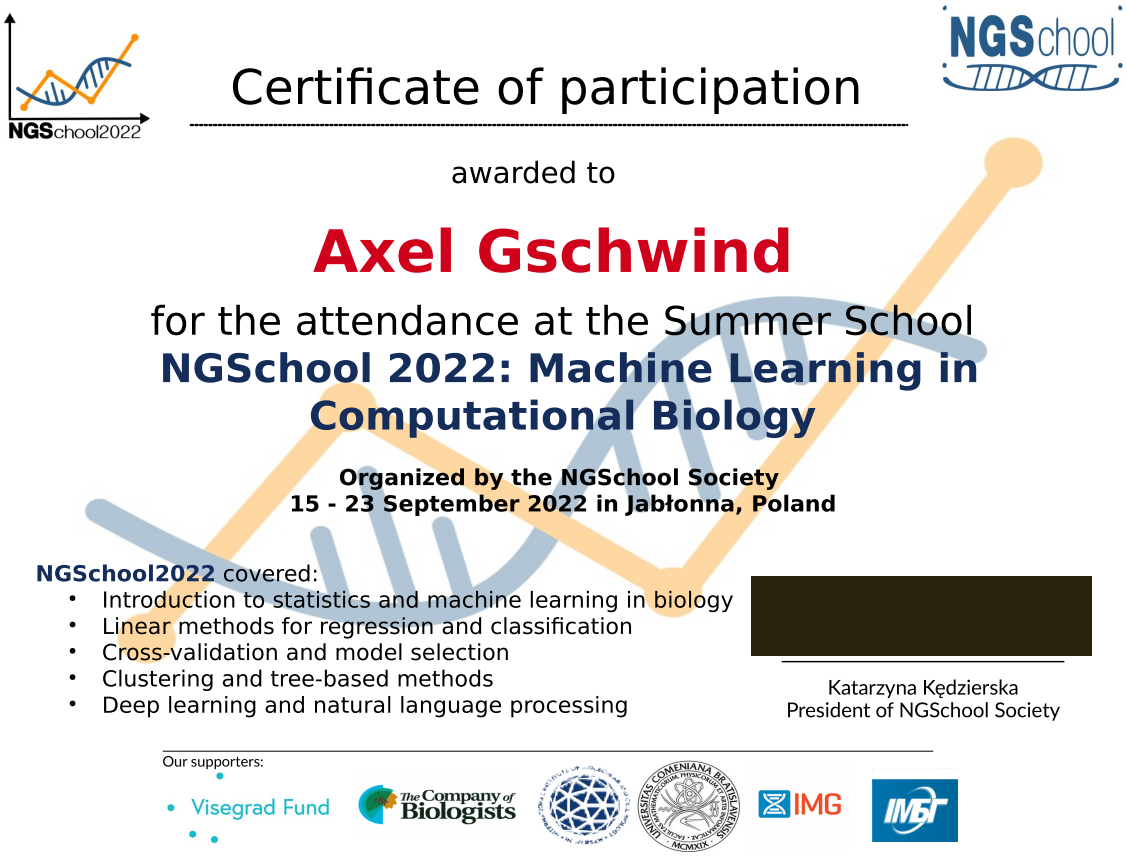

C.3 Peer Review Certificates


SPRINGER NATURE
REVIEWER CERTIFICATE
This certificate is awarded to
Axel Gschwind
in recognition of their contribution to
1 manuscript in 2026 for
Archives of Dermatological Research
26 January 2026
Springer
nature portfolio
BMC
Discover
palgrave macmillan
Birkhäuser
Adis